

Nucleon polarizabilities in covariant baryon chiral perturbation theory with explicit Δ degrees of freedom

M. Thürmann,^{1,*} E. Epelbaum^{1,†}, A. M. Gasparyan^{1,2,‡} and H. Krebs^{1,§}

¹Institut für Theoretische Physik II, Ruhr-Universität Bochum, D-44780 Bochum, Germany

²NRC Kurchatov Institute–ITEP, B. Cheremushkinskaya 25, 117218 Moscow, Russia



(Received 12 August 2020; accepted 11 February 2021; published 4 March 2021)

We compute various nucleon polarizabilities in chiral perturbation theory implementing the Δ -full (Δ -less) approach up to order $\epsilon^3 + q^4$ (q^4) in the small-scale (chiral) expansion. The calculation is carried out using the covariant formulation of χ PT by utilizing the extended on-mass shell renormalization scheme. Except for the spin-independent dipole polarizabilities used to fix the values of certain low-energy constants, our results for the nucleon polarizabilities are pure predictions. We compare our calculations with available experimental data and other theoretical results. The importance of the explicit treatment of the Δ degree of freedom in the effective field theory description of the nucleon polarizabilities is analyzed. We also study the convergence of the $1/m$ expansion and analyze the efficiency of the heavy-baryon approach for the nucleon polarizabilities.

DOI: [10.1103/PhysRevC.103.035201](https://doi.org/10.1103/PhysRevC.103.035201)

I. INTRODUCTION

Understanding the structure of the nucleon is one of the key challenges in the physics of strong interactions, and quantum chromodynamics (QCD), in particular. One of the most direct ways to access the nucleon structure is to use electromagnetic probes. In the present work we focus on the nucleon polarizabilities, which characterize the (second-order) response of the nucleon to an applied electromagnetic field. In recent decades, the nucleon polarizabilities have been intensively studied both experimentally and theoretically. At the moment, the dipole scalar (spin-independent) polarizabilities of both the proton and the neutron are determined fairly well by various methods [1] as well as the forward and backward spin polarizabilities of the proton [2–4]. Recent measurements of double-polarized Compton scattering at the Mainz Microtron allowed one to extract also other proton spin polarizabilities [5,6].

There are also experimental results for some of the generalized (Q^2 -dependent) polarizabilities of the proton and the neutron [7–11].

From the theoretical side, a significant progress has been made using lattice simulations [12–18], i.e., by directly solving QCD in the nonperturbative regime on a discrete Euclidean space-time grid. However, one is not yet in the position to perform an accurate determination of the nucleon polarizabilities calculated on the lattice for physical pion masses.

Another systematic theoretical approach is provided by effective field theories, in particular, by chiral perturbation theory (χ PT), see Refs. [19,20] for pioneering studies of the

nucleon's electromagnetic polarizabilities in this framework. Chiral perturbation theory is an effective field theory of the standard model consistent with its symmetries and the ways they are broken. It allows one to expand hadronic observables in powers of the small parameter q defined as the ratio of the typical soft scales such as the pion mass M and external-particle 3-momenta $|\vec{p}|$ and the hard scale Λ_b of the order of the ρ -meson mass. The effective chiral Lagrangian is expanded in powers of derivatives and the pion mass. In the nucleon sector, an additional complication arises due to the presence of an extra mass scale, namely the nucleon mass, which can potentially break the power counting. One way to circumvent this problem is to perform the $1/m$ expansion on the level of the effective Lagrangian. This leads to the so-called heavy-baryon approach. The heavy-baryon scheme has been intensively used for the analysis of many hadronic reactions including the nucleon Compton scattering (and, therefore, nucleon polarizabilities); see, e.g., Refs. [21–24] and [21,25] for review articles. The heavy-baryon expansion is, however, known to violate certain analytic properties of the S -matrix [26], which may lead to a slower convergence of the chiral expansion. This feature has also been observed in the actual calculations of the nucleon polarizabilities.

An alternative approach to processes involving nucleons consists in keeping the covariant structure of the effective Lagrangian and absorbing the power-counting breaking terms by a redefinition of the lower order low-energy constants [26,27]. In this work, we adopt a version of the covariant approach known as the extended on-mass-shell renormalization scheme (EOMS) [27,28]. When necessary, we will slightly modify this scheme to enable a direct comparison to the heavy-baryon results (see, e.g., Ref. [29]).

Another obstacle for the rapid convergence of the chiral expansion in the single-nucleon systems is the presence of the $\Delta(1232)$ -resonance that is located close to the pion-nucleon threshold and is known to strongly couple to the pion-nucleon

*markus.thuermann@rub.de

†evgeny.epelbaum@rub.de

‡ashot.gasparyan@rub.de

§hermann.krebs@rub.de

channel. This introduces another small scale $\Delta \equiv m_\Delta - m \approx 2 M$, which leads to the appearance of terms of order $\mathcal{O}(M/\Delta)$ in the expansion of observables. A natural way to improve this situation is to include the Δ -isobar field explicitly into the effective Lagrangian. We follow here the so-called small-scale-expansion (SSE) scheme by treating the scale Δ on the same footing as M or $|\vec{p}|$ [30]. The universal expansion parameter is then called ϵ . For recent applications of this theoretical approach to various processes in the single-nucleon sector, see Refs. [31–34]. In this work, we compare the efficiency and convergence of both the Δ -full and Δ -less schemes by calculating various nucleon polarizabilities up to orders $\epsilon^3 + q^4$ and q^4 , respectively. Our analysis is particularly instructive since we calculate a set of higher-order polarizabilities, which do not depend on any free parameters. We also perform the $1/m$ expansion of our results to analyze the efficiency of the heavy baryon approach for the nucleon polarizabilities.

There is an alternative scheme for the chiral expansion in the presence of explicit Δ degree of freedom [35] called the δ -counting. The main difference from the small-scale expansion is a different power counting assignment for the Δ -nucleon mass difference Δ by assuming the hierarchy of scales $M \ll \Delta \ll \Lambda_b$. In such an approach, loop diagrams with several Δ -lines are suppressed in contrast with the calculations within the small-scale expansion, see Refs. [36–39] for recent applications. In Sec. IV, we will compare our results with the ones obtained within the δ -counting, mostly in Ref. [40], and discuss the importance of the additional contributions in the small-scale expansion.

As a stringent test of our scheme, we also compare our results with the fixed- t dispersion-relations analyses of Refs. [41–46]. This method is based solely on the principles of analyticity and unitarity¹ and therefore defines an important benchmark for theoretical approaches.

Our paper is organized as follows. The effective Lagrangian and the power counting relevant for the construction of the Compton scattering amplitude within χ PT as well as the renormalization of the low-energy constants (LECs) are given in Sec. II. In Sec. III, the formalism for the Compton scattering is described and the nucleon polarizabilities are introduced. The numerical results for the nucleon polarizabilities are presented in Sec. IV. We summarize our results in Sec. V. Appendices A–F collect the analytic expressions for the nucleon polarizabilities.

II. COMPTON SCATTERING IN CHIRAL PERTURBATION THEORY

A. Effective Lagrangian

The description of nucleon Compton scattering in χ PT relies on an effective Lagrangian. The effective Lagrangian relevant for the problem at hand to the order we are working

consists of the following terms:

$$\begin{aligned} \mathcal{L}_{\text{eff}} = & \mathcal{L}_{\pi\pi}^{(2)} + \mathcal{L}_{\pi\pi}^{(4)} + \mathcal{L}_{WZW}^{(4)} + \mathcal{L}_{\pi N}^{(1)} + \mathcal{L}_{\pi N}^{(2)} + \mathcal{L}_{\pi N}^{(3)} \\ & + \mathcal{L}_{\pi N}^{(4)} + \mathcal{L}_{\pi N\Delta}^{(1)} + \mathcal{L}_{\pi N\Delta}^{(2)} + \mathcal{L}_{\pi\Delta\Delta}^{(1)}, \end{aligned} \quad (1)$$

where \mathcal{L}_{WZW} stays for the Wess-Zumino-Witten term [49,50]. This Lagrangian is built in terms of the pion field through the SU(2) matrix $U = u^2 = 1 + \frac{i}{F} \vec{\tau} \cdot \vec{\pi} - \frac{1}{2F^2} \vec{\pi}^2 + \dots$ (F is the pion decay constant in the chiral limit), the nucleon field N and the Rarita-Schwinger-spinor Δ -field ψ_i^μ . The electromagnetic field A^μ enters via $v_\mu = -\frac{1}{2}(1 + \tau_3)eA_\mu$ ($e > 0$ is the proton charge).

Here, we list only the terms in the pion-nucleon Lagrangian [51] appearing in the course of calculating the nucleon polarizabilities:

$$\mathcal{L}_{\pi N}^{(1)} = \bar{N} \left(iD^\mu - m + \frac{g_A}{2} \not{\psi} \gamma_5 \right) N \quad (2)$$

$$\begin{aligned} \mathcal{L}_{\pi N}^{(2)} = & c_1 \bar{N} \langle \chi_+ \rangle N - \frac{c_2}{8m^2} (\bar{N} \langle u_\mu u_\nu \rangle D^{\mu\nu} N + \text{H.c.}) + \frac{c_3}{2} \langle uu \rangle \\ & + c_4 i \bar{N} [u_\mu, u_\nu] \sigma^{\mu\nu} N + \frac{c_6}{2m} \bar{N} F_{\mu\nu}^+ N \\ & + \frac{c_7}{2m} \bar{N} \langle F_{\mu\nu}^+ \rangle \sigma^{\mu\nu} N + \dots \end{aligned} \quad (3)$$

$$\begin{aligned} \mathcal{L}_{\pi N}^{(3)} = & \frac{d_6}{2m} [i(D^\mu, \tilde{F}_{\mu\nu}^+) D^\nu + \text{H.c.}] \\ & + \frac{d_7}{2m} [i(D^\mu, \langle F_{\mu\nu}^+ \rangle) D^\nu + \text{H.c.}] + \dots \end{aligned} \quad (4)$$

$$\begin{aligned} \mathcal{L}_{\pi N}^{(4)} = & \bar{N} \left\{ -\frac{e_{54}}{2} [D^\alpha, (D_\alpha, \langle F_{\mu\nu}^+ \rangle)] \sigma^{\mu\nu} \right. \\ & - \frac{e_{74}}{2} [D^\alpha (D_\alpha, \tilde{F}_{\mu\nu}^+)] \sigma^{\mu\nu} - \frac{e_{105}}{2} \langle F_{\mu\nu}^+ \rangle \langle \chi_+ \rangle \sigma^{\mu\nu} \\ & - \frac{e_{106}}{2} \tilde{F}_{\mu\nu}^+ \langle \chi_+ \rangle \sigma^{\mu\nu} + e_{89} \langle F_{\mu\nu}^+ \rangle \langle F^{+\mu\nu} \rangle \\ & + e_{91} \tilde{F}_{\mu\nu}^+ \langle F^{+\mu\nu} \rangle + e_{93} \langle \tilde{F}_{\mu\nu}^+ \tilde{F}^{+\mu\nu} \rangle \\ & \left. + \frac{e_{118}}{2} \langle F^{-\mu\nu} F_{\mu\nu}^- + F^{+\mu\nu} F_{\mu\nu}^+ \rangle \right\} N \\ & + \left[\bar{N} \left(-\frac{e_{90}}{4m^2} \langle F_{\alpha\mu}^+ \rangle \langle F_{\alpha\nu}^+ \rangle - \frac{e_{92}}{4m^2} \tilde{F}_{\alpha\mu}^+ \langle F_{\alpha\nu}^+ \rangle \right. \right. \\ & \left. \left. - \frac{e_{94}}{4m^2} \langle \tilde{F}_{\alpha\mu}^+ \tilde{F}_{\alpha\nu}^+ \rangle - \frac{e_{117}}{8m^2} \langle F_{\alpha\mu}^- F_{\alpha\nu}^- + F_{\alpha\mu}^+ F_{\alpha\nu}^+ \rangle \right) \right. \\ & \times \{D^\mu, D^\nu\} N + \text{H.c.} \left. \right], \end{aligned} \quad (5)$$

and the terms relevant for the $\mathcal{O}(\epsilon^3)$ calculations from the $\pi N\Delta$ and $\pi\Delta\Delta$ Lagrangians:

$$\begin{aligned} \mathcal{L}_{\pi N\Delta}^{(1)} &= \frac{h_A}{2} (\bar{\Psi}_i^\mu \langle \tau_i u_\mu \rangle N + \text{H.c.}), \\ \mathcal{L}_{\pi N\Delta}^{(2)} &= \frac{b_1}{4} (i \bar{\Psi}_i^\mu \langle \tau_i F_{\mu\alpha}^+ \rangle \gamma^\alpha \gamma_5 N + \text{H.c.}), \\ \mathcal{L}_{\pi\Delta\Delta}^{(1)} &= \bar{\Psi}_i^\mu \left[\frac{i}{4} \{[\gamma_\mu, \gamma_\nu], \gamma_\alpha\} D_{ij}^\alpha - \frac{m_\Delta}{2} (\gamma_\mu, \gamma_\nu) \delta_{ij} \right] \Psi_j^\nu. \end{aligned} \quad (6)$$

¹For the application of a scheme that combines effective field theory with dispersion-relations technique for the problem under consideration see Refs. [47,48].

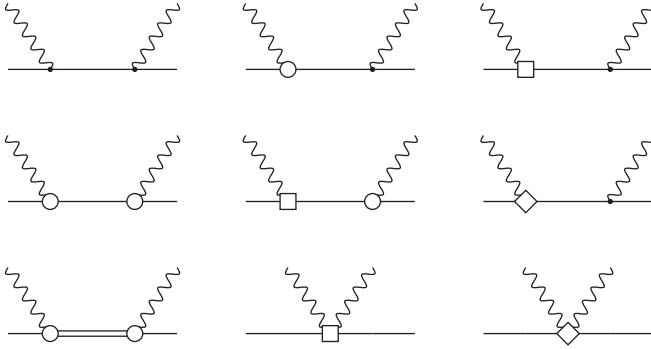


FIG. 1. Tree-level diagrams for nucleon Compton scattering which are taken into account in our analysis. Vertices of order $\mathcal{O}(q)$, $\mathcal{O}(q^2)$, $\mathcal{O}(q^3)$, and $\mathcal{O}(q^4)$ are denoted by dots, circles, squares and diamonds, respectively. Solid, wavy and double lines refer to nucleons, photons and Δ -isobars, respectively. Time-reversed and crossed diagrams as well as the diagrams with insertions of the nucleon self-energy contact terms are not shown.

The covariant derivatives and the chiral vielbein are defined as follows:

$$\begin{aligned} D_\mu &= \partial_\mu + \Gamma_\mu, & D_{ij}^\mu &= (\partial^\mu + \Gamma^\mu) \delta_{ij} - i\epsilon_{ijk}(\tau^k \Gamma^\mu), \\ \Gamma_\mu &= \frac{1}{2}[u^\dagger \partial_\mu u + u \partial_\mu u^\dagger - i(u^\dagger v_\mu u + u v_\mu u^\dagger)], \\ u_\mu &= i[u^\dagger \partial_\mu u - u \partial_\mu u^\dagger - i(u^\dagger v_\mu u - u v_\mu u^\dagger)], \end{aligned} \quad (7)$$

while the vector field strength tensors are given by

$$\begin{aligned} F_{\mu\nu}^\pm &= u v_{\mu\nu} u^\dagger \pm u^\dagger v_{\mu\nu} u, & \tilde{F}_{\mu\nu}^+ &= F_{\mu\nu}^+ - \frac{1}{2}\langle F_{\mu\nu}^+ \rangle, \\ v_{\mu\nu} &= \partial_\mu v_\nu - \partial_\nu v_\mu. \end{aligned} \quad (8)$$

Notice that the definition of b_1 differs from the one in Ref. [30] by a factor of m but is consistent with that of Ref. [31]. All redundant off-shell parameters in $\mathcal{L}_{\pi N\Delta}$ and $\mathcal{L}_{\pi\Delta\Delta}$ are set to zero (see the discussion in Refs. [52,53]). Notice further that we employ the isospin-symmetric limit throughout this work and set all particle masses to their averaged values.

For the remaining terms in Eq. (1) and further notations we refer the reader to Refs. [30,51,54,55].

B. Power counting

To calculate the nucleon Compton-scattering amplitude one needs to select the relevant Feynman diagrams according to their order D , which is determined by the power-counting formula [56]

$$D = 1 + 2L + \sum_n (2n - 2)V_{2n}^M + \sum_d (d - 1)V_d^B, \quad (9)$$

where L is the number of loops, V_{2n}^M is the number of vertices from $\mathcal{L}_{\pi\pi}^{(2n)}$ and V_d^B is the total number of vertices from $\mathcal{L}_{\pi N}^{(d)}$, $\mathcal{L}_{\pi N\Delta}^{(d)}$ and $\mathcal{L}_{\pi\Delta\Delta}^{(d)}$. Note that in the small-scale-expansion scheme, the nucleon and delta lines are counted on the same footing. In this work, we label purely nucleonic contributions (containing no Δ lines) as q^D and those involving Δ 's as ϵ^D .

The tree-level diagrams are shown in Fig. 1. Most of the nucleon pole diagrams do not contribute to the polarizabilities (as the Born terms are subtracted by definition, see Sec. III)

but are necessary for the renormalization of subdiagrams. Only the nucleon pole diagrams with the d_6 and d_7 vertices generate a small residual nonpole contribution to the generalized polarizabilities due to the specific form of the corresponding effective Lagrangian.

However, the Δ -pole graph provides a very important contribution to the nucleon polarizabilities. The pion t -channel exchange diagram with the anomalous $\pi^0\gamma\gamma$ coupling is not included in the definition of the polarizabilities either and is, therefore, not shown. Also not shown are the $\gamma N \rightarrow \gamma N$ contact terms from $\mathcal{L}_{\pi N}^{(4)}$.

Loop diagrams start to contribute at order $q^3(\epsilon^3)$. The corresponding sets of diagrams are shown in Fig. 2 for the q^3 -loops and in Fig. 3 for the ϵ^3 -loops. The subleading q^4 -loop diagrams are shown in Fig. 4.

C. Renormalization

The ultraviolet divergencies appearing in loop integrals are treated by means of dimensional regularization. Divergent parts of the integrals are canceled by the corresponding counter terms of the Lagrangian, and the resulting amplitude is expressed in terms of the finite quantities such as renormalized low-energy constants, physical masses and coupling constants. Due to the presence of an additional hard scale (the nucleon or Δ mass), baryonic loops contain power-counting-violating terms [57]. Since such terms are local, they can be absorbed by a redefinition of the low-energy constants of the effective Lagrangian. In this work, we adopt the extended on-mass-shell renormalization scheme (EOMS) [27] in a combination with on-shell renormalization conditions for the nucleon mass and magnetic moments.

For the nucleon mass and wave-function renormalization, we impose the on-shell conditions

$$\Sigma_N(m_N) = 0 \quad \text{and} \quad \Sigma'_N(m_N) = 0, \quad (10)$$

with $\Sigma_N(p)$ being the nucleon self-energy. By doing so, we fix the bare nucleon mass m and the field normalization factor Z_N . The explicit formulas relating the physical and bare parameters can be found in Ref. [32]. In what follows, we will denote the physical nucleon mass by m , which will not lead to a confusion since the bare nucleon mass will not be discussed anymore.

In a complete analogy with the nucleon field, we renormalize the Δ field. However, at the order we are working there are no loop corrections to the Δ self-energy. For the calculation of the static nucleon polarizabilities, we use the real Breit-Wigner mass of the Δ . The precise value of the renormalized Δ mass is irrelevant under the kinematic conditions considered. However, for calculation of the dynamical nucleon polarizabilities, to be able to describe the Δ region, we implement the complex-mass scheme [58,59] for the Δ resonance and use the complex Δ pole mass taking the resonance width into account explicitly.

For the renormalized constants \bar{c}_6 and \bar{c}_7 , we use the on-shell condition for the nucleon magnetic moments:

$$\bar{c}_6 = \kappa_p - \kappa_n \quad \text{and} \quad \bar{c}_7 = \kappa_n. \quad (11)$$

The explicit relation between \bar{c}_6 and \bar{c}_7 and the bare constants c_6 and c_7 is given in Appendix E.

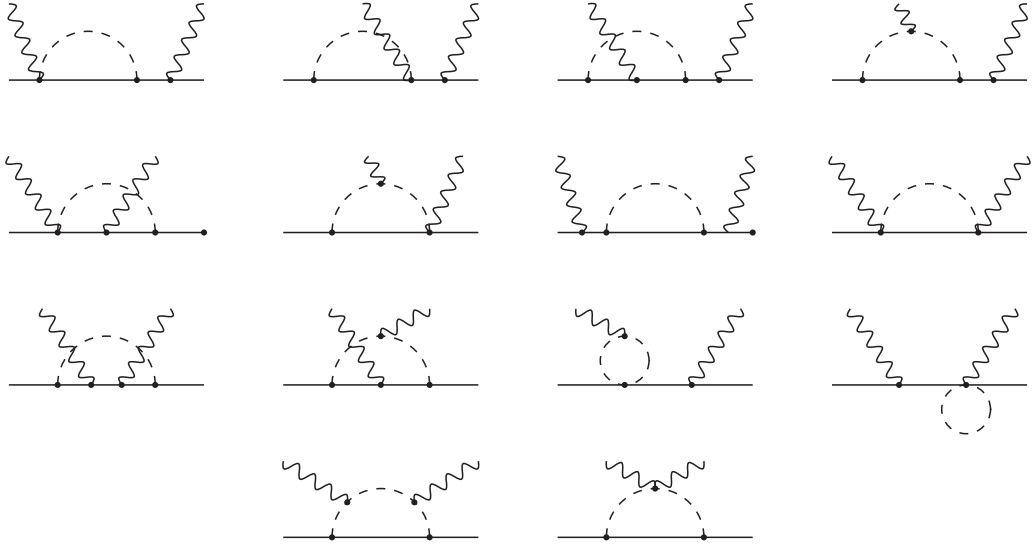


FIG. 2. $\mathcal{O}(q^3)$ loop diagrams for nucleon Compton scattering. Dashed lines refer to pions. All vertices are from the leading order Lagrangians $\mathcal{L}_{\pi\pi}^{(2)}$ and $\mathcal{L}_{\pi N}^{(1)}$. Time-reversed and crossed diagrams are not shown.

For the remaining low-energy constants ξ_i we employ the EOMS renormalization scheme. The renormalized LECs $\bar{\xi}_i$ are related to the bare quantities as follows:

$$\xi_i = \bar{\xi}_i - \frac{\beta_{\xi_i}}{F^2} \frac{A_0(M^2)}{2M^2} + \frac{\Delta_{\xi_i}}{16\pi^2 F^2},$$

$$\xi_i \in \{d_6, d_7, e_{54}, e_{74}, e_{89}, e_{89}, e_{90}, e_{91}, e_{92}, e_{93}, e_{94}, e_{117}, e_{118}\}, \quad (12)$$

with the β functions:

$$\begin{aligned} \beta_{d_6} &= -\frac{1-g_A^2}{6} + \frac{40h_A}{81}, & \beta_{d_7} &= \frac{5h_A^2}{54}, \\ \beta_{e_{54}} &= 0, & \beta_{e_{74}} &= \frac{1-g_A^2+4c_4}{12m}, \\ \beta_{e_{91}} &= \beta_{e_{92}} = 0, & 2\beta_{e_{89}} + \beta_{e_{93}} + \beta_{e_{118}} &= \frac{c_2}{12}, \\ 2\beta_{e_{90}} + \beta_{e_{94}} + \beta_{e_{117}} &= -\frac{c_2}{3}, \end{aligned} \quad (13)$$

and the finite shifts

$$\Delta_{d_6} = -\frac{g_A^2 c_6}{8}, \quad \Delta_{d_7} = \frac{3g_A^2(c_6 + 2c_7)}{16}. \quad (14)$$

The constants e_i do not receive finite shifts due to the power-counting violation because we do not consider loop diagrams of order higher than $\mathcal{O}(q^4)$. The finite shifts for d_6 and d_7 reproduce those obtained in Ref. [60] (note a different definition of the LECs). The constants e_{54} and e_{74} do not contribute to the nucleon polarizabilities after subtracting the Born terms. Nevertheless, we provide the corresponding β functions for completeness. The LECs $e_{89}, e_{90}, e_{93}, e_{94}, e_{117}, e_{118}$ enter the nucleon Compton scattering amplitude only in the linear combinations $2e_{89} + e_{93} + e_{118}$ and $2e_{90} + e_{94} + e_{117}$, for which the β functions are given in Eq. (13).

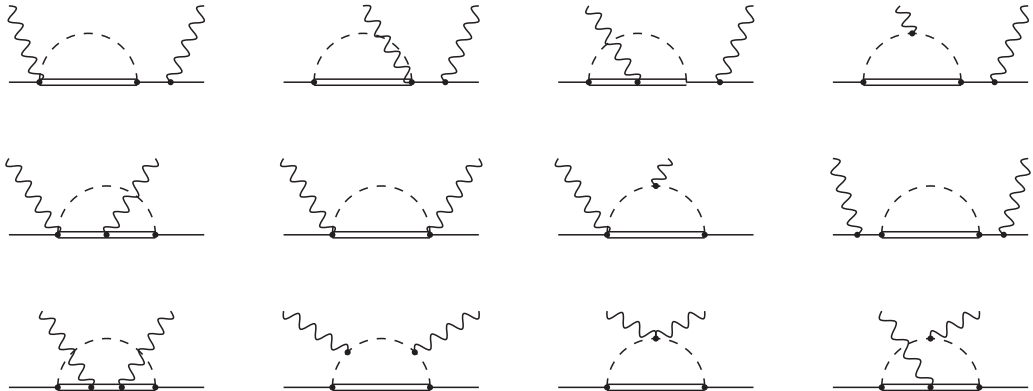


FIG. 3. $\mathcal{O}(\epsilon^3)$ loop diagrams for nucleon Compton scattering. All vertices are from the leading order Lagrangians $\mathcal{L}_{\pi\pi}^{(2)}, \mathcal{L}_{\pi N}^{(1)}, \mathcal{L}_{\pi N\Delta}^{(1)}$, and $\mathcal{L}_{\pi\Delta\Delta}^{(1)}$. Double lines denote the Δ . Time-reversed and crossed diagrams are not shown.

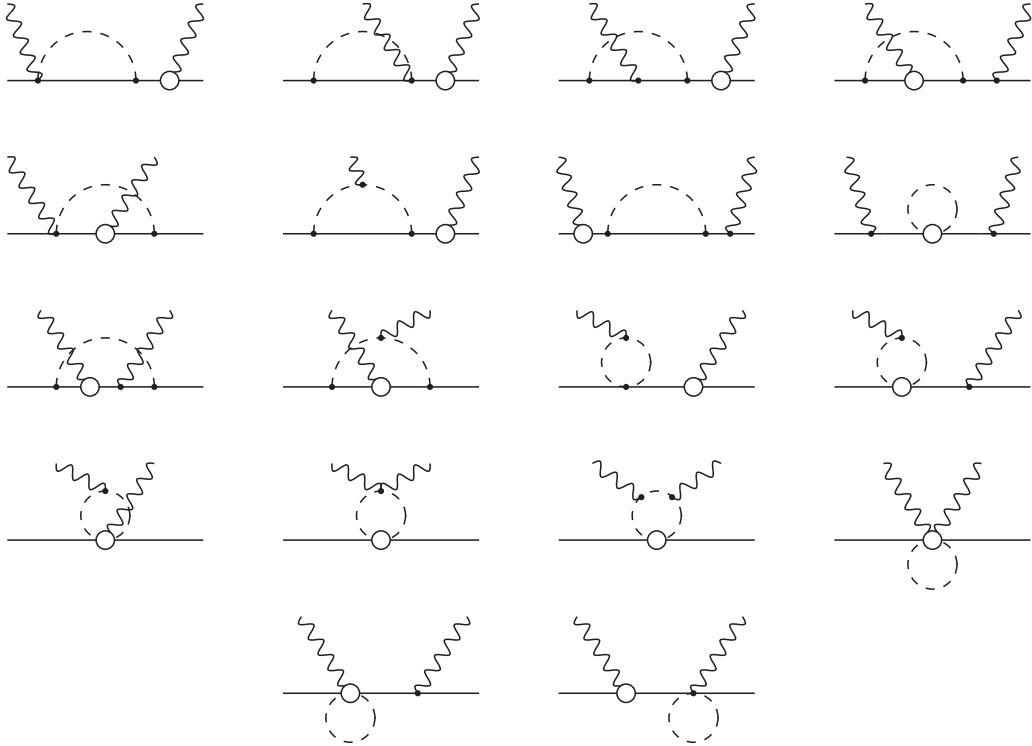


FIG. 4. $\mathcal{O}(q^4)$ loop diagrams for nucleon Compton scattering. Dots denote the leading order vertices and circles denote the vertices from $\mathcal{L}_{\pi N}^{(2)}$. Time-reversed and crossed diagrams are not shown.

The pion tadpole function in $d \approx 4$ dimensions is equal to [see Eq. (F1)]

$$A_0(M) = -2M^2 \left[\bar{\lambda} + \frac{1}{32\pi^2} \ln \left(\frac{M^2}{\mu^2} \right) \right],$$

$$\bar{\lambda} = \frac{1}{16\pi^2} \left\{ \frac{1}{d-4} + \frac{1}{2} [\gamma_E - \ln(4\pi) - 1] \right\}. \quad (15)$$

Here, γ_E is the Euler-Mascheroni constant and μ is the renormalization scale. The divergencies remaining after the renormalization of the LECs are treated in the MS [27,54] scheme, i.e., we set $\bar{\lambda} = 0$. We have checked that the residual renormalization scale dependence of the amplitude is of a higher order than we are working.

In what follows, we will omit the bars over the renormalized LECs.

III. FORMALISM

We consider nucleon Compton scattering $\gamma N \rightarrow \gamma N$ with the momenta of the initial (final) proton and photon denoted as p (p') and q (q'), respectively. We study the cases of real Compton scattering with $q^2 = q'^2 = 0$ and of double virtual Compton scattering with $Q^2 = -q^2 = -q'^2$.

To calculate the static nucleon polarizabilities, it is advantageous to work in the Breit frame from the point of view of fulfillment of the crossing symmetry constraints, see Ref. [40] for an extensive discussion. We decompose the scattering amplitude $T(q^2, z, \omega)$ in the Breit frame, where ω refers to the photon energy and $z \equiv \cos \theta$ with θ being the scattering

angle, in terms of twelve functions A_i :

$$T(q^2, z, \omega) = 2m \sum_{i=1}^{12} A_i(q^2, z, \omega) \chi_i, \quad (16)$$

with

$$\begin{aligned} \chi_1 &= \vec{\epsilon} \cdot \vec{\epsilon}^*, \\ \chi_2 &= (\hat{q} \times \vec{\epsilon}) \cdot (\hat{q}' \times \vec{\epsilon}'), \\ \chi_3 &= \hat{q} \cdot \vec{\epsilon} \hat{q} \cdot \vec{\epsilon}'^* + \hat{q}' \cdot \vec{\epsilon} \hat{q}' \cdot \vec{\epsilon}'^*, \\ \chi_4 &= \hat{q} \cdot \vec{\epsilon} \hat{q}' \cdot \vec{\epsilon}'^*, \\ \chi_5 &= i\vec{\sigma} \cdot \vec{\epsilon} \times \vec{\epsilon}'^*, \\ \chi_6 &= i\vec{\sigma} \cdot (\hat{q} \times \vec{\epsilon}) \times (\hat{q}' \times \vec{\epsilon}'), \\ \chi_7 &= i(\hat{q} \cdot \vec{\epsilon} \times \vec{\epsilon}'^* \vec{\sigma} \cdot \hat{q} + \hat{q}' \cdot \vec{\epsilon} \times \vec{\epsilon}'^* \vec{\sigma} \cdot \hat{q}'), \\ \chi_8 &= i(\hat{q} \cdot \vec{\epsilon} \times \vec{\epsilon}'^* \vec{\sigma} \cdot \hat{q}' + \hat{q}' \cdot \vec{\epsilon} \times \vec{\epsilon}'^* \vec{\sigma} \cdot \hat{q}), \\ \chi_9 &= i\hat{q} \cdot \vec{\epsilon} \hat{q}' \cdot \vec{\epsilon}'^* \vec{\sigma} \cdot \hat{q} \times \hat{q}', \\ \chi_{10} &= i(\hat{q} \cdot \vec{\epsilon} \hat{q} \cdot \vec{\epsilon}'^* \vec{\sigma} \cdot \hat{q} \times \hat{q}' + \hat{q}' \cdot \vec{\epsilon} \hat{q}' \cdot \vec{\epsilon}'^* \vec{\sigma} \cdot \hat{q} \times \hat{q}'), \\ \chi_{11} &= i(\hat{q}' \cdot \vec{\epsilon}'^* \vec{\sigma} \cdot \vec{\epsilon} \times \hat{q} - \hat{q} \cdot \vec{\epsilon} \vec{\sigma} \cdot \vec{\epsilon}'^* \times \hat{q}'), \\ \chi_{12} &= i(\hat{q}' \cdot \vec{\epsilon}'^* \vec{\sigma} \cdot \vec{\epsilon} \times \hat{q}' - \hat{q} \cdot \vec{\epsilon} \vec{\sigma} \cdot \vec{\epsilon}'^* \times \hat{q}), \end{aligned} \quad (17)$$

where \hat{q} (\hat{q}') is the unit 3-vector of the incoming (outgoing) photon. The initial (final) photon polarization vector ϵ_μ (ϵ'_μ) is defined in the Coulomb gauge ($\epsilon_0 = \epsilon'_0 = 0$). The amplitude Eq. (16) is supposed to be sandwiched between the Pauli spinors of the initial and final nucleon.

Given the presence of the Pauli matrices $\vec{\sigma}$ in Eq. (17), one can see that there are four spin-independent structures

$\chi_1 - \chi_4$ and eight spin-dependent structures $\chi_5 - \chi_{12}$. All χ_i obey crossing-invariance. For real Compton scattering, only $\chi_1, \chi_2, \chi_5, \chi_6, \chi_7, \chi_8$ survive.

The Born terms have to be subtracted from the amplitude as explained, e.g., in Ref. [61] to exclude the contributions with unexcited nucleons in the intermediate state. This procedure essentially reduces to subtracting the tree-level $Q^2 = 0$ nucleon-pole diagrams with the nucleon charge and magnetic moments replaced by the full Dirac and Pauli form factors calculated consistently within our scheme applying the same power counting. The anomalous pion t -channel exchange

diagram is also excluded from the definition of the polarizabilities.

The nucleon polarizabilities measure the response of the nucleon to an external electromagnetic field and correspond to the low-energy constants of the effective Hamiltonian quadratic in electric and magnetic fields, see Refs. [41,42]. Here, we provide the resulting expressions for the expansion of the amplitudes A_i in ω around $\omega = 0$ in terms of the nucleon polarizabilities (the dependence of the amplitudes A_i and polarizabilities on Q^2 is suppressed):

$$\begin{aligned} A_1(\omega) &= \frac{4\pi E_N}{m} \left\{ \alpha_{E1}\omega^2 + \frac{\omega^4}{12}(2z\alpha_{E2} - \beta_{M2} + 12\alpha_{E1\nu}) + \frac{\omega^6}{2700}[(30z^2 - 2)\alpha_{E3} - 20z\beta_{M3} \right. \\ &\quad \left. + 450z\alpha_{E2\nu} - 225\beta_{M2\nu} + 2700\alpha_{E1\nu^2}] + \mathcal{O}(\omega^8) \right\}, \\ A_2(\omega) &= \frac{4\pi E_N}{m} \left\{ \beta_{M1}\omega^2 + \frac{\omega^4}{12}(2z\beta_{M2} - \alpha_{E2} + 12\beta_{M1\nu}) + \frac{\omega^6}{2700}[(30z^2 - 2)\beta_{M3} - 20z\alpha_{E3} \right. \\ &\quad \left. + 450z\beta_{M2\nu} - 225\alpha_{E2\nu} + 2700\beta_{M1\nu^2}] + \mathcal{O}(\omega^8) \right\}, \\ A_5(\omega) &= \frac{4\pi E_N}{m} \left[(\gamma_{E1E1} - \gamma_{E1M2})\omega^3 + \frac{\omega^5}{5}(20z\gamma_{E2E2} + 5\gamma_{E1E1\nu} - 10z\gamma_{E2M3} \right. \\ &\quad \left. - 5\gamma_{E1M2\nu} + 2\gamma_{M2E3} + 5\gamma_{M2M2}) + \mathcal{O}(\omega^7) \right], \\ A_6(\omega) &= \frac{4\pi E_N}{m} \left[(\gamma_{M1M1} - \gamma_{M1E2})\omega^3 + \frac{\omega^5}{5}(20z\gamma_{M2M2} + 5\gamma_{M1M1\nu} - 10z\gamma_{M2E3} \right. \\ &\quad \left. - 5\gamma_{M1E2\nu} + 2\gamma_{E2M3} + 5\gamma_{E2E2}) + \mathcal{O}(\omega^7) \right], \\ A_7(\omega) &= \frac{4\pi E_N}{m} \left[\gamma_{E1M2}\omega^3 + \frac{\omega^5}{5}(15z\gamma_{E2M3} + 5\gamma_{E1M2\nu} - 7\gamma_{M2E3} - 10\gamma_{M2M2}) + \mathcal{O}(\omega^7) \right], \\ A_8(\omega) &= \frac{4\pi E_N}{m} \left[\gamma_{M1E2}\omega^3 + \frac{\omega^5}{5}(15z\gamma_{M2E3} + 5\gamma_{M1E2\nu} - 7\gamma_{E2M3} - 10\gamma_{E2E2}) + \mathcal{O}(\omega^7) \right], \end{aligned} \quad (18)$$

where E_N is the nucleon energy. We also introduce the linear combinations corresponding to the forward and backward spin polarizabilities γ_0 and γ_π ,

$$\begin{aligned} \gamma_0 &= -\gamma_{E1E1} - \gamma_{M1M1} - \gamma_{E1M2} - \gamma_{M1E2}, \\ \gamma_\pi &= -\gamma_{E1E1} + \gamma_{M1M1} - \gamma_{E1M2} + \gamma_{M1E2}, \end{aligned} \quad (19)$$

the higher-order forward spin polarizability,

$$\begin{aligned} \bar{\gamma}_0 &= -\gamma_{E1E1\nu} - \gamma_{M1M1\nu} - \gamma_{M1E2\nu} - \gamma_{E1M2\nu} \\ &\quad - \gamma_{E2E2} - \gamma_{M2M2} - \frac{8}{5}(\gamma_{E2M3} + \gamma_{M2E3}), \end{aligned} \quad (20)$$

as well as the longitudinal-transverse spin polarizability,

$$\delta_{LT} = -\frac{1}{6} \frac{d^3}{d\omega^3} \left\{ \frac{m}{4\pi E_N} [A_5(\omega) + A_{11}(\omega) + A_{12}(\omega)] \right\}_{\omega=0}. \quad (21)$$

There are similar but different amplitude decompositions used in the literature, which leads to different relations of those amplitudes to the nucleon polarizabilities. For ease of comparison, we provide the transformation matrix from the vector of amplitudes $A_{\text{this work}} = (A_1, A_2, A_5, A_6, A_7, A_8)$ defined in Eq. (17) to the vector of amplitudes $A_{\text{LMP}} = (A_1, A_2, A_3, A_4, A_5, A_6)$ considered in Ref. [40]:

$$A_{\text{LMP}} = L A_{\text{this work}}, \quad L = \begin{pmatrix} 1 & z & 0 & 0 & 0 & 0 \\ 0 & -1 & 0 & 0 & 0 & 0 \\ 0 & 0 & -1 & -z & -2 & -2z \\ 0 & 0 & 0 & -1 & 0 & 0 \\ 0 & 0 & 0 & 1 & 0 & 1 \\ 0 & 0 & 0 & 0 & 1 & 0 \end{pmatrix}. \quad (22)$$

In this work, we also analyze the so-called dynamical polarizabilities defined in terms of the center-of-mass multipoles

TABLE I. Parameters used in the current work. The values of α_{EM} , M , m , m_Δ , g_A , F_π are taken from Ref. [1]. The LECs c_6 and c_7 are related to the proton and neutron magnetic moment and d_6 and d_6 with the proton and neutron charge radii [60]. The values of the LECs b_1 and h_A are extracted from the electromagnetic and strong width of the Δ -resonance, respectively, see Ref. [31] for details and explicit expressions. For the static polarizabilities we use the real Δ mass as given in the Table, whereas for the generalized polarizabilities we use the pole mass $m_\Delta = (1210 - 50i)$ MeV.

α_{EM}^{-1}	M (MeV)	F_π (MeV)	m (MeV)	m_Δ (MeV)	g_A	c_6	c_7	h_A	b_1 [m^{-1}]
137.036	138.04	92.21	938.9	1232	1.27	3.706	-1.913	1.43	-4.98

as follows (see, e.g., Refs. [40,45,62,63]):

$$\begin{aligned}\alpha_{E1}(\omega) &= l^2(2l-1)!! \frac{(l+1)f_{EE}^{l+} + lf_{EE}^{l-}}{\omega^{2l}}, \\ \beta_{M1}(\omega) &= l^2(2l-1)!! \frac{(l+1)f_{MM}^{l+} + lf_{MM}^{l-}}{\omega^{2l}}, \\ \gamma_{E1/E1}(\omega) &= \frac{f_{EE}^{l+} - f_{EE}^{l-}}{\omega^{2l+1}}, \quad \gamma_{E1/M1\pm 1}(\omega) = (2l \pm 1)! \frac{f_{EM}^{l\pm}}{\omega^{2l\pm 1}}, \\ \gamma_{M1/M1}(\omega) &= \frac{f_{MM}^{l+} - f_{MM}^{l-}}{\omega^{2l+1}}, \quad \gamma_{M1/E1\pm 1}(\omega) = (2l \pm 1)! \frac{f_{ME}^{l\pm}}{\omega^{2l\pm 1}},\end{aligned}\quad (23)$$

for $l = 1, 2$. Note that in contrast to the equations above, in Eq. (23), ω denotes the center-of-mass photon energy.

IV. RESULTS

We are now in the position to present our numerical results for various proton and neutron polarizabilities calculated up to order $\mathcal{O}(\epsilon^3 + q^4)$. Specifically, we consider the following polarizabilities: spin-independent (scalar) dipole, quadrupole, octupole, dispersive dipole, and quadrupole polarizabilities as well as dipole, quadrupole and dispersive dipole spin polarizabilities. We also discuss selected generalized (i.e., Q^2 -dependent) and dynamical (i.e., energy-dependent) polarizabilities.

As already mentioned above, most of the results we present are pure predictions and contain no free parameters. The only exceptions are the spin-independent dipole polarizabilities α_{E1} and β_{M1} at order $\mathcal{O}(q^4)$ or $\mathcal{O}(\epsilon^3 + q^4)$, which are fitted to the experimental values. All remaining parameters are taken from other processes and are collected in Tables I, II, and III.

In the course of the calculation we have used our own code written in *Mathematica* [65] and FORM [66] for the analytical calculation of Feynman diagrams. The numerical evaluation of loop integrals have been performed with help of the *Mathematica* package *Package-X* [67]. We have also used our own Fortran code for estimating the theoretical errors.

For our complete results at order $\mathcal{O}(\epsilon^3 + q^4)$, we also provide estimations of the theoretical errors originating from two sources, namely the uncertainties in the input parameters and the errors caused by the truncation of the small-scale expansion. For the latter uncertainty, we adopt the Bayesian model used in Refs. [68,69] based on the ideas developed in Refs. [70–72]; see Ref. [34] for a recent application to radiative pion photoproduction. The observables are assumed to be expanded in parameter Q given by

$$Q = \max\left(\frac{M^{\text{eff}}}{\Lambda_b}, \frac{\sqrt{Q^2}}{\Lambda_b}, \frac{\omega}{\Lambda_b}\right), \quad (24)$$

where Q^2 on the right-hand side is the virtuality of the photon, and ω is the photon energy in the case of dynamical polarizabilities. The soft and hard scales are chosen to be $M^{\text{eff}} = 200$ MeV and $\Lambda_b = 700$ MeV in accordance with Ref. [73]. Following Refs. [68,69], we utilize the Gaussian prior distribution for the expansion coefficients c_i :

$$\begin{aligned}\text{pr}(c_i | \bar{c}) &= \frac{1}{\sqrt{2\pi}\bar{c}} e^{-c_i^2/(2\bar{c}^2)}, \\ \text{pr}(\bar{c}) &= \frac{1}{\ln(\bar{c}_>/\bar{c}_<)} \frac{1}{\bar{c}} \theta(\bar{c} - \bar{c}_<) \theta(\bar{c}_> - \bar{c}),\end{aligned}\quad (25)$$

with the cut offs $\bar{c}_< = 0.5$ and $\bar{c}_> = 10$. Further details on the employed Bayesian model can be found in Refs. [68,69].

In the following sections, we provide a detailed comparison of our results with the available experimental/empirical data as well as with other theoretical approaches based on chiral perturbation theory and on fixed- t dispersion relations. We also discuss generalized polarizabilities, investigate the convergence pattern of the $1/m$ -expansion for the calculated polarizabilities and compare the results of covariant χ PT with the heavy baryon approach. Last but not least, we emphasize that the resulting large absolute numerical values of the octupole polarizabilities are merely due to the numerical factors in their definition, which makes them consistent with the definition of polarizabilities for composite systems.

TABLE II. Numerical values of the low-energy constants used in the current work as determined by matching the solution of Roy-Steiner equations for πN scattering [64] to chiral perturbation theory in Ref. [33]. The values for $q^4 + \epsilon^3$ correspond to the ϵ^3 calculation of Ref. [33].

	q^3	q^4	ϵ^3	$q^4 + \epsilon^3$
c_1 [m^{-1}]	-0.94 ± 0.02	-1.05 ± 0.03	-1.05 ± 0.03	-1.05 ± 0.03
c_2 [m^{-1}]	2.39 ± 0.03	3.15 ± 0.03	0.96 ± 0.11	0.96 ± 0.11
c_3 [m^{-1}]	-4.60 ± 0.05	-5.35 ± 0.06	-2.13 ± 0.19	-2.13 ± 0.19

TABLE III. Numerical values of the low-energy constants obtained from the fit to the empirical values of the electric radius of the proton and neutron (d_i) and the proton and neutron spin-independent polarizabilities (e_i). Note that the e_i enter at fourth order and therefore do not have values for q^3 and ϵ^3 .

	q^3	q^4	ϵ^3	$q^4 + \epsilon^3$
$d_6 [m^{-2}]$	-0.61 [60]	-0.61 [60]	-0.80 ± 0.04	-1.27 ± 0.05
$d_7 [m^{-2}]$	-0.43 [60]	-0.44 [60]	-0.44 ± 0.01	-0.46 ± 0.01
$e_{91} [m^{-3}]$...	-0.04 ± 0.22	...	-0.46 ± 0.23
$e_{92} [m^{-3}]$...	-0.29 ± 0.79	...	-0.22 ± 0.80
$(2e_{89} + e_{93} + e_{118}) [m^{-3}]$...	-0.07 ± 0.23	...	-2.53 ± 0.50
$(2e_{90} + e_{94} + e_{117}) [m^{-3}]$...	-1.76 ± 0.80	...	2.02 ± 1.20

A. Scalar dipole polarizabilities

We start by considering the spin-independent dipole nucleon polarizabilities α_{E1} and β_{M1} . The results of the calculations at order $\mathcal{O}(q^4)$ and $\mathcal{O}(\epsilon^3 + q^4)$ as well as the individual contributions from orders $\mathcal{O}(q^3)$, $\mathcal{O}(q^4)$ pion-nucleon loops, $\mathcal{O}(\epsilon^3) \pi\Delta$ -loops and tree-level Δ -pole graphs are presented in Table IV. At order $\mathcal{O}(q^4)$, there appear low-energy constants in the effective Lagrangian that contribute to the nucleon Compton scattering. We adjust four relevant linear combinations of them (e_{91} , e_{92} , $2e_{89} + e_{93} + e_{118}$, and $2e_{90} + e_{94} + e_{117}$) in such a way as to reproduce the empirical values of the proton and neutron spin-independent dipole polarizabilities, see Table III.

In the case of the Δ -less theory, the contribution at order $\mathcal{O}(q^4)$ for the electric polarizability α_{E1} of the proton (neutron) is about two (five) times smaller than the one at order $\mathcal{O}(q^3)$, which is an indication of a reasonable convergence of the chiral expansion. For the magnetic polarizabilities β_{M1} ,

due to some cancellations among $\mathcal{O}(q^3)$ loops, the contributions at order $\mathcal{O}(q^4)$ are larger than the ones at order $\mathcal{O}(q^3)$ but are, nevertheless, comparable with those for the α_{E1} .

In the Δ -full scheme, the $\mathcal{O}(q^4)$ terms (that differ from the ones in the Δ -less case by the values of c_i 's and e_i 's) are significantly larger. This feature can be traced back to the sizable $\mathcal{O}(\epsilon^3)$ contributions, especially from the Δ -pole tree-level diagrams, that need to be compensated by adjusting the relevant contact terms. Such contributions appear to be demoted to higher orders in the Δ -less scheme. Their importance for other polarizabilities will, however, be demonstrated below. Thus, a seemingly better convergence of the Δ -less approach for the dipole polarizabilities can be argued to be accidental. Notice further that the convergence issues are not really relevant for the dipole spin-independent polarizabilities at the order we are working due to the presence of the corresponding compensating contact terms in the Lagrangian.

TABLE IV. Numerical values for the spin-independent dipole polarizabilities of the proton and the neutron in 10^{-4} fm^3 . The values are compared with the results calculated within the δ -counting scheme and obtained using fixed- t dispersion relations.

	Proton		Neutron	
	α_{E1}	β_{M1}	α_{E1}	β_{M1}
q^3 (without Δ)	7.04	-1.85	9.51	-1.10
q^4 (without Δ)	4.16	4.35	2.09	4.80
Total (without Δ)	11.2	2.5	11.6	3.7
q^3	7.04	-1.85	9.51	-1.10
$\epsilon^3 \pi\Delta$ loop	-1.45	5.54	2.78	0.96
ϵ^3 tree	-3.78	11.96	-3.78	11.96
q^4	9.40	-13.16	3.10	-8.12
Total	11.2	2.5	11.6	3.7
$\mathcal{O}(p^3) \pi N$ loops ^a [40]	6.8	-1.8	9.4	-1.1
$\mathcal{O}(p^{7/2}) \pi\Delta$ loops [40]	4.4	-1.4	4.4	-1.4
Δ pole [40]	-0.1	7.1	-0.1	7.1
Total [40]	11.2 ± 0.7	3.9 ± 0.7	13.7 ± 3.1	4.6 ± 2.7
Fixed- t DR [41,43]	12.1	1.6	12.5	2.7
HB χ PT fit [74]	10.65 ± 0.50	3.15 ± 0.50	11.55 ± 1.5	3.65 ± 1.5
B χ PT fit [75]	10.6 ± 0.5	3.2 ± 0.5
PDG [1]	11.2 ± 0.4	2.5 ± 0.4	11.6 ± 1.5	3.7 ± 2.0

^aThe small discrepancy between Ref. [40] and this paper for the πN loops at order q^3 originates mostly from the difference in the pion masses: we use the isospin-averaged value, whereas in Ref. [40] the charged pion mass is employed. This is a more natural choice if only the leading πN loops are taken into account.

TABLE V. Numerical values for the dipole spin polarizabilities of the proton (upper table) and the neutron (lower table) in 10^{-4} fm^4 . The upper errors originate from the uncertainty in the input parameters, the lower errors come from the truncation of the small-scale expansion. The values are compared with the results calculated within the δ -counting scheme and obtained using fixed- t dispersion relations.

	$\gamma_{\text{EIEI}}^{(p)}$	$\gamma_{\text{MIMI}}^{(p)}$	$\gamma_{\text{EIM2}}^{(p)}$	$\gamma_{\text{MIE2}}^{(p)}$
q^3 (without Δ)	-3.46	-0.13	0.57	0.95
q^4 (without Δ)	-0.01	0.49	-0.25	0.56
Total (without Δ)	-3.5	0.4	0.32	1.5
q^3	-3.46	-0.13	0.57	0.95
$\epsilon^3 \pi \Delta$ loops	-0.11	0.58	0.48	-0.79
$\epsilon^3 \Delta$ tree	-1.07	3.85	-0.88	1.74
q^4	-0.01	0.49	-0.25	0.56
Total	-4.7 ± 0.1	4.8 ± 0.4	-0.08 ± 0.11	2.5 ± 0.3
$\mathcal{O}(p^3) \pi N$ loops [40]	-3.4	-0.1	0.5	0.9
$\mathcal{O}(p^{7/2}) \pi \Delta$ loops [40]	0.4	-0.2	0.1	-0.2
Δ pole [40]	-0.4	3.3	-0.4	0.4
Total [40]	-3.3 ± 0.8	2.9 ± 1.5	0.2 ± 0.2	1.1 ± 0.3
Fixed- t DR [41]	-3.4	2.7	0.3	1.9
Fixed- t DR [42,45,46]	-4.3	2.9	-0.02	2.2
HB χ PT [74,78]	-1.1 ± 1.9	2.2 ± 0.8	-0.4 ± 0.6	1.9 ± 0.5
MAMI 2015 [5]	-3.5 ± 1.2	3.16 ± 0.85	-0.7 ± 1.2	1.99 ± 0.29
MAMI 2018 [6]	-3.18 ± 0.52	2.98 ± 0.43	-0.44 ± 0.67	1.58 ± 0.43
	$\gamma_{\text{EIEI}}^{(n)}$	$\gamma_{\text{MIMI}}^{(n)}$	$\gamma_{\text{EIM2}}^{(n)}$	$\gamma_{\text{MIE2}}^{(n)}$
q^3 (without Δ)	-4.86	-0.17	0.61	1.36
q^4 (without Δ)	-0.46	1.42	-0.59	0.76
Total (without Δ)	-5.3	1.3	0.0	2.1
q^3	-4.86	-0.17	0.61	1.36
$\epsilon^3 \pi \Delta$ loops	0.22	0.12	0.11	-0.27
$\epsilon^3 \Delta$ tree	-1.07	3.85	-0.88	1.74
q^4	-0.46	1.42	-0.59	0.76
Total	-6.2 ± 0.1	5.2 ± 0.4	-0.8 ± 0.1	3.6 ± 0.2
$\mathcal{O}(p^3) \pi N$ loops [40]	-4.7	-0.2	0.6	1.3
$\mathcal{O}(p^{7/2}) \pi \Delta$ loops [40]	0.4	-0.2	0.1	-0.2
Δ pole [40]	-0.4	3.3	-0.4	0.4
Total [40]	-4.7 ± 1.1	2.9 ± 1.5	0.2 ± 0.2	1.6 ± 0.4
Fixed- t DR [41]	-5.6	3.8	-0.7	2.9
Fixed- t DR [40,44,45]	-5.9	3.8	-0.9	3.1
HB χ PT [74,78]	-4.0 ± 1.9	1.3 ± 0.8	-0.1 ± 0.6	2.4 ± 0.5

In Table IV, we also provide for comparison the values for the dipole spin-independent polarizabilities obtained by analyzing experimental data using fixed- t dispersion relations [41,43], and by fitting experimental data employing various versions of the δ -counting schemes (with the loop diagrams calculated utilizing the covariant [75] or heavy-baryon approach [74]). It is particularly instructive to compare our results with [40], where the individual contributions calculated within the δ -counting scheme are presented. Such a comparison allows one to analyze the importance of the explicit Δ degrees of freedom and the sensitivity of the results to employed counting schemes for the Δ -nucleon mass difference. There are two main sources of differences between our approach and the one used in Ref. [40] (apart from slightly different numerical values of the coupling constants). First, different terms in the effective Lagrangian corresponding to the $\gamma N \Delta$ vertex are used. The $\gamma N \Delta$ Lagrangian of Ref. [40]

contains two terms with the so-called magnetic and electric $\gamma N \Delta$ -couplings g_M and g_E :

$$\mathcal{L}_{\gamma N \Delta} = \frac{3e}{2m(m_\Delta + m)} \bar{N} T_3^\dagger (ig_M \tilde{F}^{\mu\nu} - g_E \gamma_5 F^{\mu\nu}) \partial_\mu \Delta_\nu + \text{H.c.}, \quad (26)$$

which in our scheme correspond to the b_1 - and h_1 -terms (the contribution from the h_1 -term is of a higher order in our power counting and does not appear in the current calculations). The two prescriptions are identical when both the nucleon and the Delta are on the mass shell. Otherwise, the difference is compensated by local contact terms of a higher order in the $1/m$ -expansion, see Refs. [52,53,76,77] for a related discussion. Such off-shell effects manifest themselves, e.g., in the tree-level Δ -contribution to the magnetic polarizability β_{M1} . Although the residue of the Δ pole in the magnetic channel is the same in both schemes (the constants b_1 and g_M are

TABLE VI. Numerical values for the combined polarizabilities γ_0 , γ_π , $\bar{\gamma}_0$, and δ_{LT} of the proton (upper table) and the neutron (lower table). All values except for $\bar{\gamma}_0$ are given in 10^{-4} fm^4 while $\bar{\gamma}_0$ is given in 10^{-4} fm^6 . The values are compared with various results either calculated within the δ -counting scheme and obtained using fixed- t dispersion relations. The results of Ref. [31] are equivalent with our calculations without the q^4 -contribution. For remaining notation see Table V.

	$\gamma_0^{(p)}$	$\gamma_\pi^{(p)}$	$\bar{\gamma}_0^{(p)}$	$\delta_{LT}^{(p)}$
q^3 (without Δ)	2.08	3.72	2.20	1.54
q^4 (without Δ)	-0.80	1.31	-0.37	0.58
Total (without Δ)	1.3	5.0	1.8	2.12
q^3	2.08	3.72	2.20	1.54
$\epsilon^3 \pi \Delta$ loops	-0.16	-0.58	-0.01	1.21
$\epsilon^3 \Delta$ tree	-3.64	7.55	-1.24	-0.36
q^4	-0.80	1.31	-0.37	0.58
Total	-2.5 ± 0.4	12.0 ± 0.8	0.6 ± 0.1	2.98 ± 0.08
$\mathcal{O}(p^3) \pi N$ loops [40]	2.0	3.6	2.1	—
$\mathcal{O}(p^{7/2}) \pi \Delta$ loops [40]	-0.1	-0.9	-0.01	—
Δ pole [40]	-2.8	4.4	-1.0	—
Total [40]	-0.9 ± 1.4	7.2 ± 1.7	1.1 ± 0.5	—
Fixed- t DR [41]	-1.5	7.8	—	—
Fixed- t DR [42,45,46]	-0.8	9.4	0.6	—
$\text{HB}\chi\text{PT}$ [74,78]	-2.6 ± 1.9	5.6 ± 1.9	—	—
Experiment [2–4]	-1.01 ± 0.13	8.0 ± 1.8	—	—
$B\chi\text{PT}$ [31]	-1.74 ± 0.40	—	—	2.40 ± 0.01
	$\gamma_0^{(n)}$	$\gamma_\pi^{(n)}$	$\bar{\gamma}_0^{(n)}$	$\delta_{LT}^{(n)}$
q^3 (without Δ)	3.06	5.45	3.06	2.41
q^4 (without Δ)	-1.13	3.23	-0.46	0.50
Total (without Δ)	1.9	8.7	2.6	2.91
q^3	3.06	5.45	3.06	2.41
$\epsilon^3 \pi \Delta$ loops	-0.18	-0.49	-0.01	0.33
$\epsilon^3 \Delta$ tree	-3.64	7.55	-1.24	-0.36
q^4	-1.13	3.23	-0.46	0.50
Total	-1.9 ± 0.4	15.7 ± 0.8	1.4 ± 0.1	2.88 ± 0.06
$\mathcal{O}(p^3) \pi N$ loops [40]	3.0	5.3	2.9	—
$\mathcal{O}(p^{7/2}) \pi \Delta$ loops [40]	-0.1	-0.9	-0.01	—
Δ pole [40]	-2.8	4.5	-1.0	—
Total [40]	0.03 ± 1.4	9.0 ± 2.0	1.9 ± 0.7	—
Fixed- t DR [41]	-0.4	13.0	—	—
Fixed- t DR [40,44,45]	-0.1	13.7	—	—
$\text{HB}\chi\text{PT}$ [74,78]	0.5 ± 1.9	7.6 ± 1.9	—	—
$B\chi\text{PT}$ [31]	-0.77 ± 0.40	—	—	2.38 ± 0.03

roughly in agreement with each other when calculating the magnetic $\gamma N\Delta$ transition form factor), the full result differs almost by a factor of two due to the presence of the nonpole (background) terms. The nonvanishing (and sizable) contribution of the Δ -tree-level diagrams to the electric polarizabilities α_{E1} is in our scheme a pure $1/m$ -effect caused by the induced electric $\gamma N\Delta$ coupling stemming from the particular form of the effective Lagrangian. However, the Δ tree-level contribution to α_{E1} is negligible in the δ -counting scheme because of the smallness of the electric $\gamma N\Delta$ coupling g_E . Note that terms proportional to $g_E^2 (h_1^2)$ start to contribute only at order ϵ^5 in the small-scale-expansion scheme. The observed dependence of the considered polarizabilities on the off-shell effects might be an indication of the importance of such higher order contributions. Fortunately, such $1/m$ effects are strongly

suppressed for higher-order polarizabilities as will be shown below.

The second difference between the two schemes is related to power-counting of various diagrams with internal Δ -lines. While the πN loops in Ref. [40] at order $\mathcal{O}(p^3)$ are identical with the ones included in our $\mathcal{O}(q^3)$ results, the diagrams with two and three Δ -lines inside the loop are suppressed in the δ -counting and are not included in their leading-order $\pi \Delta$ -loop amplitude. However, such diagrams are required by gauge invariance (notice, however, that in the Coulomb gauge, their contribution is suppressed by a factor $1/m$).

In any case, we observe a significant difference between the size of the $\epsilon^3 \pi \Delta$ -loop contributions in our scheme and the $\mathcal{O}(p^{7/2})$ ones of Ref. [40] involving only the $\pi \Delta$ -loops with a single Δ -line.

TABLE VII. Numerical values for the dispersive and the quadrupole polarizabilities for the proton (upper table) and the neutron (lower table) in 10^{-4}fm^5 . The values are compared with the results calculated in δ -counting χPT and obtained using fixed- t dispersion relation. For remaining notation see Table V.

	$\alpha_{E2}^{(p)}$	$\beta_{M2}^{(p)}$	$\alpha_{E1v}^{(p)}$	$\beta_{M1v}^{(p)}$
q^3 (without Δ)	14.1	-8.7	0.8	1.9
q^4 (without Δ)	16.1	-15.9	-4.1	4.2
Total (without Δ)	30.2	-25	-3.3	6.1
q^3	14.1	-8.7	0.8	1.9
$\epsilon^3 \pi \Delta$ loops	5.8	-6.1	-0.9	1.1
$\epsilon^3 \Delta$ tree	1.3	-4.7	-1.6	5.0
q^4	8.3	-7.6	-2.2	2.3
Total	29.5 ± 0.9	-27 ± 1	-3.9 ± 0.4	10.2 ± 0.7
$\mathcal{O}(p^3) \pi N$ loops [40]	13.5	-8.4	0.7	1.8
$\mathcal{O}(p^{7/2}) \pi \Delta$ loops [40]	3.2	-2.7	-0.6	0.6
Δ pole [40]	0.6	-4.5	-1.5	4.7
Total [40]	17.3 ± 3.9	-15.5 ± 3.5	-1.3 ± 1.0	7.1 ± 2.5
Fixed- t DR [41,43],	27.5	-22.4	-3.8	9.1
Fixed- t DR [42,45]	27.7	-24.4	-3.9	9.3
$\alpha_{E2}^{(n)}$	$\beta_{M2}^{(n)}$	$\alpha_{E1v}^{(n)}$	$\beta_{M1v}^{(n)}$	
q^3 (without Δ)	12.9	-9.0	2.2	1.9
q^4 (without Δ)	16.0	-15.6	-3.9	3.9
Total (without Δ)	29.0	-25	-1.7	5.8
q^3	12.9	-9.0	2.2	1.9
$\epsilon^3 \pi \Delta$ loops	6.2	-6.0	-1.2	1.3
$\epsilon^3 \Delta$ tree	1.3	-4.7	-1.6	5.0
q^4	8.2	-7.3	-2.0	1.9
Total	28.7 ± 0.9	-27 ± 1	-2.6 ± 0.4	10.2 ± 0.7
$\mathcal{O}(p^3) \pi N$ loops [40]	12.4	-8.7	2.1	1.8
$\mathcal{O}(p^{7/2}) \pi \Delta$ loops [40]	3.2	-2.7	-0.6	0.6
Δ pole [40]	0.6	-4.5	-1.5	4.7
Total [40]	16.2 ± 3.7	-15.8 ± 3.6	0.1 ± 1.0	7.2 ± 2.5
Fixed- t DR [41]	27.2	-23.5	-2.4	9.2
Fixed- t DR [40,44,45]	27.9	-24.3	-2.8	9.3

B. Dipole spin polarizabilities

Next, we consider the dipole spin polarizabilities γ_{E1E1} , γ_{M1M1} , γ_{E1M2} , and γ_{M1E2} . These quantities are less sensitive to the short range dynamics as the relevant contact terms appear at order $\mathcal{O}(q^5)$. Therefore, one expects a better convergence pattern for them. At the order we are working, the spin polarizabilities are predictions and do not depend on any free parameters. The numerical values of the spin polarizabilities for the proton and neutron are collected in Table V.

We also provide theoretical errors for our complete scheme at order $\mathcal{O}(q^4 + \epsilon^3)$. The upper error reflects the uncertainty in the input parameters, whereas the lower value is the Bayesian estimate of the error coming from the truncation of the small-scale expansion.

The experimental values in Table V are obtained from the dispersion-relation analysis of the double-polarized Compton scattering asymmetries Σ_3 and Σ_{2x} [5], and, in a newer experiment, also Σ_{2z} [6].

Our predictions for the proton spin polarizabilities at order $\mathcal{O}(q^4 + \epsilon^3)$ agree with the experimental values of Ref. [5]

within the errors with only a slight deviation for γ_{M1M1} . The deviation from the values extracted in the recent MAMI experiment [6] are somewhat larger. Note that the Δ -less approach fails to reproduce γ_{M1M1} for the proton because of the missing Δ -pole contribution, which would appear as a contact term at order $\mathcal{O}(q^5)$.

The contributions of order $\mathcal{O}(q^4)$ are in all cases significantly smaller than the leading terms of order $\mathcal{O}(q^3 + \epsilon^3)$ in the Δ -full scheme (except for γ_{E1M2} where the leading-order result is small due to cancellations between individual contributions), which is an indication of a reasonable convergence of the small-scale expansion. The smallness of the $\mathcal{O}(q^4)$ -terms can probably also be traced back to the fact that the diagrams containing c_1 , c_2 , and c_3 vertices do not contribute to spin polarizabilities. Our Δ -full results also agree well with the values obtained from the fixed- t dispersion relations for the proton and the neutron, except for γ_{M1M1} , where our prediction appears to be somewhat larger.

In Table VI, we present the results for the forward and backward spin polarizabilities γ_0 and γ_π which are the linear combinations of the four spin polarizabilities and can be

TABLE VIII. Numerical values for spin-independent octupole polarizabilities α_{E3} and β_{M3} , quadrupole dispersive polarizabilities α_{E2v} and β_{M2v} as well as higher dipole dispersive polarizabilities α_{E2v^2} and β_{M2v^2} the proton [denoted with (p)] and the neutron [denoted with (n)]. All values are given in 10^{-4}fm^7 . For remaining notation see Table V.

	$\alpha_{E3}^{(p)}$	$\beta_{M3}^{(p)}$	$\alpha_{E2v}^{(p)}$	$\beta_{M2v}^{(p)}$	$\alpha_{E1v^2}^{(p)}$	$\beta_{M1v^2}^{(p)}$
q^3 (without Δ)	134.7	-95.6	-22.5	17.4	6.7	-3.4
q^4 (without Δ)	123.4	-118.6	-21.2	20.6	3.0	-2.9
Total (without Δ)	258	-214	-44	38	9.7	-6.3
q^3	134.7	-95.6	-22.5	17.4	6.7	-3.4
$\epsilon^3 \pi \Delta$ loops	52.3	-48.7	-9.1	8.7	1.3	-1.3
$\epsilon^3 \Delta$ tree	-1.2	4.3	1.7	-5.8	-1.0	2.5
q^4	61.5	-59.8	-10.5	10.2	1.4	-1.4
Total	247 ± 6	-200 ± 7	-40 ± 5	30 ± 4	8.4 ± 0.3	-3.7 ± 0.4
	$\alpha_{E3}^{(n)}$	$\beta_{M3}^{(n)}$	$\alpha_{E2v}^{(n)}$	$\beta_{M2v}^{(n)}$	$\alpha_{E1v^2}^{(n)}$	$\beta_{M1v^2}^{(n)}$
q^3 (without Δ)	136.2	-95.3	-25.1	17.3	8.3	-3.6
q^4 (without Δ)	123.4	-118.8	-21.4	21.0	3.1	-3.1
Total (without Δ)	260	-214	-47	38	11.4	-6.7
q^3	136.2	-95.3	-25.1	17.3	8.3	-3.6
$\epsilon^3 \pi \Delta$ loops	52.2	-48.7	-9.0	8.7	1.3	-1.3
$\epsilon^3 \Delta$ tree	-1.2	4.3	1.7	-5.8	-1.0	2.5
q^4	61.6	-60.0	-10.7	10.5	1.5	-3.6
Total	249 ± 6	-200 ± 7	-43 ± 5	31 ± 4	10.1 ± 0.3	-4.0 ± 0.4

more easily accessed experimentally. For these quantities, the agreement with the experimental values is slightly worse, as can be seen from Table VI.

As in the case of scalar dipole polarizabilities, we compare our Δ -tree-level and Δ -loop contributions with [40] to analyze the differences of the two Δ -full approaches and the size of the unphysical off-shell terms. For the spin polarizabilities, the off-shell effects (which we identify with the difference of the Δ -tree-level terms in two schemes considered) are smaller but, nevertheless, comparable to theoretical errors or even larger. This might indicate that our theoretical errors are somewhat underestimated. This should not come as a surprise because the Bayesian model for the error estimation that we implement is not fully trustworthy as long as only two orders in the expansion in terms of the small parameter Q are used as an input. Notice further that we treat the order $q^4 + \epsilon^3$ results as being the full fourth-order predictions when estimating truncation errors. The off-shell contributions add up constructively for the forward and backward spin polarizabilities (as can be seen in Table VI), which explains the worse agreement with experiment for these linear combinations.

The Δ -loop terms are also different in the ϵ - and δ -counting schemes, which points to the nonnegligible contribution of the diagrams with multiple Δ -lines. Note, however, that the overall absolute values of the $\epsilon^3 \Delta$ -loops are, on average, smaller than in the case of the scalar dipole polarizabilities and than the typical values of the dipole spin polarizabilities. Therefore, spin polarizabilities appear to be less sensitive to such details. However, the suppression of the $\epsilon^3 \Delta$ -loops does not exclude the possibility that the $\epsilon^4 \Delta$ -loops (with order $\mathcal{O}(q^2) \gamma N \Delta$ and $\gamma \Delta \Delta$ vertices), which are not included in the current study, yield important contributions, see also the discussion in Sec. IV D.

C. Higher-order polarizabilities

In this subsection, we focus on higher-order nucleon polarizabilities, including scalar quadrupole, dipole dispersive, octupole and quadrupole dispersive, as well as spin quadrupole and dipole dispersive polarizabilities. All relevant numerical values are collected in Tables VII–IX (we also provide the values for the higher-order forward spin polarizabilities $\tilde{\gamma}_0$ in Table VI). Note that unnaturally large values of the scalar quadrupole and, especially, octupole polarizabilities are related to the traditional l -dependent normalization factor in the definition of these polarizabilities and have no physical meaning.

We summarize the general features of the higher-order polarizabilities. Both Δ -less and Δ -full schemes give roughly the same results, except for the channels where the Δ -tree-level contribution is significant, i.e., for magnetic multipoles. Note that in the Δ -less approach, such contributions would appear only at extremely high orders, which makes the Δ -less framework rather inefficient.

The second observation concerns the loop contributions. While for all spin polarizabilities, the $\epsilon^3 \Delta$ -loops and the q^4 -loops are strongly suppressed, for scalar polarizabilities the situation is different. In the Δ -less scheme, the q^4 -loops are comparable with the q^3 -loops or larger, which spoils convergence. However, in the Δ -full scheme, a significant part of the q^4 -loop contributions is shifted to the $\epsilon^3 \Delta$ -loops. This happens due to the Δ -resonance saturation of the low-energy constants c_i , in particular, c_2 and c_3 [79,80], which do not contribute to the spin polarizabilities. As a result, the convergence pattern of the Δ -full scheme looks very convincing for both scalar and spin polarizabilities. The only exceptions are the $\gamma M2E3$ polarizabilities, where the ϵ^3 result is unnaturally small due to accidental cancellations between the q^3 -loops and the Δ -tree-level contributions.

TABLE IX. Numerical values for the quadrupole spin polarizabilities γ_{E2E2} , γ_{M2M2} , γ_{E2M3} , and γ_{M2E3} and for the dispersive spin polarizabilities γ_{E1E1v} , γ_{M1M1v} , γ_{E1M2v} and γ_{M1E2v} of the proton [indicated with (p)] and the neutron (indicated with (n)). All values are given in 10^{-6}fm^5 . For remaining notation see Table V.

	$\gamma_{E2E2}^{(p)}$	$\gamma_{M2M2}^{(p)}$	$\gamma_{E2M3}^{(p)}$	$\gamma_{M2E3}^{(p)}$
q^3 (without Δ)	-7.56	1.16	5.78	4.85
q^4 (without Δ)	-0.46	-0.63	0.32	-1.84
Total (without Δ)	-8.0	0.5	6.1	3.0
q^3	-7.56	1.16	5.78	4.85
$\epsilon^3 \pi \Delta$ loops	0.30	0.22	-0.40	-0.49
$\epsilon^3 \Delta$ tree	-1.01	-10.16	1.13	-3.11
q^4	-0.46	-0.63	0.32	-1.84
Total	-8.7 ± 0.1	-9.4 ± 1.1	6.8 ± 0.6	-0.6 ± 0.4
	$\gamma_{E2E2}^{(n)}$	$\gamma_{M2M2}^{(n)}$	$\gamma_{E2M3}^{(n)}$	$\gamma_{M2E3}^{(n)}$
q^3 (without Δ)	-1.18	1.97	5.59	3.56
q^4 (without Δ)	-0.12	-2.27	0.40	-1.66
Total (without Δ)	-1.3	0	6.0	1.9
q^3	-1.18	1.97	5.59	3.56
$\epsilon^3 \pi \Delta$ loops	0.33	0.13	-0.44	-0.33
$\epsilon^3 \Delta$ tree	-1.01	-10.16	1.13	-3.11
q^4	-0.12	-2.27	0.40	-1.66
Total	-2.0 ± 0.1	-10 ± 1	6.7 ± 0.6	-1.6 ± 0.4
	$\gamma_{E1E1v}^{(p)}$	$\gamma_{M1M1v}^{(p)}$	$\gamma_{E1M2v}^{(p)}$	$\gamma_{M1E2v}^{(p)}$
q^3 (without Δ)	-3.26	0.40	-0.29	0.85
q^4 (without Δ)	0.0003	0.24	-0.12	0.28
Total (without Δ)	-3.26	0.6	-0.41	1.13
q^3	-3.26	0.40	-0.29	0.85
$\epsilon^3 \pi \Delta$ loops	0.02	-0.02	0.02	0.001
$\epsilon^3 \Delta$ tree	-0.49	1.73	-0.56	0.70
q^4	0.0003	0.24	-0.12	0.28
Total	-3.72 ± 0.05	2.4 ± 0.2	-0.95 ± 0.06	1.83 ± 0.08
	$\gamma_{E1E1v}^{(n)}$	$\gamma_{M1M1v}^{(n)}$	$\gamma_{E1M2v}^{(n)}$	$\gamma_{M1E2v}^{(n)}$
q^3 (without Δ)	-4.62	0.46	-0.29	1.23
q^4 (without Δ)	-0.10	0.50	-0.18	0.28
Total (without Δ)	-4.72	1.0	-0.47	1.51
q^3	-4.62	0.46	-0.29	1.23
$\epsilon^3 \pi \Delta$ loops	0.03	-0.03	0.03	-0.01
$\epsilon^3 \Delta$ tree	-0.49	1.73	-0.56	0.70
q^4	-0.10	0.50	-0.18	0.28
Total	-5.17 ± 0.05	2.7 ± 0.2	-1.00 ± 0.10	2.19 ± 0.08

Our predictions at order $\mathcal{O}(q^4 + \epsilon^3)$ for all scalar quadrupole and dipole dispersive polarizabilities of the proton and the neutron agree within errors with the results based on fixed- t dispersion relations, see Table VII. Note that the predictions of the δ -counting scheme of Ref. [40] do not reproduce the fixed- t dispersion relations values for α_{E2} and β_{M2} . The main difference to our result in this channel comes from the q^4 -loops and ϵ^3 - Δ -loops. However, the difference in the tree-level- Δ contributions appears very small, indicating the insignificance of the off-shell effects, as one would expect for such high-order polarizabilities.

D. Generalized polarizabilities

Now are now in the position to discuss the generalized (Q^2 -dependent) nucleon polarizabilities. We consider the

doubly virtual Compton scattering with the initial and final virtuality of the photon equal to Q^2 . In Fig. 5, the scalar and spin dipole polarizabilities for the proton and the neutron are plotted as a function of Q^2 , and the Δ -full and Δ -less schemes are compared. The scalar polarizabilities at $Q^2 = 0$ are adjusted to the empirical values, see Sec. IV A. The difference of the Δ -full and Δ -less spin polarizabilities at $Q^2 = 0$ was discussed in Sec. IV B and can be considered as a higher-order contact-term contribution. Therefore, we focus here on the Q^2 -dependence of the polarizabilities relative to their $Q^2 = 0$ values. For the spin polarizabilities and for the electric scalar polarizability, the Δ -full and Δ -less curves go almost parallel to each other, whereas for the magnetic scalar polarizabilities the slope and the curvature of the curves are opposite in sign. This is due to a significant contribution of the Δ -tree-level

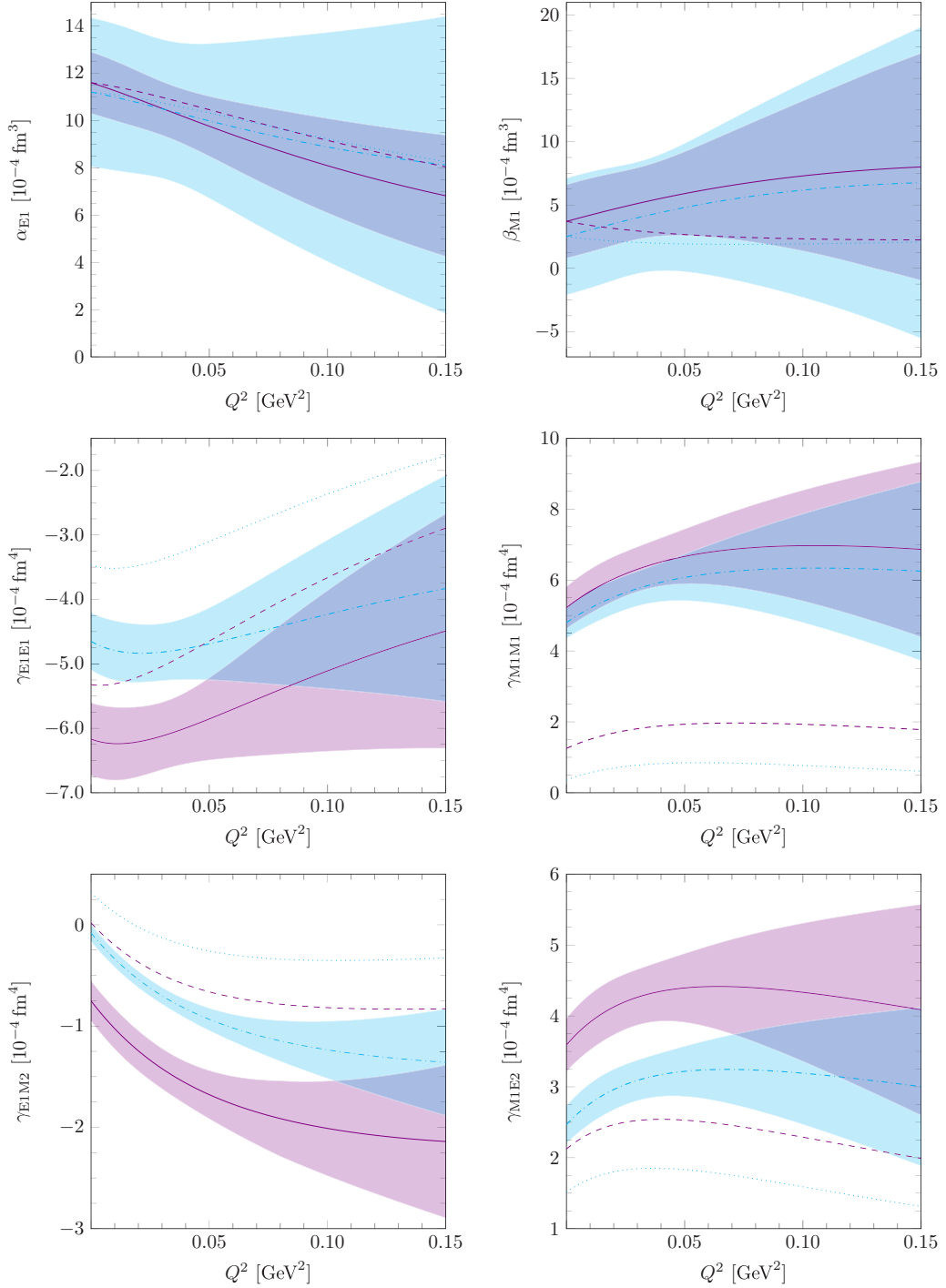


FIG. 5. Q^2 -dependence of the scalar and spin polarizabilities for the proton (dotted and dash-dotted cyan lines) and the neutron (dashed and solid purple lines). The dotted and dashed lines correspond to the Δ -less $\mathcal{O}(q^4)$ results, whereas the dash-dotted and solid lines correspond to the Δ -full $\mathcal{O}(\epsilon^3 + q^4)$ results. The bands indicate the theoretical truncation errors.

contribution in this channel. It should be emphasized that the scalar generalized polarizabilities contribute to the Lamb shift of muonic hydrogen, see, e.g., Ref. [81].

We also present the Q^2 -dependence of several combined spin polarizabilities, for some of which the experimental data are available, see Fig. 6 (their limiting values for $Q^2 = 0$ are collected in Table VI). We observe no improvement as

compared to Ref. [31] [pure $\mathcal{O}(\epsilon^3)$ calculation] due to the inclusion of the $\mathcal{O}(q^4)$ contributions. In fact, the description of γ_0 for the proton is even worse. A possible source of such a discrepancy could be a missing contribution of the Δ -loop diagrams at order $\mathcal{O}(\epsilon^4)$, as was suggested in Ref. [31]. However, taking into account a much better description of the data in Ref. [82] (within the δ -counting

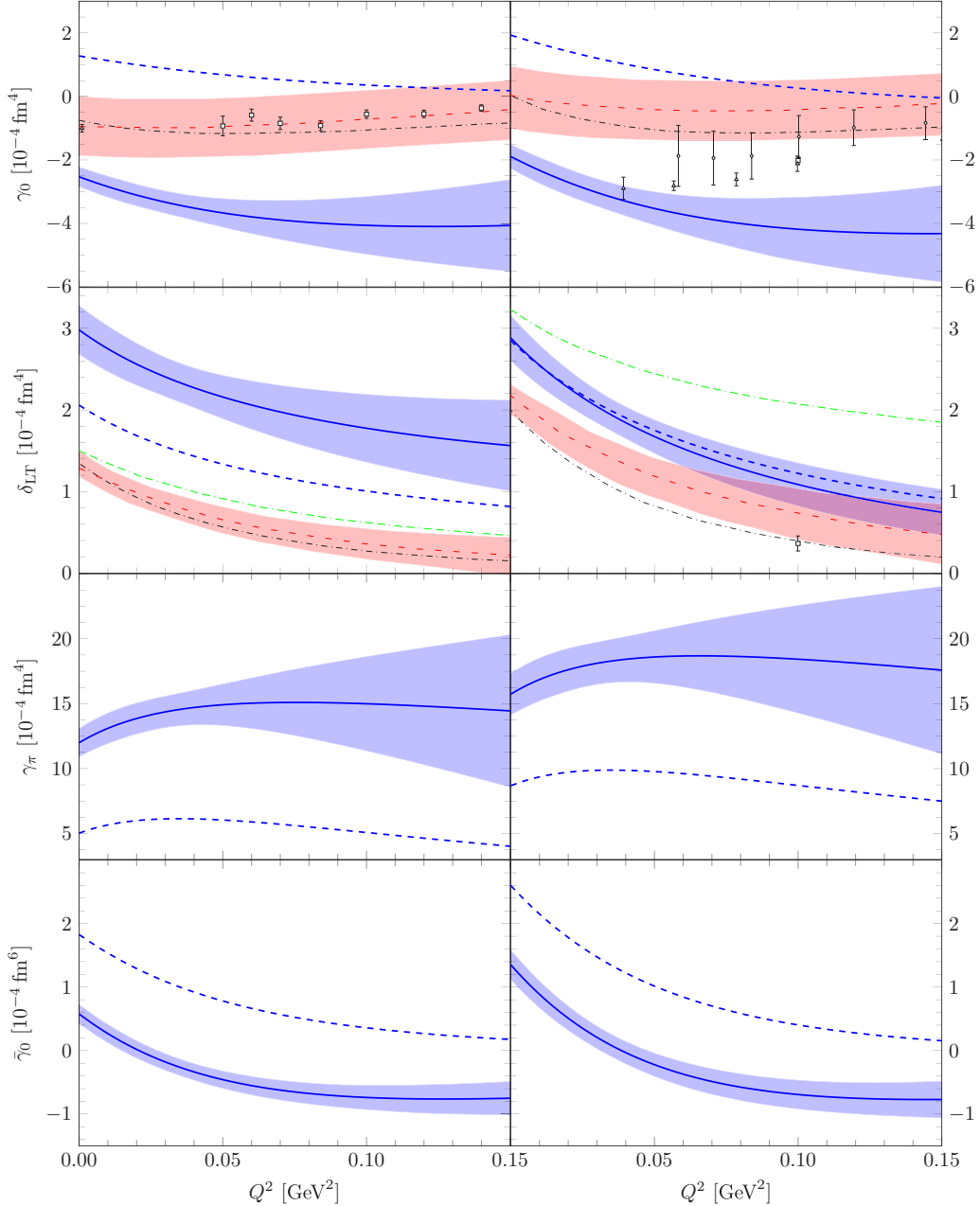


FIG. 6. Q^2 -dependencies of the forward polarizabilities γ_0 and δ_{LT} , the backward polarizability γ_π and the combined higher-order polarizability $\bar{\gamma}_0$ for the proton (left) and the neutron (right). The thick solid blue lines indicate our Δ -full $\mathcal{O}(q^4 + \epsilon^3)$ calculations with a 1σ truncation error band corresponding to 68% degree-of-belief intervals and the thick dashed blue lines show our Δ -less $\mathcal{O}(q^4)$ calculations. The red loosely dashed lines represent the NLO B χ PT calculation from Ref. [39] with the red error bands. The black dash-dotted line presents the MAID model predictions from Ref. [44] (proton) and Ref. [8] (neutron). The green double-dash-dotted line is the $\mathcal{O}(p^4)$ calculation from Ref. [83]. Empirical data are: for $\gamma_0^{(p)}$ from [10] (triangle) and [7] (squares); for $\gamma_0^{(n)}$ from Ref. [11] (preliminary, triangles), Ref. [8] (square), and Ref. [9] (diamonds); for $\delta_{LT}^{(n)}$ from Ref. [8].

scheme) and the fact that the disagreement of our result with experiment for the value of γ_0 for the proton at $Q^2 = 0$ was caused by the large contribution from the induced electric $\gamma N \Delta$ -coupling (as a $1/m$ effect), one may expect the improvement to be achieved after including the relevant higher-order $\gamma N \Delta$ -vertices from the effective Lagrangian analogously to Ref. [82].

E. Dynamical polarizabilities

One can also probe the electromagnetic structure of the nucleon by looking at dynamical (energy-dependent) polarizabilities that describe the response to the nucleon electromagnetic excitations at arbitrary energy. In Figs. 7 and 8, we present the energy dependence of the dipole and spinless

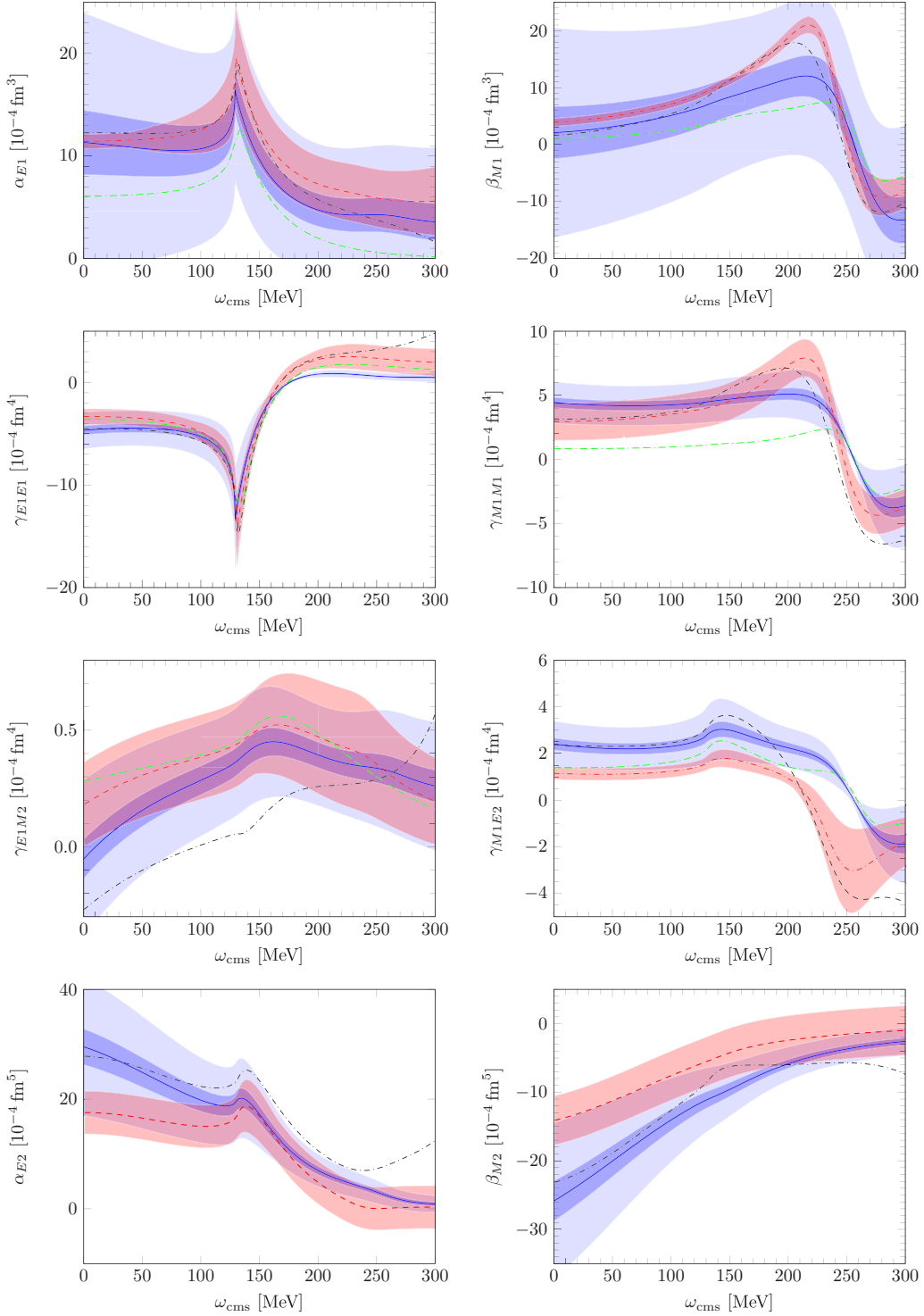


FIG. 7. The ω -dependence of the real parts of the dipole polarizabilities and the spinless quadrupole polarizabilities α_{E2} and β_{M2} for the proton. The solid blue lines represent our Δ -full $\mathcal{O}(q^4 + \epsilon^3)$ result. The inner (outer) blue bands stand for the 1σ (2σ) truncation error. The red dashed lines are the $B\chi$ PT calculation [40] with the red error bands. The black dash-dotted lines correspond to the fixed- t dispersion-relations calculation [45] and the green double-dash-dotted lines correspond to the results of Ref. [84].

quadrupole polarizabilities up to the center-of-mass energy $\omega_{\text{CM}} = 300$ MeV. For comparison, also shown are the results obtained using the δ -counting scheme [40], the fixed- t dispersion relations [45], and the Computational Hadronic Model

[84].² Note that the heavy-baryon results for these quantities are also available [85] and agree rather well in the shape

²We have extracted those data points from Ref. [40].

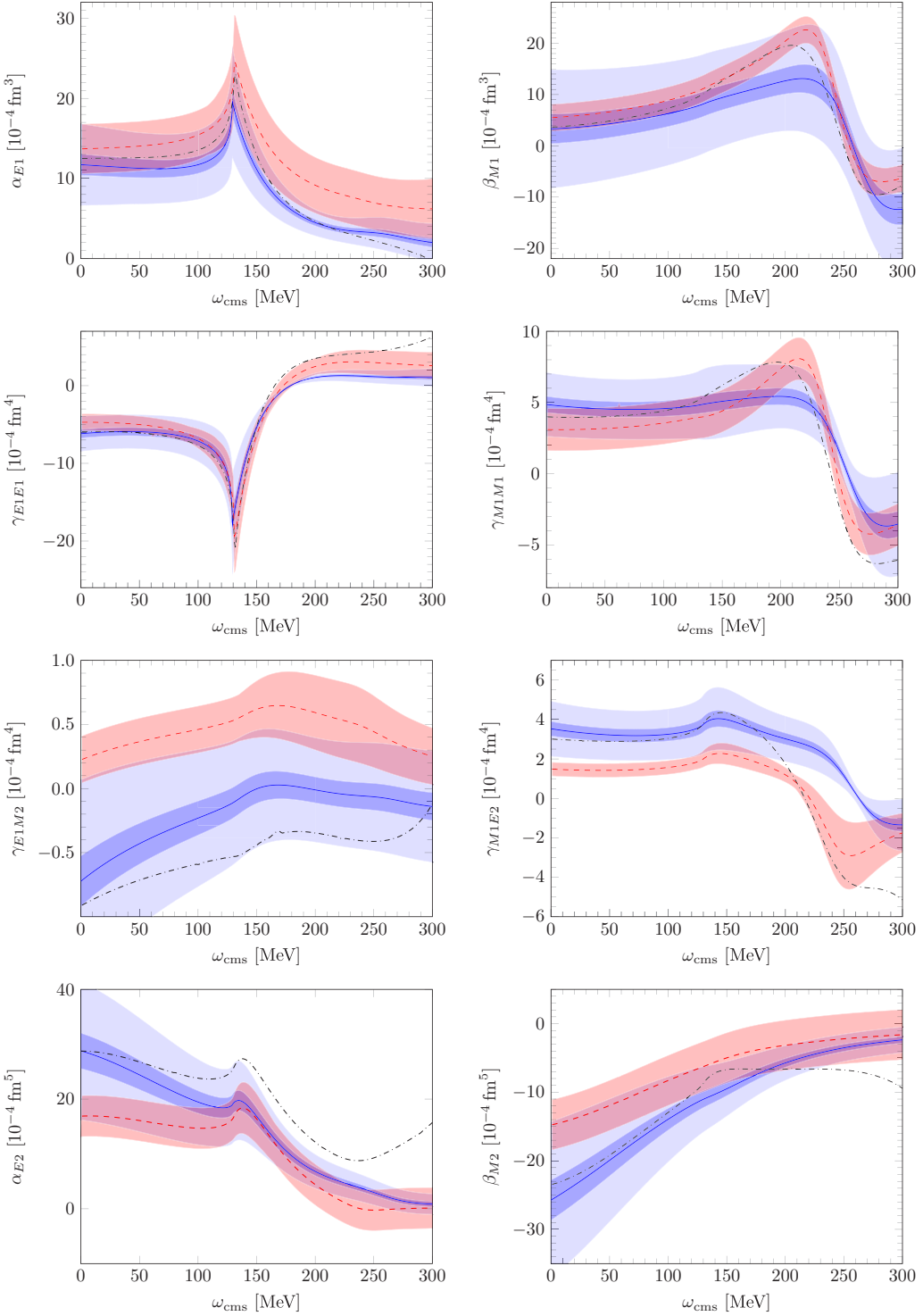


FIG. 8. The ω -dependence of the real parts of the dipole polarizabilities and the spinless quadrupole polarizabilities α_{E2} and β_{M2} for the neutron. The solid blue lines represent our Δ -full $\mathcal{O}(q^4 + \epsilon^3)$ result. The inner (outer) blue bands stand for the 1σ (2σ) truncation error. The red dashed lines are the $B\chi$ PT calculation [40] with the red error bands. The black dash-dotted lines correspond to the fixed- t dispersion-relations calculation [45].

with the other approaches. The 1σ and 2σ truncation errors corresponding to 68% and 95% degree-of-belief intervals are shown as bands in the figures. Our results agree rather well with the ones of the fixed- t dispersion relations at $\omega_{CM} = 0$ (except for γ_{E1M2}). Therefore, it is natural to compare the

two approaches at nonzero energies. As can be seen from the figures, the deviation of our results from those of the fixed- t dispersion relations increases with energy, which may provide yet another indication that our theoretical errors are underestimated (as discussed in Sec. IV C), and the convergence of the

TABLE X. Numerical values for the $1/m$ -expansion of α_{E1} . Note that the ϵ_{Tree}^3 only starts at NLO.

$\alpha_{E1}^{(p)}$	q^3	q^4	ϵ_{Loop}^3	ϵ_{Tree}^3	Full	$\alpha_{E1}^{(n)}$	q^3	q^4	ϵ_{Loop}^3	ϵ_{Tree}^3	Full
LO	12.78	8.86	7.86	...	29.50	LO	12.78	2.67	7.86	...	23.31
NLO	8.47	8.86	2.89	-5.60	14.61	NLO	9.67	2.67	4.94	-5.60	11.68
$N^2\text{LO}$	6.60	9.53	0.97	-2.98	14.13	$N^2\text{LO}$	9.50	3.22	3.03	-2.98	12.77
$N^3\text{LO}$	7.01	9.40	-1.03	-4.11	11.26	$N^3\text{LO}$	9.51	3.10	2.70	-4.11	11.19
$N^4\text{LO}$	7.04	9.40	-1.33	-3.65	11.46	$N^4\text{LO}$	9.51	3.09	2.83	-3.65	11.78
$N^5\text{LO}$	7.04	9.40	-1.49	-3.83	11.12	$N^5\text{LO}$	9.51	3.09	2.75	-3.83	11.52
Full	7.04	9.40	-1.45	-3.78	11.20	Full	9.51	3.09	2.78	-3.78	11.60

small-scale expansion becomes slower $\omega_{\text{CM}} \gtrsim 150\text{--}200$ MeV. However, for α_{E2} a large discrepancy (beyond 2σ) between the two theoretical frameworks is observed already for $\omega_{\text{CM}} \gtrsim 100\text{--}150$ MeV. This could be due to the aforementioned large induced electric $\gamma N \Delta$ -coupling in our scheme, whose effect increases with energy.

F. Heavy-Baryon expansion

In this subsection, we study the convergence of the $1/m$ -expansion of our results (the nucleon- Δ mass difference Δ is kept finite and constant) obtained within the covariant framework. Analyzing such an expansion we can test the efficiency of the heavy-baryon approach by reproducing some of its contributions appearing at higher orders. We present the $1/m$ -expansion for the dipole scalar and spin polarizabilities in Tables X–XV starting from the leading order (LO) static (m^0) results up to the order $1/m^5$ ($N^5\text{LO}$). Obviously, the static results as well as the $1/m$ -corrections to the leading-order terms coincide with the corresponding heavy-baryon calculations, see Refs. [21–24].³

We first consider the convergence of the $1/m$ -expansion of the individual contributions from the q^3 -, q^4 -, and ϵ^3 -loop diagrams, and from the Δ -tree-level terms. In general, the convergence is rather slow. The most rapid convergence is observed for the q^3 - and q^4 -loops. Sometimes (e.g., for α_{E1} , γ_{M1E2}), the expanded value approaches the “exact” one

already at NLO- $N^2\text{LO}$. In other cases, the expanded values oscillate at lower $1/m$ -orders, especially when the resulting value is small due to cancellations among various diagrams. It is natural to expect a slower convergence for the diagrams with Δ -lines as the formal expansion parameter Δ/m is roughly twice as large as M/m . Nevertheless, the expansion for the tree- Δ -graphs converges, in general, only slightly worse than the πN -loops (β_{M1} is accidentally m -independent). However, for the $\Delta\pi$ -loops, the convergence is very poor. This set of diagrams comprises loops with one, two and three Δ -lines, and cancellations among them occur quite often. Some of the values strongly oscillate and one hardly sees a sign of convergence even at $N^5\text{LO}$, e.g., for γ_{M1M1} , γ_{E1M2} .

Nevertheless, we have checked that the $1/m$ -expansion converges in principle (formally) for all diagrams. This is illustrated in Figs. 9 and 10, where the logarithm of the remainder in the $1/m$ -series is plotted against the order of expansion. As one can see from the plots, the expanded Δ -loops approach their unexpanded values very slowly, making such an expansion impractical. Note that contributions of the Δ -loops are smaller for the spin-dependent polarizabilities.

We now consider the $1/m$ -expansion of the sum of all contributions to the nucleon polarizabilities. As one can see in Tables X and XI, the electric and magnetic scalar polarizabilities at NLO agree rather well with the unexpanded values (for the absolute difference is large but the relative difference is small), while the individual contributions in some cases strongly oscillate. Such an agreement is accidental. Moreover, e.g., the $\beta_{M1}^{(p)}$ at $N^2\text{LO}$ deviates significantly from the full result and approaches it again after several oscillations. Nevertheless, these effects can be compensated by a redefinition of the q^4 contact terms.

TABLE XI. Numerical values for the $1/m$ -expansion of β_{M1} .

$\beta_{M1}^{(p)}$	q^3	q^4	ϵ_{Loop}^3	ϵ_{Tree}^3	Full	$\beta_{M1}^{(n)}$	q^3	q^4	ϵ_{Loop}^3	ϵ_{Tree}^3	Full
LO	1.28	-12.33	1.36	11.96	2.26	LO	1.28	-7.35	1.36	11.96	7.24
NLO	0.56	-12.09	1.61	11.96	2.04	NLO	-0.88	-7.60	0.34	11.96	3.83
$N^2\text{LO}$	-2.83	-13.75	9.05	11.96	4.43	$N^2\text{LO}$	-1.11	-8.27	1.28	11.96	3.85
$N^3\text{LO}$	-1.94	-13.23	5.67	11.96	2.45	$N^3\text{LO}$	-1.10	-8.12	0.69	11.96	3.43
$N^4\text{LO}$	-1.83	-13.14	6.39	11.96	3.38	$N^4\text{LO}$	-1.10	-8.12	1.09	11.96	3.83
$N^5\text{LO}$	-1.85	-13.16	5.32	11.96	2.28	$N^5\text{LO}$	-1.10	-8.12	0.90	11.96	3.64
Full	-1.85	-13.16	5.54	11.96	2.50	Full	-1.10	-8.12	0.96	11.96	3.70

TABLE XII. Numerical values for the $1/m$ -expansion of γ_{E1E1} . The dots mark entries that do not exist, e.g., the ϵ_{Tree}^3 starts at NLO and therefore does not have a LO contribution.

$\gamma_{E1E1}^{(p)}$	q^3	q^4	ϵ_{Loop}^3	ϵ_{Tree}^3	Full	$\gamma_{E1E1}^{(n)}$	q^3	q^4	ϵ_{Loop}^3	ϵ_{Tree}^3	Full
LO	-5.81	...	0.60	...	-5.22	LO	-5.81	...	0.60	...	-5.22
NLO	-1.38	...	0.96	-0.63	-1.05	NLO	-4.34	...	0.66	-0.63	-4.31
$N^2\text{LO}$	-3.03	0.20	-0.63	-1.22	-4.68	$N^2\text{LO}$	-4.83	-0.37	0.84	-1.22	-5.58
$N^3\text{LO}$	-3.57	-0.11	-1.41	-1.02	-6.11	$N^3\text{LO}$	-4.86	-0.49	0.07	-1.02	-6.30
$N^4\text{LO}$	-3.47	-0.02	0.07	-1.08	-4.50	$N^4\text{LO}$	-4.86	-0.46	0.26	-1.08	-6.15
$N^5\text{LO}$	-3.46	-0.01	-0.13	-1.06	-4.66	$N^5\text{LO}$	-4.86	-0.46	0.23	-1.06	-6.16
Full	-3.46	-0.01	-0.11	-1.07	-4.65	Full	-4.86	-0.46	0.22	-1.07	-6.17

The situation is different for the spin-dependent polarizabilities, where the NLO values in most cases deviate rather strongly from the unexpanded result, see Tables XII–XV. It should be emphasized that these differences can be absorbed into contact terms only at order q^5 .

Summarizing, we conclude that the $1/m$ -expansion (and, hence, the heavy-baryon scheme) is rather inefficient for calculating nucleon polarizabilities in the Δ -full approach, which is in line with the results of the heavy-baryon calculations mentioned above. However, the small-scale expansion seems to converge reasonably well.

V. SUMMARY AND OUTLOOK

In this work, we have presented various nucleon polarizabilities obtained within covariant chiral perturbation theory with explicit $\Delta(1232)$ degrees of freedom, calculated up to order $\mathcal{O}(\epsilon^3 + q^4)$ in the small-scale expansion. The theoretical errors were estimated by combining the uncertainties of the input parameters and the errors due to the truncation of the small-scale expansion calculated using a Bayesian model. The results were compared with the Δ -less approach at order $\mathcal{O}(q^3)$ and $\mathcal{O}(q^4)$, as well as with the empirical values and other theoretical approaches (in particular, with the δ -counting Δ -full scheme and the fixed- t dispersion-relations method).

The general conclusion of this study is that the Δ -full scheme that we adopt is quite efficient for analyzing the nucleon polarizabilities. It shows reasonable convergence, and the obtained results agree well with experiment and the fixed- t dispersion-relations values. The results obtained in the Δ -less approach are considerably worse both from the point of view of convergence and agreement with experiment.

The scalar dipole polarizabilities were used as an input to adjust four low energy constants appearing at order $\mathcal{O}(q^4)$ in the effective Lagrangian. Therefore, we were not concerned with the issue of convergence for these quantities (although the convergence is far from being satisfactory).

Our predictions for the dipole spin polarizabilities γ_{E1E1} , γ_{E1M2} , γ_{M1E2} obtained in the Δ -full scheme agree with experimental values of Ref. [5] and are slightly larger for γ_{M1M1} . The agreement is somewhat worse with the analysis of the recent MAMI experiment [5]. The same pattern is observed in the comparison with the fixed- t dispersion-relations results. However, the predictions for the forward and backward spin polarizabilities γ_0 and $\gamma + \pi$ differ noticeably from the empirical values. Such a deviation can be explained by a sizable contributions of the “induced” electric $\gamma N \Delta$ -coupling observed for these linear combinations. This effect is formally suppressed by a factor of $1/m$, but numerically it turns out to be sizable. In the δ -counting scheme of Ref. [40], the electric $\gamma N \Delta$ -coupling constant is adjusted to data and appears to be rather small. This is an indication that including higher-order Δ -pole graphs in our scheme might improve the results.

Due to small contributions of the q^4 -loops to spin polarizabilities, a rather rapid convergence is achieved for all of them.

We have also analyzed several higher-order polarizabilities. A nice convergence rate is observed for all polarizabilities calculated within the Δ -full scheme. This is, however, not the case for the higher-order scalar polarizabilities calculated in the Δ -less approach. This pattern can be understood in terms of the Δ -resonance saturation of the low-energy constants c_2 and c_3 . The main effect of the explicit treatment of the Δ is that some parts of the q^4 -loops are shifted to the ϵ^3 -loops.

TABLE XIII. Numerical values for the $1/m$ -expansion of γ_{M1M1} . The dots mark entries that do not exist, e.g., the q^4 starts at NLO and therefore does not have a LO contribution.

$\gamma_{M1M1}^{(p)}$	q^3	q^4	ϵ_{Loop}^3	ϵ_{Tree}^3	Full	$\gamma_{M1M1}^{(n)}$	q^3	q^4	ϵ_{Loop}^3	ϵ_{Tree}^3	Full
LO	-1.16	...	0.21	4.03	3.08	LO	-1.16	...	0.21	4.03	3.08
NLO	1.39	1.93	-0.12	3.40	6.59	NLO	0.31	2.05	-0.27	3.40	5.49
$N^2\text{LO}$	0.52	1.24	2.21	3.89	7.85	$N^2\text{LO}$	-0.13	1.56	0.78	3.89	6.11
$N^3\text{LO}$	-0.37	0.19	-0.44	3.87	3.26	$N^3\text{LO}$	-0.17	1.39	0.04	3.87	5.13
$N^4\text{LO}$	-0.15	0.46	0.81	3.84	4.96	$N^4\text{LO}$	-0.17	1.42	0.23	3.84	5.33
$N^5\text{LO}$	-0.12	0.50	0.39	3.86	4.62	$N^5\text{LO}$	-0.17	1.42	0.05	3.86	5.16
Full	-0.13	0.49	0.58	3.85	4.80	Full	-0.17	1.42	0.12	3.85	5.22

TABLE XIV. Numerical values for the $1/m$ -expansion of γ_{E1M2} . The dots mark entries that do not exist, e.g., the ϵ_{Tree}^3 starts at NLO and therefore does not have a LO contribution.

$\gamma_{E1M2}^{(p)}$	q^3	q^4	ϵ_{Loop}^3	ϵ_{Tree}^3	Full	$\gamma_{E1M2}^{(n)}$	q^3	q^4	ϵ_{Loop}^3	ϵ_{Tree}^3	Full
LO	1.16	...	-0.21	...	0.95	LO	1.16	...	-0.21	...	0.95
NLO	0.22	...	0.01	-0.63	-0.40	NLO	0.49	...	0.04	-0.63	-0.09
$N^2\text{LO}$	0.57	0.03	1.43	-0.92	1.11	$N^2\text{LO}$	0.60	-0.43	0.21	-0.92	-0.54
$N^3\text{LO}$	0.54	-0.36	0.84	-0.88	0.15	$N^3\text{LO}$	0.61	-0.63	0.27	-0.88	-0.64
$N^4\text{LO}$	0.56	-0.26	0.05	-0.88	-0.52	$N^4\text{LO}$	0.61	-0.59	0.03	-0.88	-0.84
$N^5\text{LO}$	0.57	-0.25	0.70	-0.88	0.14	$N^5\text{LO}$	0.61	-0.59	0.16	-0.88	-0.70
Full	0.57	-0.25	0.48	-0.88	-0.08	Full	0.61	-0.59	0.11	-0.88	-0.75

For the scalar quadrupole and dipole-dispersive polarizabilities, our predictions agree with the results of the fixed- t dispersion-relations approach. However, our results differ noticeably from the ones obtained in the δ -counting scheme. This difference is caused not only by the q^4 -loop contributions, but also by the ϵ^3 -loops with multiple Δ -lines, which contribute at higher orders in the δ -counting scheme. This points to the importance of such terms also for higher-order polarizabilities.

We also studied the Q^2 -dependence of the nucleon polarizabilities by considering generalized scalar and spin polarizabilities. We found that the Q^2 -dependence of the magnetic scalar polarizabilities is significantly different in the Δ -full and the Δ -less approach. We also observed a substantial deviation of the $\mathcal{O}(\epsilon^3 + q^4)$ results for the Q^2 -dependent polarizabilities γ_0 for the proton and for the neutron as well as δ_{LT} for the neutron from the available experimental data and no improvement compared to the $\mathcal{O}(\epsilon^3)$ -results. We expect that taking into account the $\mathcal{O}(\epsilon^4)$ terms (in particular, the tree-level graphs) might improve the description of the data.

An alternative way to study the electromagnetic structure of the nucleon is to consider dynamical (energy-dependent) polarizabilities. We have analyzed the energy dependence of the dipole and spinless quadrupole polarizabilities and compared them with other theoretical investigations. In particular, we observed a rather large deviation from the fixed- t dispersion-relations approach at energies $\omega_{\text{CM}} \gtrsim 150\text{--}200$ MeV (in some cases for $\omega_{\text{CM}} \gtrsim 100$ MeV),

which indicates the slow convergence of the small-scale expansion in that energy region.

Finally, we have analyzed the convergence of the $1/m$ -expansion of the results obtained in the covariant calculation for various polarizabilities. Such an scheme allows one to see how reliable the heavy-baryon expansion is for the evaluation of the nucleon polarizabilities. We considered the expansion up to $N^5\text{LO}$. Our conclusion is that the heavy-baryon expansion is not efficient for calculating nucleon polarizabilities in the Δ -full approach. Nevertheless, the small-scale expansion seems to converge reasonably well.

A natural extension of the current work towards increasing accuracy of the results follows from the discussion above. We expect a better accuracy and a better agreement with the experimental data after including the Δ -tree-level graphs of order $\mathcal{O}(\epsilon^4)$ with the electric $\gamma N \Delta$ -coupling as well as the $\mathcal{O}(\epsilon^4)$ -loop diagrams, that is performing a complete $\mathcal{O}(\epsilon^4)$ calculation.

ACKNOWLEDGMENTS

We are grateful to Jambul Gegelia for helpful discussions and to Veronique Bernard and Ulf-G. Meißner for sharing their insights into the considered topics. This work was supported in part by BMBF (Contract No. 05P18PCFP1), by DFG (Grant No. 426661267), and by DFG through funds provided to the Sino-German CRC 110 Symmetries and the Emergence of Structure in QCD (Grant No. TRR110).

TABLE XV. Numerical values for the $1/m$ -expansion of γ_{M1E2} . The dots mark entries that do not exist, e.g., the ϵ_{Tree}^3 starts at NLO and therefore does not have a LO contribution.

$\gamma_{M1E2}^{(p)}$	q^3	q^4	ϵ_{Loop}^3	ϵ_{Tree}^3	Full	$\gamma_{M1E2}^{(n)}$	q^3	q^4	ϵ_{Loop}^3	ϵ_{Tree}^3	Full
LO	1.16	...	-0.21	...	0.95	LO	1.16	...	-0.21	...	0.95
NLO	0.76	1.03	-0.11	1.89	3.56	NLO	1.30	0.96	-0.08	1.89	4.06
$N^2\text{LO}$	0.89	0.66	-1.32	1.59	1.82	$N^2\text{LO}$	1.36	0.87	-0.33	1.59	3.48
$N^3\text{LO}$	0.98	0.52	-1.02	1.82	2.31	$N^3\text{LO}$	1.37	0.73	-0.25	1.82	3.67
$N^4\text{LO}$	0.95	0.56	-0.80	1.71	2.42	$N^4\text{LO}$	1.36	0.76	-0.26	1.71	3.57
$N^5\text{LO}$	0.95	0.56	-0.86	1.76	2.40	$N^5\text{LO}$	1.36	0.76	-0.29	1.76	3.59
Full	0.95	0.56	-0.79	1.74	2.47	Full	1.36	0.76	-0.27	1.74	3.59

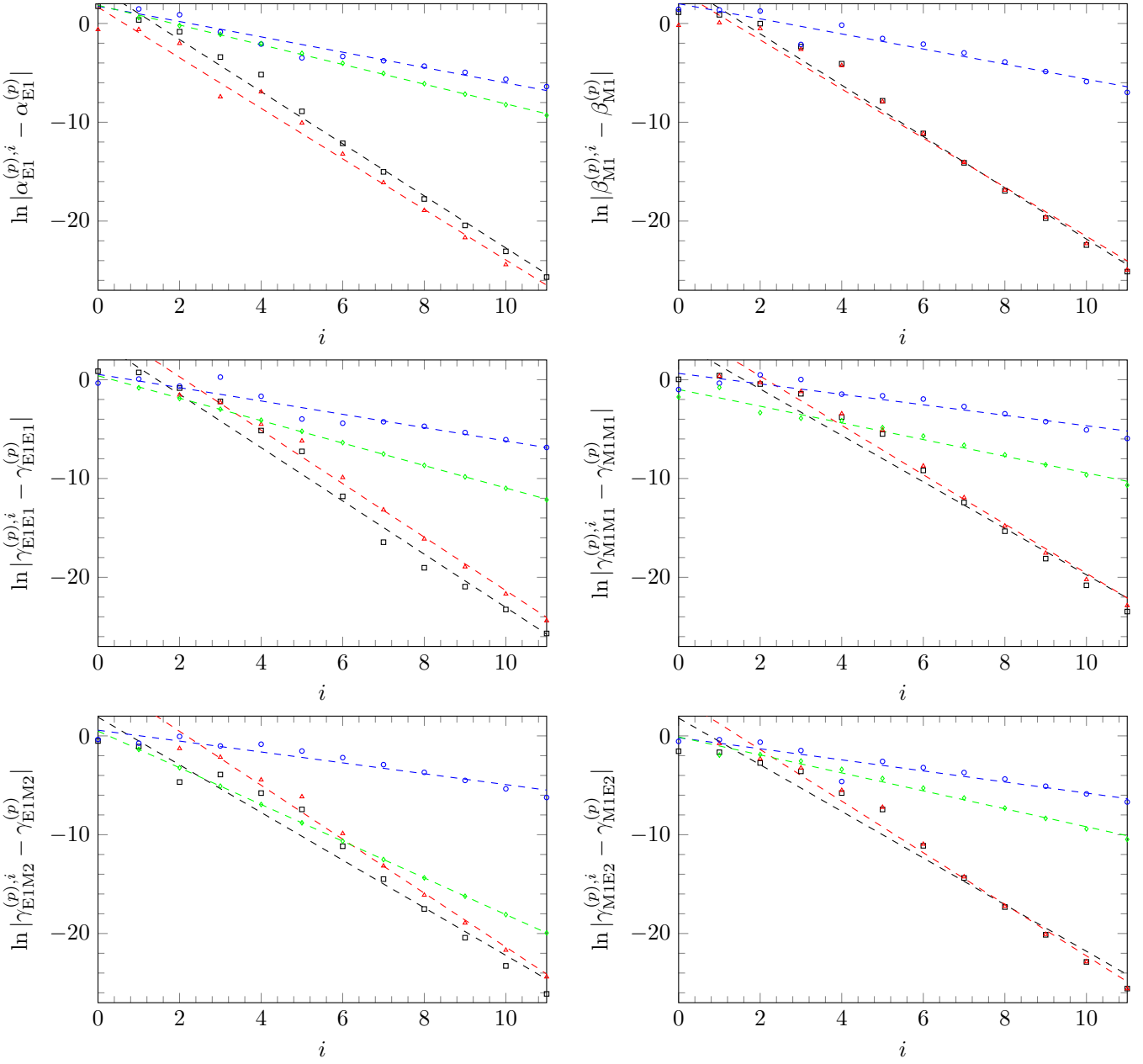


FIG. 9. Logarithmic difference of the absolute value between the HB-expanded contributions and the final, nonexpanded value for the spin-independent and spin-dependent dipole polarizabilities of the proton. i stands for the i -th order in the HB expansion. The black squares represent the q^3 contribution, the red triangles represent the q^4 contribution, the blue circles represent the ϵ^3 -loop contribution and the green diamonds represent the ϵ^3 -tree contributions. The dashed lines stand for the corresponding linear regression.

APPENDIX A: q^3 VALUES

The analytic expressions for α_{E1} , β_{M1} , α_{E2} , β_{M2} and a linear combination of the spin-dependent first-order polarizabilities for both proton and neutron were already calculated in Ref. [40] but are also given here for completeness. We have verified that our results for these quantities agree with the ones of Ref. [40]. For convenience we define $\Xi_2 = \Xi(m^2, m, M)/(\mu^2 - 4)$ where $\mu = M/m$, $\Xi_1 = \ln(\mu)$ and

$$\Xi(p^2, m_1, m_2) = \frac{1}{p^2} \sqrt{\lambda(m_1^2, m_2^2, p^2)} \ln \left[\frac{m_1^2 + m_2^2 + \sqrt{\lambda(m_1^2, m_2^2, p^2)} - p^2}{2m_1 m_2} \right],$$

$$\lambda(a, b, c) = a^2 + b^2 + c^2 - 2ab - 2bc - 2ac. \quad (\text{A1})$$

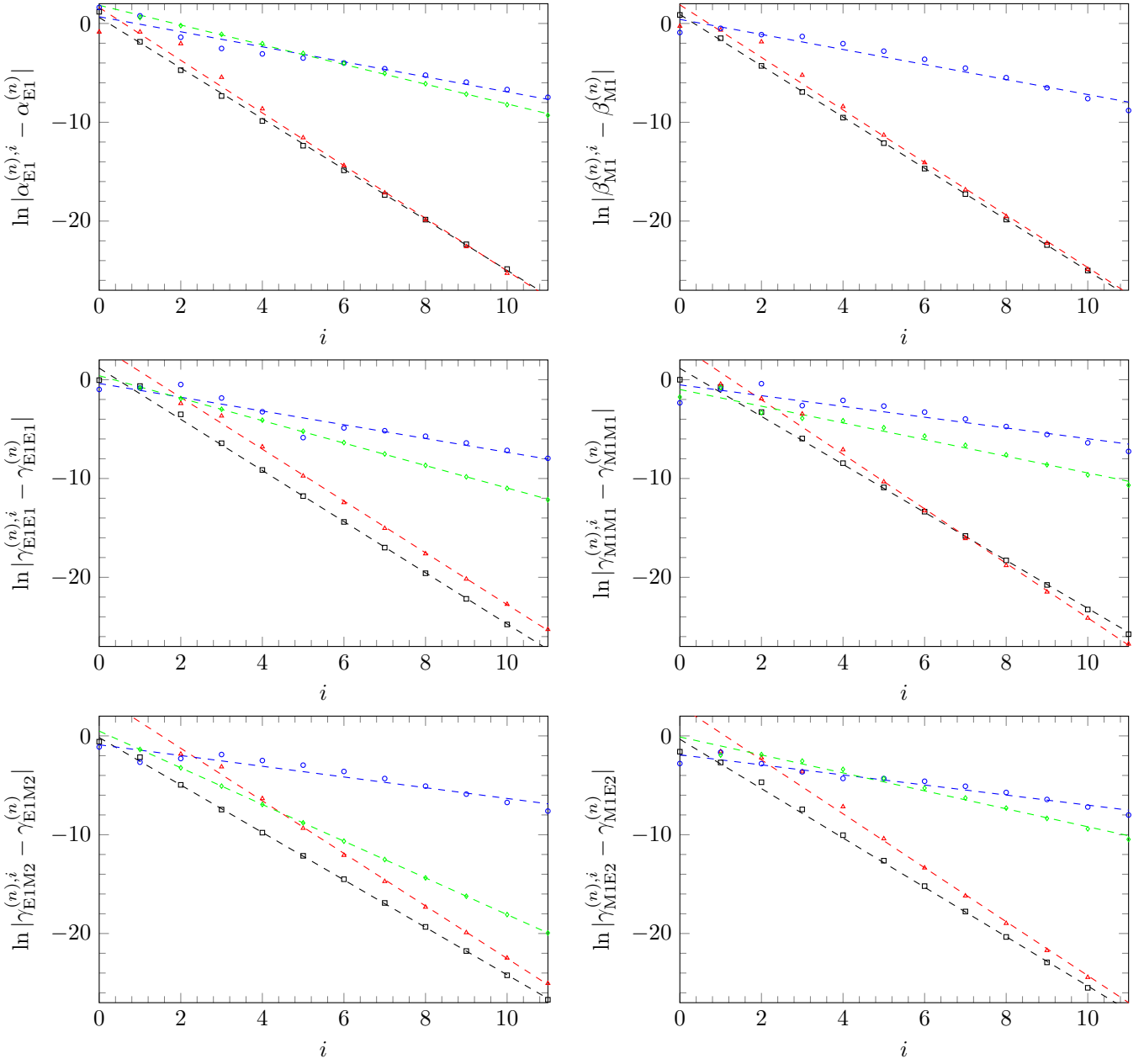


FIG. 10. Logarithmic difference of the absolute value between the HB-expanded contributions and the final, nonexpanded value for the spin-independent and spin-dependent dipole polarizabilities of the neutron. i stands for the i th order in the HB expansion. The black squares represent the q^3 contribution, the red triangles represent the q^4 contribution, the blue circles represent the ϵ^3 -loop contribution and the green diamonds represent the ϵ^3 -tree contributions. The dashed lines stand for the corresponding linear regression.

1. Proton values

a. Spin-independent first-order polarizabilities

$$\begin{aligned} \alpha_{\text{E}1}^{(p)} &= \frac{e^2 g_A^2}{192\pi^3 F^2 \mu^2 (\mu^2 - 4)^2 m} [2(-9\mu^{10} + 110\mu^8 - 479\mu^6 + 870\mu^4 - 590\mu^2 + 80)\Xi_2 \\ &\quad + (-18\mu^8 + 157\mu^6 - 407\mu^4 + 304\mu^2)] + \frac{e^2 g_A^2 (9\mu^4 - 20\mu^2 + 9)\Xi_1}{96\pi^3 F^2 m}, \\ \beta_{\text{M}1}^{(p)} &= -\frac{e^2 g_A^2}{192\pi^3 F^2 \mu^2 (\mu^2 - 4)m} [2(27\mu^8 - 212\mu^6 + 471\mu^4 - 246\mu^2 + 2)\Xi_2 \\ &\quad - (54\mu^6 - 235\mu^4 + 127\mu^2)] + \frac{e^2 g_A^2 (27\mu^4 - 50\mu^2 + 9)\Xi_1}{96\pi^3 F^2 m}. \end{aligned}$$

b. Spin-independent second-order polarizabilities

$$\begin{aligned}
\alpha_{E2}^{(p)} = & -\frac{e^2 g_A^2}{480\pi^3 F^2 \mu^4 (\mu^2 - 4)^3 m^3} [(450\mu^{14} - 7341\mu^{12} + 16584\mu^{10} - 143010\mu^8 \\
& + 212940\mu^6 - 132300\mu^4 + 18624\mu^2 + 1344)\Xi_2 - 450\mu^{12} - 5766\mu^{10} + 26437\mu^8 \\
& - 50449\mu^6 + 34592\mu^4 - 3536\mu^2] + \frac{e^2 g_A^2 \Xi_1}{160\pi^3 F^2 m^3} (150\mu^4 - 347\mu^2 + 170), \\
\beta_{M2}^{(p)} = & -\frac{e^2 g_A^2}{480\pi^3 F^2 \mu^4 (\mu^2 - 4)^2 m^3} [(990\mu^{12} - 11781\mu^{10} + 49020\mu^8 - 81330\mu^6 \\
& + 43020\mu^4 - 2700\mu^2 + 144)\Xi_2 + 990\mu^{10} - 8316\mu^8 + 20000\mu^6 - 11137\mu^4 + 92\mu^2] \\
& + \frac{e^2 g_A^2 \Xi_1}{160\pi^3 F^2 m^3} (330\mu^4 - 627\mu^2 + 170), \\
\alpha_{E1v}^{(p)} = & \frac{e^2 g_A^2}{5760\pi^3 F^2 \mu^4 (\mu^2 - 4)^4 m^3} [(-5130\mu^{16} + 102987\mu^{14} - 841656\mu^{12} \\
& + 3561462\mu^{10} - 8161020\mu^8 + 9522420\mu^6 - 4534128\mu^4 + 397824\mu^2 + 6912)\Xi_2 \\
& - 5130\mu^{14} + 85032\mu^{12} - 544482\mu^{10} + 1658251\mu^8 - 2335148\mu^6 + 1156768\mu^4 - 45504\mu^2] \\
& + \frac{e^2 g_A^2 \Xi_1}{1920\pi^3 F^2 m^3} (1710\mu^4 - 3549\mu^2 + 1210), \\
\beta_{M1v}^{(p)} = & -\frac{e^2 g_A^2}{1920\pi^3 F^2 \mu^4 (\mu^2 - 4)^3 m^3} [(1890\mu^{14} - 30129\mu^{12} + 184876\mu^{10} - 538370\mu^8 \\
& + 730660\mu^6 - 374140\mu^4 + 33056\mu^2 + 896)\Xi_2 + 1890\mu^{12} - 23514\mu^{10} + 102731\mu^8 \\
& - 178873\mu^6 + 96560\mu^4 - 4032\mu^2] + \frac{e^2 g_A^2 \Xi_1}{1920\pi^3 F^2 m^3} (1890\mu^4 - 3669\mu^2 + 1210).
\end{aligned}$$

c. Spin-dependent first-order polarizabilities

$$\begin{aligned}
\gamma_{E1E1}^{(p)} = & \frac{e^2 g_A^2}{384\pi^3 F^2 \mu^2 (\mu^2 - 4)^2 m^2} [2(-9\mu^{10} + 134\mu^8 - 739\mu^6 + 1790\mu^4 - 1650\mu^2 \\
& + 264)\Xi_2 - (18\mu^8 - 205\mu^6 + 764\mu^4 - 900\mu^2 + 80)] + \frac{e^2 g_A^2 \Xi_1}{192\pi^3 F^2 m^2} (9\mu^4 - 44\mu^2 + 29), \\
\gamma_{M1M1}^{(p)} = & \frac{e^2 g_A^2}{384\pi^3 F^2 \mu^2 (\mu^2 - 4)^2 m^2} [2(-63\mu^{10} + 744\mu^8 - 3059\mu^6 + 4970\mu^4 - 2534\mu^2 + 152)\Xi_2 \\
& - (126\mu^8 - 1047\mu^6 + 2462\mu^4 - 1308\mu^2 + 16)] + \frac{e^2 g_A^2 \Xi_1}{192\pi^3 F^2 m^2} (63\mu^4 - 114\mu^2 + 29), \\
\gamma_{E1M2}^{(p)} = & -\frac{e^2 g_A^2}{384\pi^3 F^2 \mu^2 (\mu^2 - 4)^2 m^2} [2((3(\mu^2 - 5)(3\mu^4 - 19\mu^2 + 34)\mu^2 + 46)\mu^2 \\
& + 56)\Xi_2 + (-18\mu^8 + 141\mu^6 - 284\mu^4 + 4\mu^2 + 16)] + \frac{e^2 g_A^2 \Xi_1}{64\pi^3 F^2 m^2} (3\mu^4 - 4\mu^2 - 1), \\
\gamma_{M1E2}^{(p)} = & \frac{e^2 g_A^2}{384\pi^3 F^2 \mu^2 (\mu^2 - 4) m^2} [2(9\mu^8 - 68\mu^6 + 141\mu^4 - 66\mu^2 + 6)\Xi_2 + (18\mu^6 - 73\mu^4 + 30\mu^2 - 4)] \\
& - \frac{e^2 g_A^2 \Xi_1}{192\pi^3 F^2 m^2} (9\mu^4 - 14\mu^2 + 3).
\end{aligned}$$

d. Spin-dependent second-order polarizabilities

$$\begin{aligned}
\gamma_{E2E2}^{(p)} = & -\frac{e^2 g_A^2}{138240 \pi^3 F^2 \mu^4 (\mu^2 - 4)^3 m^4} [(6030\mu^{14} - 107814\mu^{12} + 764796\mu^{10} \\
& - 2694300\mu^8 + 4759500\mu^6 - 3591840\mu^4 + 577056\mu^2 + 36096) \Xi_2 + 6030\mu^{12} \\
& - 86709\mu^{10} + 461861\mu^8 - 1079504\mu^6 + 954200\mu^4 - 100864\mu^2 - 3328] \\
& + \frac{e^2 g_A^2 \Xi_1}{23040 \pi^3 F^2 m^4} (1005\mu^4 - 3899\mu^2 + 2530), \\
\gamma_{M2M2}^{(p)} = & -\frac{e^2 g_A^2}{138240 \pi^3 F^2 \mu^4 (\mu^2 - 4)^3 m^4} [(29250\mu^{14} - 462354\mu^{12} + 2802636\mu^{10} \\
& - 8007300\mu^8 + 10510020\mu^6 - 5011200\mu^4 + 379296\mu^2 + 7296) \Xi_2 + 29250\mu^{12} \\
& - 359979\mu^{10} + 1545103\mu^8 - 2601080\mu^6 + 1278024\mu^4 - 40480\mu^2 - 256] \\
& + \frac{e^2 g_A^2 \Xi_1}{23040 \pi^3 F^2 m^4} (4875\mu^4 - 8809\mu^2 + 2530), \\
\gamma_{E2M3}^{(p)} = & \frac{e^2 g_A^2}{69120 \pi^3 F^2 \mu^4 (\mu^2 - 4)^3 m^4} [(-1710\mu^{14} + 26382\mu^{12} - 153696\mu^{10} \\
& + 407652\mu^8 - 447780\mu^6 + 91920\mu^4 + 28032\mu^2 + 3072) \Xi_2 - 1710\mu^{12} + 20397\mu^{10} \\
& - 82493\mu^8 + 119300\mu^6 - 19808\mu^4 - 7040\mu^2 - 512] + \frac{e^2 g_A^2 \Xi_1}{11520 \pi^3 F^2 m^4} (285\mu^4 - 407\mu^2 - 32), \\
\gamma_{M2E3}^{(p)} = & \frac{e^2 g_A^2}{69120 \pi^3 F^2 \mu^4 (\mu^2 - 4)^2 m^4} [(912\mu^{12} - 11118\mu^{10} + 42072\mu^8 - 58260\mu^6 + 19860\mu^4 - 1920\mu^2 \\
& - 768) \Xi_2 + 990\mu^{10} - 7653\mu^8 + 15413\mu^6 - 4112\mu^4 + 832\mu^2 + 128] \\
& - \frac{e^2 g_A^2 \Xi_1}{11520 \pi^3 F^2 m^4} (165\mu^4 - 203\mu^2 + 32), \\
\gamma_{E1E1v}^{(p)} = & \frac{e^2 g_A^2}{46080 \pi^3 F^2 \mu^4 (\mu^2 - 4)^4 m^4} [(-33750\mu^{16} + 688446\mu^{14} - 5745756\mu^{12} \\
& + 25026300\mu^{10} - 59825628\mu^8 + 74731920\mu^6 - 40404960\mu^4 + 4788480\mu^2 \\
& + 299520) \Xi_2 - 33750\mu^{14} + 570321\mu^{12} - 3752313\mu^{10} + 11906948\mu^8 - 18015768\mu^6 \\
& + 10422016\mu^4 - 748416\mu^2 - 64512] + \frac{e^2 g_A^2 \Xi_1}{7680 \pi^3 F^2 m^4} (5625\mu^4 - 13491\mu^2 + 6038), \\
\gamma_{M1M1v}^{(p)} = & \frac{e^2 g_A^2}{15360 \pi^3 F^2 \mu^4 (\mu^2 - 4)^4 m^4} [(-18270\mu^{16} + 364014\mu^{14} - 2946868\mu^{12} \\
& + 12320172\mu^{10} - 27795996\mu^8 + 31816880\mu^6 - 14929824\mu^4 + 1383552\mu^2 \\
& + 45056) \Xi_2 - 18270\mu^{14} + 300069\mu^{12} - 1898193\mu^{10} + 5684492\mu^8 - 7821048\mu^6 \\
& + 3793952\mu^4 - 184320\mu^2 - 1024] + \frac{e^2 g_A^2 \Xi_1}{7680 \pi^3 F^2 m^4} (9135\mu^4 - 17577\mu^2 + 6038), \\
\gamma_{E1M2v}^{(p)} = & -\frac{e^2 g_A^2}{115200 \pi^3 F^2 \mu^4 (\mu^2 - 4)^4 m^4} [(72090\mu^{16} - 1426818\mu^{14} + 11444436\mu^{12} \\
& - 47196324\mu^{10} + 104160132\mu^8 - 114538560\mu^6 + 48945312\mu^4 - 3267456\mu^2
\end{aligned}$$

$$\begin{aligned}
& + 3072) \Xi_2 + 72090\mu^{14} - 1174503\mu^{12} + 7339287\mu^{10} - 21533144\mu^8 + 28502616\mu^6 \\
& - 12369760\mu^4 + 243968\mu^2 + 7168] + \frac{e^2 g_A^2 \Xi_1}{19200\pi^3 F^2 m^4} (12015\mu^4 - 21533\mu^2 + 5922), \\
\gamma_{M1E2v}^{(p)} = & - \frac{e^2 g_A^2}{115200\pi^3 F^2 \mu^4 (\mu^2 - 4)^3 m^4} [(20790\mu^{14} - 358638\mu^{12} + 2436924\mu^{10} \\
& - 8138508\mu^8 + 13400220\mu^6 - 9090480\mu^4 + 1224672\mu^2 + 54912) \Xi_2 + 20790\mu^{12} \\
& - 285873\mu^{10} + 1438497\mu^8 - 3110380\mu^6 + 2403672\mu^4 - 197280\mu^2 + 3328] \\
& + \frac{e^2 g_A^2 \Xi_1}{19200\pi^3 F^2 m^4} 7(495\mu^4 - 1609\mu^2 + 846).
\end{aligned}$$

2. Neutron values

a. Spin-independent first-order polarizabilities

$$\begin{aligned}
\alpha_{E1}^{(n)} = & \frac{e^2 g_A^2}{192\pi^3 F^2 \mu^2 (\mu^2 - 4)^2 m} [2(-3\mu^6 + 30\mu^4 - 98\mu^2 + 80) \Xi_2 - (\mu^4 - 16\mu^2)] + \frac{e^2 g_A^2 \Xi_1}{32\pi^3 F^2 m}, \\
\beta_{M1}^{(n)} = & - \frac{e^2 g_A^2}{192\pi^3 F^2 \mu^2 (\mu^2 - 4)m} [2(3(\mu^2 - 6)\mu^2 + 2) \Xi_2 - 11\mu^2] + \frac{e^2 g_A^2 \Xi_1}{32\pi^3 F^2 m}.
\end{aligned}$$

b. Spin-independent second-order polarizabilities

$$\begin{aligned}
\alpha_{E2}^{(n)} = & - \frac{e^2 g_A^2}{480\pi^3 F^2 \mu^4 (\mu^2 - 4)^3 m^3} [(120\mu^{10} - 1680\mu^8 + 8400\mu^6 - 17700\mu^4 + 9984\mu^2 \\
& + 1344) \Xi_2 + 113\mu^8 - 1119\mu^6 + 4272\mu^4 - 3536\mu^2] + \frac{e^2 g_A^2 \Xi_1}{4\pi^3 F^2 m^3}, \\
\beta_{M2}^{(n)} = & \frac{e^2 g_A^2}{480\pi^3 F^2 \mu^4 (\mu^2 - 4)^2 m^3} [(-120\mu^8 + 1200\mu^6 - 3600\mu^4 + 1500\mu^2 - 144) \Xi_2 \\
& - 127\mu^6 + 885\mu^4 - 92\mu^2] + \frac{e^2 g_A^2 \Xi_1}{4\pi^3 F^2 m^3}, \\
\alpha_{E1v}^{(n)} = & \frac{e^2 g_A^2}{5760\pi^3 F^2 \mu^4 (\mu^2 - 4)^4 m^3} [(-240\mu^{12} + 4320\mu^{10} - 30240\mu^8 + 97380\mu^6 - 132528\mu^4 + 38784\mu^2 \\
& + 6912) \Xi_2 - 261\mu^{10} + 4031\mu^8 - 18540\mu^6 + 28928\mu^4 - 3520\mu^2] + \frac{e^2 g_A^2 \Xi_1}{24\pi^3 F^2 m^3}, \\
\beta_{M1v}^{(n)} = & - \frac{e^2 g_A^2}{1920\pi^3 F^2 \mu^4 (\mu^2 - 4)^3 m^3} [(80\mu^{10} - 1120\mu^8 + 5600\mu^6 - 12340\mu^4 \\
& + 7136\mu^2 + 896) \Xi_2 + 73\mu^8 - 687\mu^6 + 3168\mu^4 - 2752\mu^2] + \frac{e^2 g_A^2 \Xi_1}{24\pi^3 F^2 m^3}.
\end{aligned}$$

c. Spin-dependent first-order polarizabilities

$$\begin{aligned}
\gamma_{E1E1}^{(p)} = & - \frac{e^2 g_A^2}{192\pi^3 F^2 \mu^2 (\mu^2 - 4)m^2} [(5(\mu^2 - 6)\mu^2 + 22) \Xi_2 + (10 - 7\mu^2)] + \frac{5e^2 g_A^2 \Xi_1}{192\pi^3 F^2 m^2}, \\
\gamma_{M1M1}^{(p)} = & \frac{e^2 g_A^2}{192\pi^3 F^2 \mu^2 (\mu^2 - 4)^2 m^2} [(-5\mu^6 + 50\mu^4 - 166\mu^2 + 88) \Xi_2 - (3\mu^4 - 38\mu^2 + 8)] + \frac{5e^2 g_A^2 \Xi_1}{192\pi^3 F^2 m^2},
\end{aligned}$$

$$\gamma_{\text{E1M2}}^{(p)} = \frac{e^2 g_A^2}{192\pi^3 F^2 \mu^2 (\mu^2 - 4)^2 m^2} [(\mu^6 - 10\mu^4 + 46\mu^2 - 40)\Xi_2 - (\mu^4 + 10\mu^2 - 8)] - \frac{e^2 g_A^2 \Xi_1}{192\pi^3 F^2 m^2},$$

$$\gamma_{\text{M1E2}}^{(p)} = \frac{e^2 g_A^2}{192\pi^3 F^2 \mu^2 (\mu^2 - 4) m^2} [(\mu^4 - 6\mu^2 - 2)\Xi_2 + (3\mu^2 - 2)] - \frac{e^2 g_A^2 \Xi_1}{192\pi^3 F^2 m^2}.$$

d. Spin-dependent second-order polarizabilities

$$\gamma_{\text{E2E2}}^{(n)} = -\frac{e^2 g_A^2}{34560\pi^3 F^2 \mu^4 (\mu^2 - 4)^3 m^4} [(450\mu^{10} - 6300\mu^8 + 31410\mu^6 - 62340\mu^4 + 29304\mu^2 + 9024)\Xi_2 + 472\mu^8 - 4927\mu^6 + 15802\mu^4 - 11136\mu^2 - 832] + \frac{e^2 g_A^2 5\Xi_1}{384\pi^3 F^2 m^4},$$

$$\gamma_{\text{M2M2}}^{(n)} = -\frac{e^2 g_A^2}{34560\pi^3 F^2 \mu^4 (\mu^2 - 4)^3 m^4} [(450\mu^{10} - 6300\mu^8 + 31590\mu^6 - 74220\mu^4 + 27864\mu^2 + 1824)\Xi_2 + 428\mu^8 - 4495\mu^6 + 16486\mu^4 - 6280\mu^2 - 64] + \frac{e^2 g_A^2 5\Xi_1}{384\pi^3 F^2 m^4},$$

$$\gamma_{\text{E2M3}}^{(n)} = \frac{e^2 g_A^2}{17280\pi^3 F^2 \mu^4 (\mu^2 - 4)^3 m^4} [(36\mu^{10} - 504\mu^8 + 2610\mu^6 - 6780\mu^4 + 3888\mu^2 + 768)\Xi_2 + 14\mu^8 - 155\mu^6 + 1844\mu^4 - 1440\mu^2 - 128] - \frac{e^2 g_A^2 \Xi_1}{480\pi^3 F^2 m^4},$$

$$\gamma_{\text{M2E3}}^{(n)} = \frac{e^2 g_A^2}{17280\pi^3 F^2 \mu^4 (\mu^2 - 4)^2 m^4} [(36\mu^8 - 360\mu^6 + 990\mu^4 + 60\mu^2 - 192)\Xi_2 + 58\mu^6 - 355\mu^4 - 32\mu^2 + 32] - \frac{e^2 g_A^2 \Xi_1}{480\pi^3 F^2 m^4},$$

$$\gamma_{\text{E1E1v}}^{(n)} = -\frac{e^2 g_A^2}{11520\pi^3 F^2 \mu^4 (\mu^2 - 4)^3 m^4} [(342\mu^{10} - 4788\mu^8 + 24210\mu^6 - 51780\mu^4 + 26664\mu^2 + 3744)\Xi_2 + 276\mu^8 - 2935\mu^6 + 11506\mu^4 - 4680\mu^2 - 4032] + \frac{19e^2 g_A^2 \Xi_1}{640\pi^3 F^2 m^4},$$

$$\gamma_{\text{M1M1v}}^{(n)} = \frac{e^2 g_A^2}{3840\pi^3 F^2 \mu^4 (\mu^2 - 4)^4 m^4} [(-114\mu^{12} + 2052\mu^{10} - 14274\mu^8 + 45700\mu^6 - 65928\mu^4 + 21984\mu^2 + 8192)\Xi_1 - 136\mu^{10} + 1969\mu^8 - 8702\mu^6 + 17624\mu^4 - 8960\mu^2 - 256] + \frac{19e^2 g_A^2 \Xi_1}{640\pi^3 F^2 m^4},$$

$$\gamma_{\text{E1M2v}}^{(n)} = \frac{e^2 g_A^2}{14400\pi^3 F^2 \mu^4 (\mu^2 - 4)^4 m^4} [(-393\mu^{12} + 7074\mu^{10} - 49923\mu^8 + 174660\mu^6 - 279684\mu^4 + 127152\mu^2 + 1536)\Xi_2 - 294\mu^{10} + 4282\mu^8 - 28623\mu^6 + 68156\mu^4 - 30016\mu^2 - 896] + \frac{e^2 g_A^2 \Xi_1}{4800\pi^3 F^2 m^4},$$

$$\gamma_{\text{M1E2v}}^{(n)} = -\frac{e^2 g_A^2}{14400\pi^3 F^2 \mu^4 (\mu^2 - 4)^3 m^4} [(393\mu^{10} - 5502\mu^8 + 27105\mu^6 - 49140\mu^4 + 19044\mu^2 + 8784)\Xi_2 + (\mu^2 - 1)(492\mu^6 - 4613\mu^4 + 8404\mu^2 - 416)] + \frac{131e^2 g_A^2 \Xi_1}{4800\pi^3 F^2 m^4}.$$

APPENDIX B: ϵ^3 -TREE VALUES

We give here the explicit analytic expressions for the Δ -tree contribution to the nucleon polarizabilities:

$$\alpha_{E1} = -\frac{b_1^2 e^2 (\mu_\Delta^2 + \mu_\Delta + 1)}{18\pi m^3 \mu_\Delta^2 (\mu_\Delta + 1)},$$

$$\beta_{M1} = \frac{b_1^2 e^2}{18\pi m^3(\mu_\Delta - 1)},$$

$$\alpha_{E2} = \frac{b_1^2 e^2(6\mu_\Delta^2 + 3\mu_\Delta + 1)}{12\pi m^5(\mu_\Delta - 1)\mu_\Delta^2(\mu_\Delta + 1)^2},$$

$$\beta_{M2} = -\frac{b_1^2 e^2(6\mu_\Delta^2 - 3\mu_\Delta + 1)}{12\pi m^5(\mu_\Delta - 1)^2\mu_\Delta^2(\mu_\Delta + 1)},$$

$$\alpha_{E1v} = -\frac{b_1^2 e^2(18\mu_\Delta^4 + 15\mu_\Delta^3 + 31\mu_\Delta^2 + 9\mu_\Delta + 7)}{144\pi m^5(\mu_\Delta - 1)^2\mu_\Delta^2(\mu_\Delta + 1)^3},$$

$$\beta_{M1v} = \frac{b_1^2 e^2(18\mu_\Delta^4 - 15\mu_\Delta^3 + 31\mu_\Delta^2 - 9\mu_\Delta + 7)}{144\pi m^5(\mu_\Delta - 1)^3\mu_\Delta^2(\mu_\Delta + 1)^2},$$

$$\alpha_{E3} = -\frac{5b_1^2 e^2(6\mu_\Delta^2 + 3\mu_\Delta + 1)}{4\pi m^7(\mu_\Delta - 1)^2\mu_\Delta^2(\mu_\Delta + 1)^3},$$

$$\beta_{M3} = \frac{5b_1^2 e^2(6\mu_\Delta^2 - 3\mu_\Delta + 1)}{4\pi m^7(\mu_\Delta - 1)^3\mu_\Delta^2(\mu_\Delta + 1)^2},$$

$$\alpha_{E2v} = \frac{b_1^2 e^2(42\mu_\Delta^4 + 27\mu_\Delta^3 + 67\mu_\Delta^2 + 23\mu_\Delta + 13)}{18\pi m^7(\mu_\Delta - 1)^3\mu_\Delta^2(\mu_\Delta + 1)^4},$$

$$\beta_{M2v} = -\frac{b_1^2 e^2(42\mu_\Delta^4 - 27\mu_\Delta^3 + 67\mu_\Delta^2 - 23\mu_\Delta + 13)}{18\pi m^7(\mu_\Delta - 1)^4\mu_\Delta^2(\mu_\Delta + 1)^3},$$

$$\alpha_{E1v^2} = -\frac{b_1^2 e^2(162\mu_\Delta^6 + 141\mu_\Delta^5 + 243\mu_\Delta^4 + 188\mu_\Delta^3 + 258\mu_\Delta^2 + 71\mu_\Delta + 57)}{360\pi m^7(\mu_\Delta - 1)^4\mu_\Delta^2(\mu_\Delta + 1)^5},$$

$$\beta_{M1v^2} = \frac{b_1^2 e^2(162\mu_\Delta^6 - 141\mu_\Delta^5 + 243\mu_\Delta^4 - 188\mu_\Delta^3 + 258\mu_\Delta^2 - 71\mu_\Delta + 57)}{360\pi m^7(\mu_\Delta - 1)^5\mu_\Delta^2(\mu_\Delta + 1)^4}$$

$$\gamma_{E1E1} = -\frac{b_1^2 e^2(\mu_\Delta^3 + \mu_\Delta^2 - 1)}{18\pi m^4(\mu_\Delta - 1)\mu_\Delta(\mu_\Delta + 1)^2},$$

$$\gamma_{M1M1} = \frac{b_1^2 e^2(2\mu_\Delta^4 - 3\mu_\Delta^3 + \mu_\Delta^2 + 3\mu_\Delta - 1)}{36\pi m^4(\mu_\Delta - 1)^2\mu_\Delta^2(\mu_\Delta + 1)},$$

$$\gamma_{E1M2} = -\frac{b_1^2 e^2(2\mu_\Delta - 1)}{36\pi m^4(\mu_\Delta^2 - 1)},$$

$$\gamma_{M1E2} = \frac{b_1^2 e^2(2\mu_\Delta^3 + 1)}{36\pi m^4\mu_\Delta^2(\mu_\Delta^2 - 1)},$$

$$\gamma_{E2E2} = -\frac{b_1^2 e^2(4\mu_\Delta^6 + 3\mu_\Delta^5 - 17\mu_\Delta^4 - 8\mu_\Delta^3 + 4\mu_\Delta^2 + 57\mu_\Delta + 13)}{1728\pi m^6(\mu_\Delta - 1)^2\mu_\Delta^2(\mu_\Delta + 1)^3},$$

$$\gamma_{M2M2} = \frac{b_1^2 e^2(4\mu_\Delta^6 - 5\mu_\Delta^5 - 15\mu_\Delta^4 + 12\mu_\Delta^3 - 59\mu_\Delta + 15)}{1728\pi m^6(\mu_\Delta - 1)^3(\mu_\Delta^2)^2(\mu_\Delta + 1)^2},$$

$$\gamma_{E2M3} = -\frac{b_1^2 e^2(4\mu_\Delta^5 - \mu_\Delta^4 - 16\mu_\Delta^3 + 8\mu_\Delta^2 - 4\mu_\Delta + 1)}{864\pi m^6\mu_\Delta^2(\mu_\Delta^2 - 1)^2},$$

$$\gamma_{M2E3} = \frac{b_1^2 e^2(4\mu_\Delta^5 - \mu_\Delta^4 - 16\mu_\Delta^3 - 4\mu_\Delta^2 - 4\mu_\Delta + 3)}{864\pi m^6\mu_\Delta^2(\mu_\Delta^2 - 1)^2},$$

$$\gamma_{E1E1v} = \frac{b_1^2 e^2(12\mu_\Delta^8 + 9\mu_\Delta^7 - 63\mu_\Delta^6 - 45\mu_\Delta^5 - 53\mu_\Delta^4 - 69\mu_\Delta^3 - 93\mu_\Delta^2 + 73\mu_\Delta + 37)}{576\pi m^6(\mu_\Delta - 1)^3\mu_\Delta^2(\mu_\Delta + 1)^4},$$

$$\gamma_{M1M1v} = -\frac{b_1^2 e^2(12\mu_\Delta^8 - 15\mu_\Delta^7 - 57\mu_\Delta^6 + 63\mu_\Delta^5 - 71\mu_\Delta^4 + 51\mu_\Delta^3 - 75\mu_\Delta^2 - 67\mu_\Delta + 31)}{576\pi m^6(\mu_\Delta - 1)^4\mu_\Delta^2(\mu_\Delta + 1)^3},$$

$$\gamma_{E1M2\nu} = \frac{b_1^2 e^2 (36\mu_\Delta^7 - 9\mu_\Delta^6 - 180\mu_\Delta^5 + 33\mu_\Delta^4 - 152\mu_\Delta^3 - 11\mu_\Delta^2 - 104\mu_\Delta + 67)}{1440\pi m^6 \mu_\Delta^2 (\mu_\Delta^2 - 1)^3},$$

$$\gamma_{M1E2\nu} = -\frac{b_1^2 e^2 (36\mu_\Delta^7 - 9\mu_\Delta^6 - 180\mu_\Delta^5 + 21\mu_\Delta^4 - 152\mu_\Delta^3 - 43\mu_\Delta^2 - 104\mu_\Delta - 49)}{1440\pi m^6 \mu_\Delta^2 (\mu_\Delta^2 - 1)^3}.$$

APPENDIX C: ϵ^3 -LOOP VALUES

Due to the length of the expressions, we only provide here the expressions for the first-order polarizabilities. In addition to the definition from Appendix A, we now have m_Δ as an additional mass scale and it is convenient to introduce $\mu_\Delta = m_\Delta/m$, $\Xi_3 = \ln(\mu_\Delta)$ as well as $\Xi_4 = \Xi(m^2, m_\Delta, M)/(\mu^2 - 4)$.

1. Proton values

a. Spin-independent first-order polarizabilities

$$\begin{aligned} \alpha_{E1}^{(p)} = & -\frac{e^2 h_A^2 \Xi_4}{7776 F^2 m \pi^3 \mu_\Delta^6 (-\mu^2 + \mu_\Delta^2 - 2\mu_\Delta + 1)^2 (-\mu^2 + \mu_\Delta^2 + 2\mu_\Delta + 1)} [-81\mu_\Delta^{16} \\ & + 228\mu_\Delta^{15} + (486\mu^2 - 56)\mu_\Delta^{14} - 2(522\mu^2 + 325)\mu_\Delta^{13} + (-1215\mu^4 - 136\mu^2 \\ & + 445)\mu_\Delta^{12} + 6(300\mu^4 + 301\mu^2 + 148)\mu_\Delta^{11} + 30(54\mu^6 + 34\mu^4 + 32\mu^2 - 11)\mu_\Delta^{10} \\ & - 6(220\mu^6 + 204\mu^4 + 343\mu^2 + 126)\mu_\Delta^9 - (1215\mu^8 + 1586\mu^6 + 3036\mu^4 + 666\mu^2 \\ & + 407)\mu_\Delta^8 + 2(90\mu^8 - 325\mu^6 + 573\mu^4 + 3\mu^2 + 581)\mu_\Delta^7 + 2(243\mu^{10} + 412\mu^8 \\ & + 692\mu^6 - 315\mu^4 + 295\mu^2 - 25)\mu_\Delta^6 + 6(42\mu^{10} + 164\mu^8 - 121\mu^6 + 6\mu^4 + 171\mu^2 \\ & - 262)\mu_\Delta^5 - 3(\mu^2 - 1)^2(27\mu^8 + 34\mu^6 - 32\mu^4 - 462\mu^2 - 449)\mu_\Delta^4 \\ & - 6(\mu^2 - 1)^3(16\mu^6 + 90\mu^4 + 83\mu^2 + 91)\mu_\Delta^3 - 28(\mu^2 - 1)^4(5\mu^4 + 17\mu^2 + 32)\mu_\Delta^2 \\ & - 14(\mu^2 - 1)^5(\mu^2 + 11)\mu_\Delta + 14(\mu^2 - 1)^6(\mu^2 + 2)] \\ & + \frac{e^2 h_A^2 \Xi_1}{7776 F^2 m \pi^3 \mu_\Delta^6} [81\mu_\Delta^{12} - 66\mu_\Delta^{11} - 4(81\mu^2 + 19)\mu_\Delta^{10} + 6(17\mu^2 + 56)\mu_\Delta^9 + (486\mu^4 \\ & + 482\mu^2 + 440)\mu_\Delta^8 + 6(15\mu^4 + 29\mu^2 + 13)\mu_\Delta^7 - 2(162\mu^6 + 326\mu^4 + 248\mu^2 \\ & + 131)\mu_\Delta^6 - 6(37\mu^6 + 138\mu^4 + 22\mu^2 + 52)\mu_\Delta^5 + (81\mu^8 + 148\mu^6 - 84\mu^4 - 324\mu^2 \\ & + 67)\mu_\Delta^4 + 6(16\mu^8 + 46\mu^6 - 35\mu^4 + 104\mu^2 - 77)\mu_\Delta^3 + 28(4\mu^8 + 4\mu^6 - 3\mu^4 \\ & + 22\mu^2 - 17)\mu_\Delta^2 + 42(\mu^8 + 2\mu^6 + 12\mu^4 - 14\mu^2 + 5)\mu_\Delta - 14(\mu^{10} - 2\mu^8 - 2\mu^6 - 8\mu^4 + 7\mu^2 - 2)] \\ & + \frac{e^2 h_A^2 \Xi_3}{7776 F^2 m \pi^3 \mu_\Delta^6} [-81\mu_\Delta^{12} + 66\mu_\Delta^{11} + 4(81\mu^2 + 19)\mu_\Delta^{10} - 6(17\mu^2 + 56)\mu_\Delta^9 \\ & - 2(243\mu^4 + 241\mu^2 + 220)\mu_\Delta^8 - 6(15\mu^4 + 29\mu^2 + 13)\mu_\Delta^7 + (324\mu^6 + 652\mu^4 \\ & + 496\mu^2 + 262)\mu_\Delta^6 + 6(37\mu^6 + 138\mu^4 + 22\mu^2 - 170)\mu_\Delta^5 + (-81\mu^8 - 148\mu^6 + 84\mu^4 \\ & + 324\mu^2 + 31)\mu_\Delta^4 - 6(16\mu^8 + 46\mu^6 - 35\mu^4 - 104\mu^2 + 77)\mu_\Delta^3 - 28(\mu^2 - 1)^2(4\mu^4 \\ & + 12\mu^2 + 17)\mu_\Delta^2 - 42(\mu^2 - 1)^3(\mu^2 + 5)\mu_\Delta + 14(\mu^2 - 1)^4(\mu^2 + 2)] \end{aligned}$$

$$\begin{aligned}
& + \frac{e^2 h_A^2}{46656 F^2 m \pi^3 \mu_\Delta^6 (-\mu^2 + \mu_\Delta^2 - 2\mu_\Delta + 1)} [486\mu_\Delta^{12} - 1368\mu_\Delta^{11} - 3(648\mu^2 - 355)\mu_\Delta^{10} \\
& + 168(21\mu^2 + 11)\mu_\Delta^9 + 3(972\mu^4 + 253\mu^2 - 425)\mu_\Delta^8 - 12(198\mu^4 + 325\mu^2 \\
& + 432)\mu_\Delta^7 - (1944\mu^6 + 4209\mu^4 + 4278\mu^2 - 6401)\mu_\Delta^6 - 4(90\mu^6 + 144\mu^4 - 1773\mu^2 \\
& + 598)\mu_\Delta^5 + (486\mu^8 + 1797\mu^6 + 3573\mu^4 - 4251\mu^2 + 1501)\mu_\Delta^4 + 2(288\mu^8 + 1272\mu^6 \\
& - 999\mu^4 - 818\mu^2 + 82)\mu_\Delta^3 + 14(48\mu^8 + 57\mu^6 - 510\mu^4 + 427\mu^2 - 85)\mu_\Delta^2 + 14(6\mu^8 \\
& - 135\mu^6 + 85\mu^4 + 4\mu^2 - 14)\mu_\Delta - 14(6\mu^{10} - 15\mu^8 + 73\mu^6 - 108\mu^4 + 54\mu^2 - 10)], \\
\beta_{M1}^{(p)} = & - \frac{e^2 h_A^2 \Xi_4}{7776 F^2 m \pi^3 \mu_\Delta^6 (-\mu^2 + \mu_\Delta^2 - 2\mu_\Delta + 1)} [-243\mu_\Delta^{12} + 456\mu_\Delta^{11} + 2(486\mu^2 + 71)\mu_\Delta^{10} \\
& - 8(147\mu^2 + 136)\mu_\Delta^9 - 2(729\mu^4 + 385\mu^2 - 477)\mu_\Delta^8 + 2(396\mu^4 + 715\mu^2 \\
& + 388)\mu_\Delta^7 + 2(486\mu^6 + 479\mu^4 + 44\mu^2 - 950)\mu_\Delta^6 + 2(60\mu^6 - 48\mu^4 - 613\mu^2 + 477)\mu_\Delta^5 \\
& + (-243\mu^8 - 160\mu^6 - 228\mu^4 + 620\mu^2 + 95)\mu_\Delta^4 - 4(48\mu^8 + 58\mu^6 \\
& - 145\mu^4 - 97\mu^2 + 136)\mu_\Delta^3 - 4(\mu^2 - 1)^2(46\mu^4 + 35\mu^2 - 102)\mu_\Delta^2 - 14(\mu^2 - 1)^4\mu_\Delta + 14(\mu^2 - 1)^5] \\
& - \frac{e^2 h_A^2 \Xi_1}{7776 F^2 m \pi^3 \mu_\Delta^6} [-243\mu_\Delta^{12} - 30\mu_\Delta^{11} + (972\mu^2 + 568)\mu_\Delta^{10} + 6(47\mu^2 - 63)\mu_\Delta^9 \\
& - 2(729\mu^4 + 619\mu^2 + 256)\mu_\Delta^8 - 6(111\mu^4 + 59\mu^2 - 203)\mu_\Delta^7 + 2(486\mu^6 + 308\mu^4 \\
& + 62\mu^2 + 47)\mu_\Delta^6 + 6(101\mu^6 + 111\mu^4 - 58\mu^2 - 142)\mu_\Delta^5 + (-243\mu^8 + 224\mu^6 \\
& + 336\mu^4 + 197)\mu_\Delta^4 - 12(16\mu^8 - 9\mu^6 - 41\mu^4 - 52\mu^2 + 18)\mu_\Delta^3 - 4(46\mu^8 - 71\mu^6 - 84\mu^4 - 197\mu^2 \\
& + 88)\mu_\Delta^2 - 42(\mu^8 - 4\mu^6 - 18\mu^4 + 4\mu^2 - 1)\mu_\Delta + 14(\mu^{10} - 5\mu^8 + 10\mu^6 + 22\mu^4 - 5\mu^2 + 1)] \\
& + \frac{e^2 h_A^2 \Xi_3}{7776 F^2 m \pi^3 \mu_\Delta^6} [-243\mu_\Delta^{12} - 30\mu_\Delta^{11} + (972\mu^2 + 568)\mu_\Delta^{10} + 6(47\mu^2 - 63)\mu_\Delta^9 \\
& - 2(729\mu^4 + 619\mu^2 + 256)\mu_\Delta^8 - 6(111\mu^4 + 59\mu^2 - 203)\mu_\Delta^7 + 2(486\mu^6 + 308\mu^4 \\
& + 62\mu^2 + 47)\mu_\Delta^6 + 6(101\mu^6 + 111\mu^4 - 58\mu^2 + 80)\mu_\Delta^5 + (-243\mu^8 + 224\mu^6 + 336\mu^4 \\
& - 233)\mu_\Delta^4 - 12(16\mu^8 - 9\mu^6 - 41\mu^4 + 52\mu^2 - 18)\mu_\Delta^3 - 4(\mu^2 - 1)^2(46\mu^4 + 21\mu^2 \\
& - 88)\mu_\Delta^2 - 42(\mu^2 - 1)^4\mu_\Delta + 14(\mu^2 - 1)^5] \\
& + \frac{e^2 h_A^2}{46656 F^2 m \pi^3 \mu_\Delta^6} [1458\mu_\Delta^{10} + 180\mu_\Delta^9 - 3(1458\mu^2 + 893)\mu_\Delta^8 - 18(84\mu^2 - 131)\mu_\Delta^7 \\
& + 6(729\mu^4 + 670\mu^2 + 309)\mu_\Delta^6 + 18(138\mu^4 + 217\mu^2 - 162)\mu_\Delta^5 + (-1458\mu^6 \\
& - 405\mu^4 + 1656\mu^2 + 1445)\mu_\Delta^4 - 12(96\mu^6 + 15\mu^4 + 90\mu^2 - 119)\mu_\Delta^3 - 2(510\mu^6 - 450\mu^4 \\
& - 370\mu^2 + 503)\mu_\Delta^2 - 42(6\mu^6 + 39\mu^4 - 22\mu^2 + 4)\mu_\Delta + 14(6\mu^8 - 27\mu^6 - 65\mu^4 + 16\mu^2 - 2)].
\end{aligned}$$

b. Spin-dependent first-order polarizabilities

$$\begin{aligned}
 \gamma_{\text{EIE1}}^{(p)} = & \frac{e^2 h_A^2 \Xi_4}{15552 F^2 m^2 \pi^3 \mu_\Delta^6 (\mu^2 - \mu_\Delta^2 + 2\mu_\Delta - 1)^3 (\mu^2 - \mu_\Delta^2 - 2\mu_\Delta - 1)^2} (-81\mu_\Delta^{20} \\
 & + 282\mu_\Delta^{19} + (648\mu^2 - 361)\mu_\Delta^{18} - 2(723\mu^2 - 94)\mu_\Delta^{17} - 4(567\mu^4 - 501\mu^2 - 886)\mu_\Delta^{16} \\
 & + (2226\mu^4 - 3596\mu^2 - 6942)\mu_\Delta^{15} + (4536\mu^6 - 5007\mu^4 - 13196\mu^2 - 10489)\mu_\Delta^{14} \\
 & + 6(203\mu^6 + 2281\mu^4 + 3724\mu^2 + 3951)\mu_\Delta^{13} + (-5670\mu^8 + 8181\mu^6 + 19029\mu^4 \\
 & + 25959\mu^2 + 16267)\mu_\Delta^{12} - 2(4305\mu^8 + 10535\mu^6 + 11493\mu^4 + 14259\mu^2 + 19673)\mu_\Delta^{11} \\
 & + (4536\mu^{10} - 10677\mu^8 - 12326\mu^6 - 18558\mu^4 - 23154\mu^2 - 14543)\mu_\Delta^{10} + 2(6279\mu^{10} \\
 & + 6380\mu^8 + 2604\mu^6 + 804\mu^4 + 47\mu^2 + 19122)\mu_\Delta^9 + (-2268\mu^{12} + 11121\mu^{10} - 1169\mu^8 + 230\mu^6 - 78\mu^4 \\
 & + 12487\mu^2 + 6389)\mu_\Delta^8 - 6(1519\mu^{12} - 212\mu^{10} - 511\mu^8 - 776\mu^6 - 403\mu^4 - 3676\mu^2 + 3835)\mu_\Delta^7 \\
 & + (648\mu^{14} - 7989\mu^{12} + 10752\mu^{10} - 1203\mu^8 - 1636\mu^6 + 4107\mu^4 - 6000\mu^2 + 1321)\mu_\Delta^6 + 2(\mu^2 - 1)^2(1707\mu^{10} \\
 & + 1057\mu^8 + 425\mu^6 - 1038\mu^4 - 760\mu^2 + 3901)\mu_\Delta^5 - (\mu^2 - 1)^3(81\mu^{10} - 3084\mu^8 + 38\mu^6 + 150\mu^4 - 2265\mu^2 \\
 & - 3194)\mu_\Delta^4 - 2(\mu^2 - 1)^4(264\mu^8 + 319\mu^6 + 13\mu^4 - 869\mu^2 + 252)\mu_\Delta^3 \\
 & - 2(\mu^2 - 1)^5(303\mu^6 + 34\mu^4 - 137\mu^2 + 556)\mu_\Delta^2 - 84(\mu^2 - 1)^6(\mu^2 + 5)\mu_\Delta + 7(\mu^2 - 1)^7(\mu^4 - 2\mu^2 - 5)) \\
 & - \frac{e^2 h_A^2 \Xi_1}{15552 F^2 m^2 \pi^3 \mu_\Delta^6} (-81\mu_\Delta^{12} + 120\mu_\Delta^{11} + (324\mu^2 - 283)\mu_\Delta^{10} + 12(14\mu^2 + 29)\mu_\Delta^9 \\
 & + (-486\mu^4 + 1136\mu^2 + 2954)\mu_\Delta^8 + (-1224\mu^4 + 158\mu^2 + 874)\mu_\Delta^7 + (324\mu^6 \\
 & - 1987\mu^4 - 1888\mu^2 - 4039)\mu_\Delta^6 + 6(244\mu^6 - 166\mu^4 - 117\mu^2 - 354)\mu_\Delta^5 + (-81\mu^8 \\
 & + 1705\mu^6 - 825\mu^4 - 165\mu^2 + 1030)\mu_\Delta^4 - 6(88\mu^8 - 84\mu^6 + 26\mu^4 - 24\mu^2 - 75)\mu_\Delta^3 \\
 & + (-578\mu^8 + 496\mu^6 + 300\mu^4 + 340\mu^2 - 482)\mu_\Delta^2 - 14(\mu^8 + 2\mu^6 - 30\mu^4 + 46\mu^2 \\
 & - 25)\mu_\Delta + 7(\mu^{10} - 5\mu^8 + 4\mu^6 + 16\mu^4 + 13\mu^2 - 5)) \\
 & - \frac{e^2 h_A^2 \Xi_3}{15552 F^2 m^2 \pi^3 \mu_\Delta^6} (81\mu_\Delta^{12} - 120\mu_\Delta^{11} + (283 - 324\mu^2)\mu_\Delta^{10} - 12(14\mu^2 + 29)\mu_\Delta^9 \\
 & + 2(243\mu^4 - 568\mu^2 - 1477)\mu_\Delta^8 + 2(612\mu^4 - 79\mu^2 - 437)\mu_\Delta^7 + (-324\mu^6 + 1987\mu^4 + 1888\mu^2 \\
 & + 4039)\mu_\Delta^6 + (-1464\mu^6 + 996\mu^4 + 702\mu^2 + 3048)\mu_\Delta^5 + (81\mu^8 - 1705\mu^6 + 825\mu^4 + 165\mu^2 \\
 & + 820)\mu_\Delta^4 + 6(88\mu^8 - 84\mu^6 + 26\mu^4 + 84\mu^2 + 75)\mu_\Delta^3 + (578\mu^8 - 496\mu^6 - 300\mu^4 \\
 & + 700\mu^2 - 482)\mu_\Delta^2 + 14(\mu^2 - 1)^2(\mu^4 + 4\mu^2 + 25)\mu_\Delta - 7(\mu^2 - 1)^3(\mu^4 - 2\mu^2 - 5)) \\
 & - \frac{e^2 h_A^2}{93312 F^2 m^2 \pi^3 \mu_\Delta^6 (\mu^2 - \mu_\Delta^2 + 2\mu_\Delta - 1)^2 (\mu^2 - \mu_\Delta^2 - 2\mu_\Delta - 1)} (486\mu_\Delta^{16} - 1692\mu_\Delta^{15} \\
 & - 3(972\mu^2 - 965)\mu_\Delta^{14} + 6(882\mu^2 - 611)\mu_\Delta^{13} + 3(2430\mu^4 - 3293\mu^2 - 5708)\mu_\Delta^{12}
 \end{aligned}$$

$$\begin{aligned}
& -12(90\mu^4 - 1637\mu^2 - 3453)\mu_\Delta^{11} + (-9720\mu^6 + 13950\mu^4 + 36153\mu^2 + 26911)\mu_\Delta^{10} \\
& -2(7380\mu^6 + 16422\mu^4 + 27279\mu^2 + 49276)\mu_\Delta^9 + (7290\mu^8 - 14952\mu^6 - 23619\mu^4 \\
& -30092\mu^2 + 225)\mu_\Delta^8 + 2(11610\mu^8 + 8664\mu^6 + 6543\mu^4 + 8679\mu^2 + 46169)\mu_\Delta^7 \\
& -(2916\mu^{10} - 16563\mu^8 + 3972\mu^6 + 10382\mu^4 + 13357\mu^2 + 25208)\mu_\Delta^6 + (-14148\mu^{10} \\
& + 3630\mu^8 + 9990\mu^6 - 34308\mu^4 + 68166\mu^2 - 28466)\mu_\Delta^5 + (486\mu^{12} - 12087\mu^{10} \\
& + 20124\mu^8 - 22834\mu^6 + 28369\mu^4 - 21493\mu^2 + 6763)\mu_\Delta^4 + 2(1584\mu^{12} - 2046\mu^{10} \\
& -7245\mu^8 + 10135\mu^6 - 4430\mu^4 - 1415\mu^2 + 393)\mu_\Delta^3 + (3552\mu^{12} - 11877\mu^{10} \\
& + 16691\mu^8 - 25025\mu^6 + 31935\mu^4 - 20510\mu^2 + 5234)\mu_\Delta^2 + 168(\mu^2 - 1)^2(27\mu^6 \\
& -52\mu^4 + 47\mu^2 - 13)\mu_\Delta - 7(\mu^2 - 1)^3(6\mu^8 - 27\mu^6 - 137\mu^4 + 76\mu^2 - 26), \\
\gamma_{\text{M1MI}}^{(p)} = & \frac{e^2 h_A^2 \Xi_4}{15552 F^2 m^2 \pi^3 \mu_\Delta^6 (\mu^2 - \mu_\Delta^2 + 2\mu_\Delta - 1)^2 (\mu^2 - \mu_\Delta^2 - 2\mu_\Delta - 1)} (-567\mu_\Delta^{16} \\
& + 1446\mu_\Delta^{15} + (3402\mu^2 + 1649)\mu_\Delta^{14} - 6(1149\mu^2 + 893)\mu_\Delta^{13} - (8505\mu^4 + 6710\mu^2 \\
& + 2767)\mu_\Delta^{12} + 4(3195\mu^4 + 3432\mu^2 + 2113)\mu_\Delta^{11} + 2(5670\mu^6 + 5025\mu^4 + 4973\mu^2 \\
& + 2336)\mu_\Delta^{10} - 2(5550\mu^6 + 4365\mu^4 + 5225\mu^2 + 4044)\mu_\Delta^9 - (8505\mu^8 + 6073\mu^6 \\
& + 10931\mu^4 + 8455\mu^2 + 6140)\mu_\Delta^8 + 6(645\mu^8 - 433\mu^6 + 208\mu^4 + 339\mu^2 + 1116)\mu_\Delta^7 \\
& + (3402\mu^{10} + 277\mu^8 + 3576\mu^6 + 892\mu^4 + 3154\mu^2 + 3885)\mu_\Delta^6 + 2(117\mu^{10} + 1632\mu^8 \\
& - 335\mu^6 + 971\mu^4 + 1116\mu^2 - 2381)\mu_\Delta^5 - (567\mu^{12} - 1128\mu^{10} + 343\mu^8 - 1548\mu^6 \\
& + 657\mu^4 + 850\mu^2 + 259)\mu_\Delta^4 - 2(\mu^2 - 1)^2(168\mu^8 + 489\mu^6 - 26\mu^4 + \mu^2 - 849)\mu_\Delta^3 \\
& - 2(\mu^2 - 1)^3(164\mu^6 + 215\mu^4 + 302\mu^2 - 261)\mu_\Delta^2 - 84(\mu^2 - 1)^4(3\mu^2 + 1)\mu_\Delta + 7(\mu^2 - 1)^5(\mu^4 - 7) \\
& + \frac{e^2 h_A^2 \Xi_1}{15552 F^2 m^2 \pi^3 \mu_\Delta^6} (567\mu_\Delta^{12} - 312\mu_\Delta^{11} - (2268\mu^2 + 2273)\mu_\Delta^{10} + (600\mu^2 - 322)\mu_\Delta^9 \\
& + (3402\mu^4 + 5122\mu^2 + 3314)\mu_\Delta^8 + (72\mu^4 + 2062\mu^2 + 2410)\mu_\Delta^7 - (2268\mu^6 \\
& + 3125\mu^4 + 3048\mu^2 + 1481)\mu_\Delta^6 - 6(116\mu^6 + 353\mu^4 + 361\mu^2 + 304)\mu_\Delta^5 + (567\mu^8 \\
& - 31\mu^6 - 159\mu^4 - 321\mu^2 + 986)\mu_\Delta^4 + (336\mu^8 + 364\mu^6 - 366\mu^4 + 324\mu^2 + 612)\mu_\Delta^3 \\
& + (314\mu^8 + 88\mu^6 - 204\mu^4 + 692\mu^2 - 494)\mu_\Delta^2 + 14(\mu^8 + 16\mu^6 + 12\mu^4 - 20\mu^2 \\
& + 1)\mu_\Delta - 7(\mu^{10} - 3\mu^8 - 4\mu^6 - 20\mu^4 + 21\mu^2 - 7)) \\
& + \frac{e^2 h_A^2 \Xi_3}{15552 F^2 m^2 \pi^3 \mu_\Delta^6} (-567\mu_\Delta^{12} + 312\mu_\Delta^{11} + (2268\mu^2 + 2273)\mu_\Delta^{10} + (322 - 600\mu^2)\mu_\Delta^9 \\
& - 2(1701\mu^4 + 2561\mu^2 + 1657)\mu_\Delta^8 - 2(36\mu^4 + 1031\mu^2 + 1205)\mu_\Delta^7 + (2268\mu^6 \\
& + 3125\mu^4 + 3048\mu^2 + 1481)\mu_\Delta^6 + 6(116\mu^6 + 353\mu^4 + 361\mu^2 + 458)\mu_\Delta^5 + (-567\mu^8 + 31\mu^6 + 159\mu^4
\end{aligned}$$

$$\begin{aligned}
& + 321\mu^2 + 1196)\mu_{\Delta}^4 + (-336\mu^8 - 364\mu^6 + 366\mu^4 + 324\mu^2 + 612)\mu_{\Delta}^3 + (-314\mu^8 - 88\mu^6 \\
& + 204\mu^4 + 692\mu^2 - 494)\mu_{\Delta}^2 - 14(\mu^2 - 1)^2(\mu^4 + 18\mu^2 - 1)\mu_{\Delta} + 7(\mu^2 - 1)^3(\mu^4 - 7) \\
& - \frac{e^2 h_A^2}{93312 F^2 m^2 \pi^3 \mu_{\Delta}^6 (\mu^2 - \mu_{\Delta}^2 + 2\mu_{\Delta} - 1)} (3402\mu_{\Delta}^{12} - 8676\mu_{\Delta}^{11} - 3(4536\mu^2 \\
& + 1597)\mu_{\Delta}^{10} + 18(1334\mu^2 + 1063)\mu_{\Delta}^9 + 3(6804\mu^4 + 5123\mu^2 + 2666)\mu_{\Delta}^8 \\
& - 6(3330\mu^4 + 3516\mu^2 + 3829)\mu_{\Delta}^7 - (13608\mu^6 + 14565\mu^4 + 18741\mu^2 + 6716)\mu_{\Delta}^6 \\
& + (2628\mu^6 - 2898\mu^4 + 9408\mu^2 + 23984)\mu_{\Delta}^5 + (3402\mu^8 + 2145\mu^6 + 6003\mu^4 - 843\mu^2 - 14987)\mu_{\Delta}^4 \\
& + (2016\mu^8 + 4860\mu^6 + 3270\mu^4 - 8018\mu^2 + 298)\mu_{\Delta}^3 + (1884\mu^8 - 267\mu^6 - 3495\mu^4 - 1038\mu^2 \\
& + 2090)\mu_{\Delta}^2 - 84(30\mu^6 - 41\mu^4 + 28\mu^2 - 8)\mu_{\Delta} - 7(6\mu^{10} - 21\mu^8 + 196\mu^6 - 349\mu^4 + 218\mu^2 - 50)), \\
\gamma_{\text{E1M2}}^{(p)} = & - \frac{e^2 h_A^2 \Xi_4}{15552 F^2 m^2 \pi^3 \mu_{\Delta}^6 (\mu^2 - \mu_{\Delta}^2 + 2\mu_{\Delta} - 1)^2 (\mu^2 - \mu_{\Delta}^2 - 2\mu_{\Delta} - 1)} (81\mu_{\Delta}^{16} - 210\mu_{\Delta}^{15} \\
& - (486\mu^2 + 475)\mu_{\Delta}^{14} + 6(183\mu^2 + 178)\mu_{\Delta}^{13} + (1215\mu^4 + 1714\mu^2 + 1583)\mu_{\Delta}^{12} \\
& - 4(585\mu^4 + 642\mu^2 + 428)\mu_{\Delta}^{11} - 2(810\mu^6 + 1077\mu^4 + 1765\mu^2 + 2159)\mu_{\Delta}^{10} \\
& + 2(1290\mu^6 + 654\mu^4 - 511\mu^2 + 901)\mu_{\Delta}^9 + (1215\mu^8 + 983\mu^6 + 1733\mu^4 \\
& + 5733\mu^2 + 5652)\mu_{\Delta}^8 + (-1530\mu^8 + 762\mu^6 + 3840\mu^4 + 1570\mu^2 - 804)\mu_{\Delta}^7 - (486\mu^{10} + 47\mu^8 \\
& - 968\mu^6 + 1340\mu^4 - 546\mu^2 + 3607)\mu_{\Delta}^6 + 2(225\mu^{10} - 237\mu^8 - 587\mu^6 + 1003\mu^4 \\
& - 352\mu^2 - 248)\mu_{\Delta}^5 + (81\mu^{12} + 48\mu^{10} - 937\mu^8 + 1484\mu^6 + 483\mu^4 - 2438\mu^2 + 1279)\mu_{\Delta}^4 \\
& - 2(\mu^2 - 1)^2(24\mu^8 + 117\mu^6 + 92\mu^4 + 209\mu^2 - 197)\mu_{\Delta}^3 - 2(\mu^2 - 1)^3(38\mu^6 + 19\mu^4 + 205\mu^2 - 94)\mu_{\Delta}^2 \\
& + 42(\mu^2 - 1)^5(\mu^2 + 1)\mu_{\Delta} + 7(\mu^2 - 1)^5(\mu^4 + 4\mu^2 + 1)) \\
& + \frac{e^2 h_A^2 \Xi_1}{15552 F^2 m^2 \pi^3 \mu_{\Delta}^6} (81\mu_{\Delta}^{12} - 48\mu_{\Delta}^{11} - (324\mu^2 + 571)\mu_{\Delta}^{10} + 4(48\mu^2 - 59)\mu_{\Delta}^9 \\
& + 2(243\mu^4 + 607\mu^2 + 644)\mu_{\Delta}^8 + (-288\mu^4 + 758\mu^2 + 1958)\mu_{\Delta}^7 - (324\mu^6 + 763\mu^4 \\
& + 300\mu^2 + 501)\mu_{\Delta}^6 + 2(96\mu^6 - 255\mu^4 - 611\mu^2 - 1006)\mu_{\Delta}^5 + (81\mu^8 + 175\mu^6 \\
& - 587\mu^4 - 179\mu^2 - 1000)\mu_{\Delta}^4 - 2(24\mu^8 + 20\mu^6 + 75\mu^4 + 270\mu^2 - 96)\mu_{\Delta}^3 \\
& + (-62\mu^8 + 24\mu^6 - 246\mu^4 - 800\mu^2 + 300)\mu_{\Delta}^2 + 28(\mu^8 - 4\mu^6 - 21\mu^4 - 2\mu^2 + 2)\mu_{\Delta} \\
& + 7(\mu^{10} + \mu^8 - 8\mu^6 - 32\mu^4 + \mu^2 + 1)) \\
& - \frac{e^2 h_A^2 \Xi_3}{15552 F^2 m^2 \pi^3 \mu_{\Delta}^6} (81\mu_{\Delta}^{12} - 48\mu_{\Delta}^{11} - (324\mu^2 + 571)\mu_{\Delta}^{10} + 4(48\mu^2 - 59)\mu_{\Delta}^9 \\
& + 2(243\mu^4 + 607\mu^2 + 644)\mu_{\Delta}^8 + (-288\mu^4 + 758\mu^2 + 1958)\mu_{\Delta}^7 - (324\mu^6 + 763\mu^4 \\
& + 300\mu^2 + 501)\mu_{\Delta}^6 + 2(96\mu^6 - 255\mu^4 - 611\mu^2 - 544)\mu_{\Delta}^5 + (81\mu^8 + 175\mu^6 \\
& - 587\mu^4 - 179\mu^2 + 1182)\mu_{\Delta}^4 - 2(24\mu^8 + 20\mu^6 + 75\mu^4 - 54\mu^2 + 96)\mu_{\Delta}^3
\end{aligned}$$

$$\begin{aligned}
& + (-62\mu^8 + 24\mu^6 - 246\mu^4 + 584\mu^2 - 300)\mu_\Delta^2 + 28(\mu^2 - 1)^2(\mu^4 - 2\mu^2 - 2)\mu_\Delta \\
& + 7(\mu^2 - 1)^3(\mu^4 + 4\mu^2 + 1) \\
& - \frac{e^2 h_A^2}{93312 F^2 m^2 \pi^3 \mu_\Delta^6 (\mu^2 - \mu_\Delta^2 + 2\mu_\Delta - 1)} (486\mu_\Delta^{12} - 1260\mu_\Delta^{11} - 3(648\mu^2 + 707)\mu_\Delta^{10} \\
& + 18(226\mu^2 + 251)\mu_\Delta^9 + 3(972\mu^4 + 1285\mu^2 + 2038)\mu_\Delta^8 - 12(387\mu^4 + 180\mu^2 - 134)\mu_\Delta^7 \\
& - (1944\mu^6 + 1635\mu^4 + 5055\mu^2 + 23338)\mu_\Delta^6 + 2(1062\mu^6 - 927\mu^4 - 8307\mu^2 + 4691)\mu_\Delta^5 \\
& + (486\mu^8 + 231\mu^6 - 4683\mu^4 + 465\mu^2 + 4651)\mu_\Delta^4 - 2(144\mu^8 + 378\mu^6 + 2154\mu^4 \\
& + 11\mu^2 - 1707)\mu_\Delta^3 - 3(124\mu^8 - 229\mu^6 - 629\mu^4 - 980\mu^2 + 944)\mu_\Delta^2 \\
& + 126(2\mu^8 + 27\mu^6 - 29\mu^4 + 16\mu^2 - 2)\mu_\Delta + 7(6\mu^{10} + 3\mu^8 + 160\mu^6 - 249\mu^4 + 102\mu^2 - 22),
\end{aligned}$$

$$\begin{aligned}
\gamma_{M1E2}^{(p)} = & - \frac{e^2 h_A^2 \Xi_4}{15552 F^2 m^2 \pi^3 \mu_\Delta^6 (\mu^2 - \mu_\Delta^2 + 2\mu_\Delta - 1)^2 (\mu^2 - \mu_\Delta^2 - 2\mu_\Delta - 1)} (-81\mu_\Delta^{16} \\
& + 114\mu_\Delta^{15} + (486\mu^2 + 233)\mu_\Delta^{14} - 2(261\mu^2 + 347)\mu_\Delta^{13} + (-1215\mu^4 - 932\mu^2 \\
& + 41)\mu_\Delta^{12} + 4(225\mu^4 + 533\mu^2 + 453)\mu_\Delta^{11} + 2(810\mu^6 + 687\mu^4 + 317\mu^2 - 763)\mu_\Delta^{10} \\
& - 2(330\mu^6 + 1124\mu^4 + 2069\mu^2 + 442)\mu_\Delta^9 + (-1215\mu^8 - 829\mu^6 - 1623\mu^4 + 1709\mu^2 \\
& + 1544)\mu_\Delta^8 + 2(45\mu^8 + 425\mu^6 + 1725\mu^4 + 455\mu^2 - 781)\mu_\Delta^7 + (486\mu^{10} + 61\mu^8 \\
& + 1324\mu^6 - 1744\mu^4 - 894\mu^2 + 613)\mu_\Delta^6 + 2(63\mu^{10} + 14\mu^8 - 705\mu^6 + 360\mu^4 \\
& - 572\mu^2 + 924)\mu_\Delta^5 + (-81\mu^{12} + 138\mu^{10} - 541\mu^8 + 508\mu^6 - 1005\mu^4 + 2404\mu^2 \\
& - 1423)\mu_\Delta^4 - 2(\mu^2 - 1)^2(24\mu^8 + 103\mu^6 + 39\mu^4 + 63\mu^2 + 296)\mu_\Delta^3 \\
& - 2(\mu^2 - 1)^3(26\mu^6 - 15\mu^4 - 153\mu^2 + 310)\mu_\Delta^2 + 42(\mu^2 - 1)^4(\mu^4 + 4\mu^2 - 1)\mu_\Delta \\
& + 7(\mu^2 - 1)^5(\mu^4 + 2\mu^2 + 3) \\
& + \frac{e^2 h_A^2 \Xi_1}{15552 F^2 m^2 \pi^3 \mu_\Delta^6} (-81\mu_\Delta^{12} - 48\mu_\Delta^{11} + (324\mu^2 + 137)\mu_\Delta^{10} + 6(32\mu^2 - 43)\mu_\Delta^9 \\
& - 2(243\mu^4 + 170\mu^2 + 230)\mu_\Delta^8 + (-288\mu^4 + 242\mu^2 + 570)\mu_\Delta^7 + (324\mu^6 + 245\mu^4 \\
& + 796\mu^2 + 267)\mu_\Delta^6 + 6(32\mu^6 + 8\mu^4 - 91\mu^2 + 52)\mu_\Delta^5 - (81\mu^8 + 11\mu^6 + 315\mu^4 \\
& + 285\mu^2 - 568)\mu_\Delta^4 - 6(8\mu^8 + 10\mu^6 - 40\mu^4 - 48\mu^2 + 59)\mu_\Delta^3 + (-38\mu^8 + 40\mu^6 + 66\mu^4 \\
& + 520\mu^2 - 452)\mu_\Delta^2 + 28(\mu^8 + 3\mu^6 + 12\mu^4 - 11\mu^2 + 3)\mu_\Delta + 7(\mu^{10} - \mu^8 + 4\mu^4 - 7\mu^2 + 3)) \\
& + \frac{e^2 h_A^2 \Xi_3}{15552 F^2 m^2 \pi^3 \mu_\Delta^6} (81\mu_\Delta^{12} + 48\mu_\Delta^{11} - (324\mu^2 + 137)\mu_\Delta^{10} - 6(32\mu^2 - 43)\mu_\Delta^9 \\
& + (486\mu^4 + 340\mu^2 + 460)\mu_\Delta^8 + (288\mu^4 - 242\mu^2 - 570)\mu_\Delta^7 - (324\mu^6 + 245\mu^4 \\
& + 796\mu^2 + 267)\mu_\Delta^6 - 6(32\mu^6 + 8\mu^4 - 91\mu^2 - 102)\mu_\Delta^5 + (81\mu^8 + 11\mu^6 + 315\mu^4 \\
& + 285\mu^2 + 1282)\mu_\Delta^4 + 6(8\mu^8 + 10\mu^6 - 40\mu^4 + 60\mu^2 - 59)\mu_\Delta^3 + (38\mu^8 - 40\mu^6
\end{aligned}$$

$$\begin{aligned}
& -66\mu^4 + 520\mu^2 - 452)\mu_\Delta^2 - 28(\mu^2 - 1)^2(\mu^4 + 5\mu^2 - 3)\mu_\Delta - 7(\mu^2 - 1)^3(\mu^4 + 2\mu^2 + 3) \\
& - \frac{e^2 h_A^2}{93312 F^2 m^2 \pi^3 \mu_\Delta^6 (\mu^2 - \mu_\Delta^2 + 2\mu_\Delta - 1)} (-486\mu_\Delta^{12} + 684\mu_\Delta^{11} + 3(648\mu^2 + 223)\mu_\Delta^{10} \\
& - 6(294\mu^2 + 523)\mu_\Delta^9 - 3(972\mu^4 + 689\mu^2 - 484)\mu_\Delta^8 + 6(198\mu^4 + 816\mu^2 + 217)\mu_\Delta^7 \\
& + (1944\mu^6 + 1983\mu^4 + 3315\mu^2 + 1874)\mu_\Delta^6 + 2(90\mu^6 - 711\mu^4 - 1944\mu^2 - 3338)\mu_\Delta^5 \\
& + (-486\mu^8 - 399\mu^6 - 2499\mu^4 + 4659\mu^2 + 9271)\mu_\Delta^4 + (-288\mu^8 - 588\mu^6 + 5916\mu^4 \\
& + 970\mu^2 - 4090)\mu_\Delta^3 + (-228\mu^8 + 711\mu^6 - 4995\mu^4 + 4248\mu^2 - 1444)\mu_\Delta^2 + 42(6\mu^8 \\
& - 87\mu^6 + 115\mu^4 - 56\mu^2 + 10)\mu_\Delta + 7(6\mu^{10} - 9\mu^8 - 146\mu^6 + 313\mu^4 - 218\mu^2 + 54)).
\end{aligned}$$

2. Neutron values

a. Spin-independent first-order polarizabilities

$$\begin{aligned}
\alpha_{EI}^{(n)} = & - \frac{e^2 h_A^2 \Xi_4}{3888 F^2 m \pi^3 \mu_\Delta^6 (-\mu^2 + \mu_\Delta^2 - 2\mu_\Delta + 1)^2 (-\mu^2 + \mu_\Delta^2 + 2\mu_\Delta + 1)} [-8\mu_\Delta^{14} \\
& + 70\mu_\Delta^{13} + (50\mu^2 - 239)\mu_\Delta^{12} + (105 - 348\mu^2)\mu_\Delta^{11} + (-132\mu^4 + 936\mu^2 + 429)\mu_\Delta^{10} \\
& + 3(230\mu^4 - 135\mu^2 - 93)\mu_\Delta^9 + 2(95\mu^6 - 681\mu^4 - 150\mu^2 - 157)\mu_\Delta^8 + (-680\mu^6 \\
& + 597\mu^4 + 90\mu^2 + 133)\mu_\Delta^7 + (-160\mu^8 + 868\mu^6 - 651\mu^4 + 98\mu^2 + 217)\mu_\Delta^6 \\
& + 3(110\mu^8 - 137\mu^6 + 81\mu^4 + 5\mu^2 - 59)\mu_\Delta^5 + 3(\mu^2 - 1)^2(26\mu^6 - 17\mu^4 + 104\mu^2 \\
& + 13)\mu_\Delta^4 - 6(\mu^2 - 1)^3(10\mu^4 + 9\mu^2 + 21)\mu_\Delta^3 - 4(\mu^2 - 1)^4(5\mu^4 + 17\mu^2 + 32)\mu_\Delta^2 \\
& - 2(\mu^2 - 1)^5(\mu^2 + 11)\mu_\Delta + 2(\mu^2 - 1)^6(\mu^2 + 2)] \\
& + \frac{e^2 h_A^2 \Xi_1}{3888 F^2 m \pi^3 \mu_\Delta^6} [-2\mu^{10} + 4\mu^8 + 4\mu^6 + 16\mu^4 - 14\mu^2 + 8\mu_\Delta^{10} - 54\mu_\Delta^9 + (131 \\
& - 34\mu^2)\mu_\Delta^8 + 3(52\mu^2 + 47)\mu_\Delta^7 + (56\mu^4 - 238\mu^2 - 31)\mu_\Delta^6 - 3(48\mu^4 + 41\mu^2 \\
& + 33)\mu_\Delta^5 - (44\mu^6 - 87\mu^4 + 126\mu^2 + 35)\mu_\Delta^4 + 6(6\mu^6 - 5\mu^4 + 4\mu^2 - 3)\mu_\Delta^3 + 4(4\mu^8 \\
& + 4\mu^6 - 3\mu^4 + 22\mu^2 - 17)\mu_\Delta^2 + 6(\mu^8 + 2\mu^6 + 12\mu^4 - 14\mu^2 + 5)\mu_\Delta + 4] \\
& + \frac{e^2 h_A^2 \Xi_3}{3888 F^2 m \pi^3 \mu_\Delta^6} [-8\mu_\Delta^{10} + 54\mu_\Delta^9 + (34\mu^2 - 131)\mu_\Delta^8 - 3(52\mu^2 + 47)\mu_\Delta^7 + (-56\mu^4 \\
& + 238\mu^2 + 31)\mu_\Delta^6 + 3(48\mu^4 + 41\mu^2 - 71)\mu_\Delta^5 + (44\mu^6 - 87\mu^4 + 126\mu^2 - 53)\mu_\Delta^4 \\
& - 6(6\mu^6 - 5\mu^4 - 4\mu^2 + 3)\mu_\Delta^3 - 4(\mu^2 - 1)^2(4\mu^4 + 12\mu^2 + 17)\mu_\Delta^2 - 6(\mu^2 - 1)^3(\mu^2 \\
& + 5)\mu_\Delta + 2(\mu^2 - 1)^4(\mu^2 + 2)] \\
& + \frac{e^2 h_A^2}{23328 F^2 m \pi^3 \mu_\Delta^6 (-\mu^2 + \mu_\Delta^2 - 2\mu_\Delta + 1)} [48\mu_\Delta^{10} - 420\mu_\Delta^9 - 6(34\mu^2 - 251)\mu_\Delta^8
\end{aligned}$$

$$\begin{aligned}
& + 12(104\mu^2 - 123)\mu_{\Delta}^7 + (336\mu^4 - 2838\mu^2 + 413)\mu_{\Delta}^6 + (-1224\mu^4 + 1764\mu^2 + 62)\mu_{\Delta}^5 \\
& + (-264\mu^6 + 1188\mu^4 - 399\mu^2 + 1)\mu_{\Delta}^4 + 2(192\mu^6 - 9\mu^4 - 230\mu^2 + 22)\mu_{\Delta}^3 \\
& + 2(48\mu^8 + 57\mu^6 - 510\mu^4 + 427\mu^2 - 85)\mu_{\Delta}^2 + 2(6\mu^8 - 135\mu^6 + 85\mu^4 + 4\mu^2 - 14)\mu_{\Delta} \\
& + 2(-6\mu^{10} + 15\mu^8 - 73\mu^6 + 108\mu^4 - 54\mu^2 + 10)], \\
\beta_{M1}^{(n)} = & - \frac{e^2 h_A^2 \Xi_4}{3888 F^2 m \pi^3 \mu_{\Delta}^6 (-\mu^2 + \mu_{\Delta}^2 - 2\mu_{\Delta} + 1)} [-8\mu_{\Delta}^{10} + 70\mu_{\Delta}^9 + (34\mu^2 - 183)\mu_{\Delta}^8 \\
& + (245 - 208\mu^2)\mu_{\Delta}^7 + (-56\mu^4 + 358\mu^2 - 241)\mu_{\Delta}^6 + (204\mu^4 - 305\mu^2 + 45)\mu_{\Delta}^5 \\
& + (44\mu^6 - 177\mu^4 + 38\mu^2 + 107)\mu_{\Delta}^4 + (-64\mu^6 + 52\mu^4 + 100\mu^2 - 88)\mu_{\Delta}^3 \\
& - 4(\mu^2 - 1)^2(4\mu^4 + 5\mu^2 - 12)\mu_{\Delta}^2 - 2(\mu^2 - 1)^4\mu_{\Delta} + 2(\mu^2 - 1)^5] \\
& - \frac{e^2 h_A^2 \Xi_1}{3888 F^2 m \pi^3 \mu_{\Delta}^6} [-8\mu_{\Delta}^{10} + 54\mu_{\Delta}^9 + (34\mu^2 - 59)\mu_{\Delta}^8 + (3 - 156\mu^2)\mu_{\Delta}^7 + (-56\mu^4 \\
& + 118\mu^2 + 7)\mu_{\Delta}^6 + 3(48\mu^4 - 29\mu^2 - 63)\mu_{\Delta}^5 + (44\mu^6 - 69\mu^4 + 18\mu^2 - 37)\mu_{\Delta}^4 \\
& + 12\mu^2(-3\mu^4 + 5\mu^2 + 2)\mu_{\Delta}^3 + (-16\mu^8 + 20\mu^6 + 48\mu^4 + 92\mu^2 - 40)\mu_{\Delta}^2 - 6(\mu^8 \\
& - 4\mu^6 - 18\mu^4 + 4\mu^2 - 1)\mu_{\Delta} + 2(\mu^{10} - 5\mu^8 + 10\mu^6 + 22\mu^4 - 5\mu^2 + 1)] \\
& + \frac{e^2 h_A^2 \Xi_3}{3888 F^2 m \pi^3 \mu_{\Delta}^6} [-8\mu_{\Delta}^{10} + 54\mu_{\Delta}^9 + (34\mu^2 - 59)\mu_{\Delta}^8 + (3 - 156\mu^2)\mu_{\Delta}^7 + (-56\mu^4 \\
& + 118\mu^2 + 7)\mu_{\Delta}^6 + 3(48\mu^4 - 29\mu^2 + 41)\mu_{\Delta}^5 + (44\mu^6 - 69\mu^4 + 18\mu^2 + 19)\mu_{\Delta}^4 \\
& - 12\mu^2(3\mu^4 - 5\mu^2 + 2)\mu_{\Delta}^3 - 4(\mu^2 - 1)^2(4\mu^4 + 3\mu^2 - 10)\mu_{\Delta}^2 - 6(\mu^2 - 1)^4\mu_{\Delta} + 2(\mu^2 - 1)^5] \\
& + \frac{e^2 h_A^2}{23328 F^2 m \pi^3 \mu_{\Delta}^6} [48\mu_{\Delta}^8 - 324\mu_{\Delta}^7 - 6(26\mu^2 - 63)\mu_{\Delta}^6 + 36(17\mu^2 + 1)\mu_{\Delta}^5 + (180\mu^4 \\
& - 360\mu^2 + 371)\mu_{\Delta}^4 - 12(21\mu^4 + 6\mu^2 - 17)\mu_{\Delta}^3 - 2(42\mu^6 - 18\mu^4 - 94\mu^2 + 77)\mu_{\Delta}^2 \\
& - 6(6\mu^6 + 39\mu^4 - 22\mu^2 + 4)\mu_{\Delta} + 2(6\mu^8 - 27\mu^6 - 65\mu^4 + 16\mu^2 - 2)].
\end{aligned}$$

b. Spin-dependent first-order polarizabilities

$$\begin{aligned}
\gamma_{E1E1}^{(n)} = & \frac{e^2 h_A^2 \Xi_4}{7776 F^2 m^2 \pi^3 \mu_{\Delta}^6 (\mu^2 - \mu_{\Delta}^2 + 2\mu_{\Delta} - 1)^3 (\mu^2 - \mu_{\Delta}^2 - 2\mu_{\Delta} - 1)^2} [-34\mu_{\Delta}^{18} \\
& + 122\mu_{\Delta}^{17} + (273\mu^2 - 38)\mu_{\Delta}^{16} - 7(122\mu^2 + 51)\mu_{\Delta}^{15} + (-960\mu^4 + 316\mu^2 - 49)\mu_{\Delta}^{14} \\
& + 3(854\mu^4 + 457\mu^2 + 347)\mu_{\Delta}^{13} + (1932\mu^6 - 1107\mu^4 + 708\mu^2 + 733)\mu_{\Delta}^{12} - 2(2135\mu^6 \\
& + 744\mu^4 + 1347\mu^2 + 1265)\mu_{\Delta}^{11} - 2(1218\mu^8 - 1067\mu^6 + 1116\mu^4 + 507\mu^2 + 625)\mu_{\Delta}^{10} \\
& + (4270\mu^8 - 630\mu^6 + 2142\mu^4 + 898\mu^2 + 3456)\mu_{\Delta}^9 + (1974\mu^{10} - 2465\mu^8 + 2858\mu^6 \\
& - 1008\mu^4 + 946\mu^2 + 935)\mu_{\Delta}^8 - 3(854\mu^{10} - 825\mu^8 + 228\mu^6 - 482\mu^4 - 754\mu^2
\end{aligned}$$

$$\begin{aligned}
& + 915) \mu_{\Delta}^7 + (-1008 \mu^{12} + 1728 \mu^{10} - 1557 \mu^8 + 1256 \mu^6 + 540 \mu^4 - 804 \mu^2 - 155) \mu_{\Delta}^6 \\
& + (\mu^2 - 1)^2 (854 \mu^8 - 125 \mu^6 - 579 \mu^4 + 97 \mu^2 + 1265) \mu_{\Delta}^5 + (\mu^2 - 1)^3 (300 \mu^8 \\
& + 199 \mu^6 - 51 \mu^4 + 411 \mu^2 + 323) \mu_{\Delta}^4 - 2(\mu^2 - 1)^4 (61 \mu^6 + 7 \mu^4 - 167 \mu^2 + 96) \mu_{\Delta}^3 \\
& - 2(\mu^2 - 1)^5 (21 \mu^6 + 34 \mu^4 - 35 \mu^2 + 88) \mu_{\Delta}^2 - 12(\mu^2 - 1)^6 (\mu^2 + 5) \mu_{\Delta} + (\mu^2 - 1)^7 (\mu^4 - 2 \mu^2 - 5) \Big] \\
& + \frac{e^2 h_A^2 \Xi_1}{7776 F^2 m^2 \pi^3 \mu_{\Delta}^6} \left[-\mu^{10} + 5 \mu^8 - 4 \mu^6 - 16 \mu^4 - 13 \mu^2 + 34 \mu_{\Delta}^{10} - 54 \mu_{\Delta}^9 - (137 \mu^2 + 2) \mu_{\Delta}^8 \right. \\
& + (160 \mu^2 + 41) \mu_{\Delta}^7 + (208 \mu^4 + 46 \mu^2 + 451) \mu_{\Delta}^6 + (-156 \mu^4 + 39 \mu^2 + 159) \mu_{\Delta}^5 \\
& - (142 \mu^6 + 81 \mu^4 - 60 \mu^2 + 151) \mu_{\Delta}^4 + 6(8 \mu^6 - 14 \mu^4 + 12 \mu^2 - 25) \mu_{\Delta}^3 \\
& + 2(19 \mu^8 + 16 \mu^6 - 66 \mu^4 - 14 \mu^2 + 43) \mu_{\Delta}^2 + 2(\mu^8 + 2 \mu^6 - 30 \mu^4 + 46 \mu^2 - 25) \mu_{\Delta} + 5 \Big] \\
& - \frac{e^2 h_A^2 \Xi_3}{7776 F^2 m^2 \pi^3 \mu_{\Delta}^6} \left[34 \mu_{\Delta}^{10} - 54 \mu_{\Delta}^9 - (137 \mu^2 + 2) \mu_{\Delta}^8 + (160 \mu^2 + 41) \mu_{\Delta}^7 + (208 \mu^4 \right. \\
& + 46 \mu^2 + 451) \mu_{\Delta}^6 + (-156 \mu^4 + 39 \mu^2 + 279) \mu_{\Delta}^5 + (-142 \mu^6 - 81 \mu^4 + 60 \mu^2 \\
& + 121) \mu_{\Delta}^4 + 6(8 \mu^6 - 14 \mu^4 + 8 \mu^2 + 25) \mu_{\Delta}^3 + 2(19 \mu^8 + 16 \mu^6 - 66 \mu^4 + 74 \mu^2 \\
& - 43) \mu_{\Delta}^2 + 2(\mu^2 - 1)^2 (\mu^4 + 4 \mu^2 + 25) \mu_{\Delta} - (\mu^2 - 1)^3 (\mu^4 - 2 \mu^2 - 5) \Big] \\
& + \frac{e^2 h_A^2}{46656 F^2 m^2 \pi^3 \mu_{\Delta}^6 (\mu^2 - \mu_{\Delta}^2 + 2 \mu_{\Delta} - 1)^2 (\mu^2 - \mu_{\Delta}^2 - 2 \mu_{\Delta} - 1)} \left[-204 \mu_{\Delta}^{14} + 732 \mu_{\Delta}^{13} \right. \\
& + 6(205 \mu^2 - 89) \mu_{\Delta}^{12} - 12(305 \mu^2 + 132) \mu_{\Delta}^{11} + (-3096 \mu^4 + 2367 \mu^2 + 230) \mu_{\Delta}^{10} \\
& + (7320 \mu^4 + 3186 \mu^2 + 5678) \mu_{\Delta}^9 + (4170 \mu^6 - 4173 \mu^4 + 2261 \mu^2 - 1530) \mu_{\Delta}^8 \\
& - 2(3660 \mu^6 - 297 \mu^4 + 4827 \mu^2 + 4253) \mu_{\Delta}^7 + (-3180 \mu^8 + 3702 \mu^6 - 5173 \mu^4 \\
& + 4783 \mu^2 + 4820) \mu_{\Delta}^6 + (3660 \mu^8 - 5058 \mu^6 + 5706 \mu^4 - 8298 \mu^2 + 2966) \mu_{\Delta}^5 \\
& + (1314 \mu^{10} - 1728 \mu^8 + 2605 \mu^6 - 6124 \mu^4 + 6079 \mu^2 - 2050) \mu_{\Delta}^4 + (-732 \mu^{10} \\
& + 3510 \mu^8 - 4274 \mu^6 + 3220 \mu^4 - 1262 \mu^2 + 402) \mu_{\Delta}^3 + (-240 \mu^{12} + 411 \mu^{10} + 115 \mu^8 \\
& + 1127 \mu^6 - 3369 \mu^4 + 2714 \mu^2 - 758) \mu_{\Delta}^2 - 24(\mu^2 - 1)^2 (27 \mu^6 - 52 \mu^4 + 47 \mu^2 - 13) \mu_{\Delta} \\
& \left. + (\mu^2 - 1)^3 (6 \mu^8 - 27 \mu^6 - 137 \mu^4 + 76 \mu^2 - 26) \right], \\
\gamma_{\text{MIIMI}}^{(n)} = & \frac{e^2 h_A^2 \Xi_4}{7776 F^2 m^2 \pi^3 \mu_{\Delta}^6 (\mu^2 - \mu_{\Delta}^2 + 2 \mu_{\Delta} - 1)^2 (\mu^2 - \mu_{\Delta}^2 - 2 \mu_{\Delta} - 1)} \left[-34 \mu_{\Delta}^{14} \right. \\
& + 102 \mu_{\Delta}^{13} + (205 \mu^2 - 262) \mu_{\Delta}^{12} + (139 - 510 \mu^2) \mu_{\Delta}^{11} + (-516 \mu^4 + 1114 \mu^2 + 613) \mu_{\Delta}^{10} \\
& + (1020 \mu^4 - 493 \mu^2 - 543) \mu_{\Delta}^9 + (695 \mu^6 - 1841 \mu^4 - 727 \mu^2 - 659) \mu_{\Delta}^8 - 3(340 \mu^6 \\
& - 227 \mu^4 + 62 \mu^2 - 193) \mu_{\Delta}^7 + (-530 \mu^8 + 1464 \mu^6 - 497 \mu^4 + 562 \mu^2 + 567) \mu_{\Delta}^6 \\
& \left. + 5(102 \mu^8 - 95 \mu^6 + 149 \mu^4 + 15 \mu^2 - 107) \mu_{\Delta}^5 + (219 \mu^{10} - 556 \mu^8 + 726 \mu^6 - 360 \mu^4 \right]
\end{aligned}$$

$$\begin{aligned}
& + 149\mu^2 - 178)\mu_{\Delta}^4 - 2(\mu^2 - 1)^2(51\mu^6 + 10\mu^4 + 43\mu^2 - 135)\mu_{\Delta}^3 - 2(\mu^2 \\
& - 1)^3(20\mu^6 + 17\mu^4 + 50\mu^2 - 27)\mu_{\Delta}^2 - 12(\mu^2 - 1)^4(3\mu^2 + 1)\mu_{\Delta} + (\mu^2 - 1)^5(\mu^4 - 7) \\
& + \frac{e^2 h_A^2 \Xi_1}{7776 F^2 m^2 \pi^3 \mu_{\Delta}^6} [-\mu^{10} + 3\mu^8 + 4\mu^6 + 20\mu^4 - 21\mu^2 + 34\mu_{\Delta}^{10} - 34\mu_{\Delta}^9 + (194 \\
& - 137\mu^2)\mu_{\Delta}^8 + (100\mu^2 + 181)\mu_{\Delta}^7 + (208\mu^4 - 390\mu^2 - 149)\mu_{\Delta}^6 - 3(32\mu^4 + 81\mu^2 \\
& + 59)\mu_{\Delta}^5 + (-142\mu^6 + 201\mu^4 - 96\mu^2 + 137)\mu_{\Delta}^4 + 2(14\mu^6 + 15\mu^4 - 6\mu^2 + 78)\mu_{\Delta}^3 \\
& + 2(19\mu^8 - 4\mu^6 + 6\mu^4 + 46\mu^2 - 25)\mu_{\Delta}^2 + 2(\mu^8 + 16\mu^6 + 12\mu^4 - 20\mu^2 + 1)\mu_{\Delta} + 7] \\
& + \frac{e^2 h_A^2 \Xi_3}{7776 F^2 m^2 \pi^3 \mu_{\Delta}^6} [-34\mu_{\Delta}^{10} + 34\mu_{\Delta}^9 + (137\mu^2 - 194)\mu_{\Delta}^8 - (100\mu^2 + 181)\mu_{\Delta}^7 \\
& + (-208\mu^4 + 390\mu^2 + 149)\mu_{\Delta}^6 + 3(32\mu^4 + 81\mu^2 + 99)\mu_{\Delta}^5 + (142\mu^6 - 201\mu^4 \\
& + 96\mu^2 + 167)\mu_{\Delta}^4 - 2(14\mu^6 + 15\mu^4 + 6\mu^2 - 78)\mu_{\Delta}^3 - 2(19\mu^8 - 4\mu^6 + 6\mu^4 - 46\mu^2 \\
& + 25)\mu_{\Delta}^2 - 2(\mu^2 - 1)^2(\mu^4 + 18\mu^2 - 1)\mu_{\Delta} + (\mu^2 - 1)^3(\mu^4 - 7)] \\
& - \frac{e^2 h_A^2}{46656 F^2 m^2 \pi^3 \mu_{\Delta}^6 (\mu^2 - \mu_{\Delta}^2 + 2\mu_{\Delta} - 1)} [-6\mu^{10} + 21\mu^8 - 196\mu^6 + 349\mu^4 - 218\mu^2 \\
& + 204\mu_{\Delta}^{10} - 612\mu_{\Delta}^9 + (1878 - 822\mu^2)\mu_{\Delta}^8 + 12(153\mu^2 - 191)\mu_{\Delta}^7 + (1248\mu^4 \\
& - 3855\mu^2 - 242)\mu_{\Delta}^6 + (-1836\mu^4 + 1650\mu^2 + 2390)\mu_{\Delta}^5 - (852\mu^6 - 2097\mu^4 + 285\mu^2 \\
& + 2024)\mu_{\Delta}^4 + 2(306\mu^6 + 501\mu^4 - 727\mu^2 + 11)\mu_{\Delta}^3 + (228\mu^8 - 141\mu^6 - 129\mu^4 \\
& - 498\mu^2 + 422)\mu_{\Delta}^2 - 12(30\mu^6 - 41\mu^4 + 28\mu^2 - 8)\mu_{\Delta} + 50], \\
\gamma_{\text{EIM2}}^{(n)} = & - \frac{e^2 h_A^2 \Xi_4}{7776 F^2 m^2 \pi^3 \mu_{\Delta}^6 (\mu^2 - \mu_{\Delta}^2 + 2\mu_{\Delta} - 1)^2 (\mu^2 - \mu_{\Delta}^2 - 2\mu_{\Delta} - 1)} [2\mu_{\Delta}^{14} \\
& + 48\mu_{\Delta}^{13} - (11\mu^2 + 148)\mu_{\Delta}^{12} + (247 - 246\mu^2)\mu_{\Delta}^{11} + (24\mu^4 + 574\mu^2 - 229)\mu_{\Delta}^{10} \\
& + (510\mu^4 - 881\mu^2 - 325)\mu_{\Delta}^9 + (-25\mu^6 - 817\mu^4 + 741\mu^2 + 669)\mu_{\Delta}^8 + (-540\mu^6 \\
& + 1185\mu^4 - 50\mu^2 + 63)\mu_{\Delta}^7 + (10\mu^8 + 488\mu^6 - 785\mu^4 + 234\mu^2 - 397)\mu_{\Delta}^6 + (300\mu^8 \\
& - 739\mu^6 + 653\mu^4 - 173\mu^2 - 97)\mu_{\Delta}^5 + (3\mu^{10} - 82\mu^8 + 254\mu^6 - 156\mu^4 - 143\mu^2 + 124)\mu_{\Delta}^4 \\
& - 2(\mu^2 - 1)^2(39\mu^6 - 28\mu^4 + 59\mu^2 - 35)\mu_{\Delta}^3 - 2(\mu^2 - 1)^3(2\mu^6 + 13\mu^4 \\
& + 19\mu^2 - 10)\mu_{\Delta}^2 + 6(\mu^2 - 1)^5(\mu^2 + 1)\mu_{\Delta} + (\mu^2 - 1)^5(\mu^4 + 4\mu^2 + 1)] \\
& + \frac{e^2 h_A^2 \Xi_1}{7776 F^2 m^2 \pi^3 \mu_{\Delta}^6} [\mu^{10} + \mu^8 - 8\mu^6 - 32\mu^4 - 2(32\mu^4 - 51\mu^2 + 30)\mu_{\Delta}^3 \mu^2 + \mu^2 + 2\mu_{\Delta}^{10} \\
& + 52\mu_{\Delta}^9 - (7\mu^2 + 44)\mu_{\Delta}^8 - 5(32\mu^2 - 31)\mu_{\Delta}^7 + (8\mu^4 + 66\mu^2 - 21)\mu_{\Delta}^6 + (168\mu^4 \\
& - 241\mu^2 - 227)\mu_{\Delta}^5 + (-2\mu^6 + \mu^4 - 68\mu^2 - 139)\mu_{\Delta}^4 - 2(\mu^8 + 12\mu^6 - 3\mu^4 + 64\mu^2 \\
& - 18)\mu_{\Delta}^2 + 4(\mu^8 - 4\mu^6 - 21\mu^4 - 2\mu^2 + 2)\mu_{\Delta} + 1]
\end{aligned}$$

$$\begin{aligned}
& - \frac{e^2 h_A^2 \Xi_3}{7776 F^2 m^2 \pi^3 \mu_\Delta^6} [2\mu_\Delta^{10} + 52\mu_\Delta^9 - (7\mu^2 + 44)\mu_\Delta^8 - 5(32\mu^2 - 31)\mu_\Delta^7 + (8\mu^4 + 66\mu^2 \\
& - 21)\mu_\Delta^6 + (168\mu^4 - 241\mu^2 - 107)\mu_\Delta^5 + (-2\mu^6 + \mu^4 - 68\mu^2 + 165)\mu_\Delta^4 - 2\mu^2(32\mu^4 \\
& - 51\mu^2 + 42)\mu_\Delta^3 - 2(\mu^8 + 12\mu^6 - 3\mu^4 - 28\mu^2 + 18)\mu_\Delta^2 + 4(\mu^2 - 1)^2(\mu^4 - 2\mu^2 \\
& - 2)\mu_\Delta + (\mu^2 - 1)^3(\mu^4 + 4\mu^2 + 1)] \\
& - \frac{e^2 h_A^2}{46656 F^2 m^2 \pi^3 \mu_\Delta^6 (\mu^2 - \mu_\Delta^2 + 2\mu_\Delta - 1)} [6\mu^{10} + 3\mu^8 + 160\mu^6 - 249\mu^4 + 102\mu^2 \\
& + 12\mu_\Delta^{10} + 288\mu_\Delta^9 - 6(7\mu^2 + 145)\mu_\Delta^8 + (2454 - 900\mu^2)\mu_\Delta^7 + (48\mu^4 + 1659\mu^2 \\
& - 3388)\mu_\Delta^6 + 4(243\mu^4 - 684\mu^2 + 328)\mu_\Delta^5 + (-12\mu^6 - 705\mu^4 + 627\mu^2 + 172)\mu_\Delta^4 \\
& - 2(198\mu^6 + 102\mu^4 + 125\mu^2 - 285)\mu_\Delta^3 - 3(4\mu^8 + 29\mu^6 - 179\mu^4 - 92\mu^2 + 128)\mu_\Delta^2 \\
& + 18(2\mu^8 + 27\mu^6 - 29\mu^4 + 16\mu^2 - 2)\mu_\Delta - 22], \\
\gamma_{\text{MIE2}}^{(n)} & = - \frac{e^2 h_A^2 \Xi_4}{7776 F^2 m^2 \pi^3 \mu_\Delta^6 (\mu^2 - \mu_\Delta^2 + 2\mu_\Delta - 1)^2 (\mu^2 - \mu_\Delta^2 - 2\mu_\Delta - 1)} [2\mu_\Delta^{14} \\
& + 44\mu_\Delta^{13} - (11\mu^2 + 184)\mu_\Delta^{12} + (219 - 226\mu^2)\mu_\Delta^{11} + (24\mu^4 + 730\mu^2 + 67)\mu_\Delta^{10} \\
& + (470\mu^4 - 811\mu^2 - 281)\mu_\Delta^9 + (-25\mu^6 - 1083\mu^4 + 269\mu^2 + 161)\mu_\Delta^8 + (-500\mu^6 \\
& + 1119\mu^4 + 46\mu^2 - 131)\mu_\Delta^7 + (10\mu^8 + 712\mu^6 - 673\mu^4 - 54\mu^2 - 17)\mu_\Delta^6 + (280\mu^8 \\
& - 681\mu^6 + 333\mu^4 - 199\mu^2 + 291)\mu_\Delta^5 + (3\mu^{10} - 178\mu^8 + 274\mu^6 - 150\mu^4 + 169\mu^2 \\
& - 118)\mu_\Delta^4 - 2(\mu^2 - 1)^2(37\mu^6 - 3\mu^4 - 27\mu^2 + 68)\mu_\Delta^3 - 2(\mu^2 - 1)^3(2\mu^6 + 3\mu^4 \\
& - 27\mu^2 + 46)\mu_\Delta^2 + 6(\mu^2 - 1)^4(\mu^4 + 4\mu^2 - 1)\mu_\Delta + (\mu^2 - 1)^5(\mu^4 + 2\mu^2 + 3)] \\
& + \frac{e^2 h_A^2 \Xi_1}{7776 F^2 m^2 \pi^3 \mu_\Delta^6} [\mu^{10} - \mu^8 + 4\mu^4 - 7\mu^2 + 2\mu_\Delta^{10} + 48\mu_\Delta^9 - (7\mu^2 + 88)\mu_\Delta^8 + (39 \\
& - 148\mu^2)\mu_\Delta^7 + (8\mu^4 + 166\mu^2 + 51)\mu_\Delta^6 + 3(52\mu^4 - 41\mu^2 + 15)\mu_\Delta^5 - (2\mu^6 + 69\mu^4 \\
& + 24\mu^2 - 85)\mu_\Delta^4 - 6(10\mu^6 - 12\mu^4 + 4\mu^2 + 1)\mu_\Delta^3 - 2(\mu^8 + 4\mu^6 - 15\mu^4 - 44\mu^2 \\
& + 34)\mu_\Delta^2 + 4(\mu^8 + 3\mu^6 + 12\mu^4 - 11\mu^2 + 3)\mu_\Delta + 3] \\
& - \frac{e^2 h_A^2 \Xi_3}{7776 F^2 m^2 \pi^3 \mu_\Delta^6} [2\mu_\Delta^{10} + 48\mu_\Delta^9 - (7\mu^2 + 88)\mu_\Delta^8 + (39 - 148\mu^2)\mu_\Delta^7 + (8\mu^4 + 166\mu^2 \\
& + 51)\mu_\Delta^6 + 3(52\mu^4 - 41\mu^2 - 25)\mu_\Delta^5 - (2\mu^6 + 69\mu^4 + 24\mu^2 + 187)\mu_\Delta^4 + (-60\mu^6 \\
& + 72\mu^4 + 6)\mu_\Delta^3 - 2(\mu^8 + 4\mu^6 - 15\mu^4 + 44\mu^2 - 34)\mu_\Delta^2 + 4(\mu^2 - 1)^2(\mu^4 + 5\mu^2 \\
& - 3)\mu_\Delta + (\mu^2 - 1)^3(\mu^4 + 2\mu^2 + 3)] \\
& - \frac{e^2 h_A^2}{46656 F^2 m^2 \pi^3 \mu_\Delta^6 (\mu^2 - \mu_\Delta^2 + 2\mu_\Delta - 1)} [6\mu^{10} - 9\mu^8 - 146\mu^6 + 313\mu^4 - 218\mu^2 \\
& + 12\mu_\Delta^{10} + 264\mu_\Delta^9 - 6(7\mu^2 + 181)\mu_\Delta^8 - 18(46\mu^2 - 65)\mu_\Delta^7 + (48\mu^4 + 2163\mu^2
\end{aligned}$$

$$\begin{aligned}
& + 8)\mu_{\Delta}^6 + 4(225\mu^4 - 483\mu^2 - 256)\mu_{\Delta}^5 + (-12\mu^6 - 1077\mu^4 + 1275\mu^2 + 1444)\mu_{\Delta}^4 \\
& - 2(186\mu^6 - 642\mu^4 + 61\mu^2 + 299)\mu_{\Delta}^3 + (-12\mu^8 + 9\mu^6 - 621\mu^4 + 576\mu^2 - 196)\mu_{\Delta}^2 \\
& + 6(6\mu^8 - 87\mu^6 + 115\mu^4 - 56\mu^2 + 10)\mu_{\Delta} + 54].
\end{aligned}$$

APPENDIX D: q^4 VALUES

Here, we use the notation

$$\tilde{e}_{117} \equiv e_{117} + 2e_{90} + e_{94} + g_A^2 \frac{2c_6 + 3c_7}{128m\pi^2 F^2} \quad \text{and} \quad \tilde{e}_{118} \equiv e_{118} + 2e_{89} + e_{93} - g_A^2 \frac{13c_6 + 15c_7}{512m\pi^2 F^2}.$$

1. Proton values

a. Spin-independent first-order polarizabilities

$$\begin{aligned}
\alpha_{E1}^p &= -\frac{e^2 g_A^2}{64\pi^3 F^2 m} [c_6 \Xi_2(5\mu^4 - 17\mu^2 + 4) + 3c_7 \Xi_2(3\mu^4 - 11\mu^2 + 4) + 5c_6 \mu^2 \\
&\quad + 9c_7 \mu^2] - \frac{e^2(\tilde{e}_{117} + 2\tilde{e}_{118} + e_{92} + 2e_{91})}{\pi} - \frac{e^2(4c_1 + c_2 - 2c_3)}{192\pi^3 F^2} \\
&\quad + \frac{e^2 \Xi_1}{192\pi^3 F^2 m} [3g_A^2 c_6 \mu^2(5\mu^2 - 7) + 9g_A^2 c_7 \mu^2(3\mu^2 - 5) - 2c_2 m], \\
\beta_{M1}^p &= \frac{e^2 g_A^2}{64\pi^3 F^2 (\mu^2 - 4)m} [c_6 \Xi_2(-15\mu^6 + 113\mu^4 - 230\mu^2 + 96) + c_7 \Xi_2(-21\mu^6 \\
&\quad + 159\mu^4 - 328\mu^2 + 144) + c_6(15\mu^4 - 55\mu^2 + 4) + c_7(21\mu^4 - 78\mu^2 + 8)] \\
&\quad + \frac{2e^2(\tilde{e}_{118} + e_{91})}{\pi} + \frac{e^2(4c_1 - c_2 - 2c_3)}{192\pi^3 F^2} \\
&\quad + \frac{e^2}{192\pi^3 F^2 m} \Xi_1 [3c_6 g_A^2(15\mu^4 - 23\mu^2 + 2) + 3c_7 g_A^2(21\mu^4 - 33\mu^2 + 4) - 2c_2 m].
\end{aligned}$$

b. Spin-independent second-order polarizabilities

$$\begin{aligned}
\alpha_{E2}^{(p)} &= \frac{e^2 g_A^2}{64\pi^3 F^2 (\mu^2 - 4)m^3} [c_6 \Xi_2(-45\mu^6 + 340\mu^4 - 696\mu^2 + 276) + c_7 \Xi_2(-81\mu^6 \\
&\quad + 628\mu^4 - 1356\mu^2 + 636) - c_7(81\mu^4 - 358\mu^2 + 212) - c_6(45\mu^4 - 190\mu^2 + 92)] \\
&\quad + \frac{e^2 \Xi_1}{64\pi^3 F^2 m^3} [2c_2 m + g_A^2 c_6(45\mu^4 - 70\mu^2 + 6) + g_A^2 c_7(81\mu^4 - 142\mu^2 + 18)] \\
&\quad + \frac{e^2(-32c_1 + 15\mu^2 c_2 - 44c_3)}{960\pi^3 F^2 \mu^2 m^2} + \frac{3e^2 \tilde{e}_{117}}{2\pi m^2}, \\
\beta_{M2}^{(p)} &= \frac{e^2 g_A^2}{64\pi^3 F^2 \mu^2 (\mu^2 - 4)^2 m^3} [c_6 \Xi_2(-105\mu^{10} + 1208\mu^8 - 4756\mu^6 + 7100\mu^4 \\
&\quad - 2920\mu^2 + 64) + c_7 \Xi_2(-153\mu^{10} + 1772\mu^8 - 7056\mu^6 + 10780\mu^4 - 4720\mu^2 + 160) \\
&\quad + c_6(-105\mu^6 + 848\mu^4 - 1882\mu^2 + 848) + c_7(-153\mu^6 + 1250\mu^4 - 2848\mu^2 + 1400)]
\end{aligned}$$

$$\begin{aligned}
& + \frac{e^2 \Xi_1}{64\pi^3 F^2 m^3} [2c_2 m + g_A^2 c_6 (105\mu^4 - 158\mu^2 + 26) + g_A^2 c_7 (153\mu^4 - 242\mu^2 + 46)] \\
& + \frac{e^2 (32c_1 + (15\mu^2 + 8)c_2 + 44c_3)}{960\pi^3 F^2 \mu^2 m^2} + \frac{3e^2 \tilde{\epsilon}_{117}}{2\pi m^2}, \\
\alpha_{E1\nu}^{(p)} = & \frac{e^2 g_A^2}{768\pi^3 F^2 \mu^2 (\mu^2 - 4)^2 m^3} [c_6 \Xi_2 (-567\mu^{10} + 6616\mu^8 - 26660\mu^6 + 41620\mu^4 \\
& - 19080\mu^2 + 576) + c_7 \Xi_2 (1312 - 5\mu^2 (171\mu^8 - 2004\mu^6 + 8136\mu^4 - 12900\mu^2 \\
& + 6176)) + c_6 (-567\mu^6 + 4624\mu^4 - 10434\mu^2 + 4784) + 3c_7 (-285\mu^6 + 2338\mu^4 - 5348\mu^2 + 2568)] \\
& + \frac{e^2 \Xi_1}{768\pi^3 F^2 m^3} [g_A^2 c_6 (567\mu^4 - 946\mu^2 + 190) + 15g_A^2 c_7 (57\mu^4 - 98\mu^2 + 22) - 2c_2 m] \\
& + \frac{e^2 (96c_1 + (16 - 15\mu^2)c_2 + 132c_3)}{11520\pi^3 F^2 \mu^2 m^2} - \frac{e^2 \tilde{\epsilon}_{117}}{8\pi m^2}, \\
\beta_{M1\nu}^{(p)} = & - \frac{e^2 g_A^2}{768\pi^3 F^2 \mu^2 (\mu^2 - 4)^3 m^3} [c_6 \Xi_2 (627\mu^{12} - 9764\mu^{10} + 57904\mu^8 - 159740\mu^6 \\
& + 196496\mu^4 - 80992\mu^2 + 4352) + c_7 \Xi_2 (927\mu^{12} - 14484\mu^{10} + 86300\mu^8 - 239764\mu^6 \\
& + 298416\mu^4 - 125504\mu^2 + 6400) - c_6 (-627\mu^{10} + 7562\mu^8 - 31376\mu^6 + 49112\mu^4 \\
& - 19392\mu^2 + 256) - c_7 (-927\mu^{10} + 11226\mu^8 - 46880\mu^6 + 74336\mu^4 - 30464\mu^2 + 512)] \\
& + \frac{e^2 \Xi_1}{768\pi^3 F^2 m^3} [g_A^2 c_6 (627\mu^4 - 986\mu^2 + 210) + g_A^2 c_7 (927\mu^4 - 1506\mu^2 + 326) - 2c_2 m] \\
& - \frac{e^2 (32c_1 + (5\mu^2 + 8)c_2 + 44c_3)}{3840\pi^3 F^2 \mu^2 m^2} - \frac{e^2 \tilde{\epsilon}_{117}}{8\pi m^2}.
\end{aligned}$$

c. Spin-dependent first-order polarizabilities

$$\begin{aligned}
\gamma_{E1E1}^{(p)} = & \frac{e^2 g_A^2}{384\pi^3 F^2 (\mu^2 - 4)^2 m^2} [-c_6 \Xi_2 (54\mu^8 - 635\mu^6 + 2582\mu^4 - 4056\mu^2 + 1704) \\
& - c_7 \Xi_2 (72\mu^8 - 851\mu^6 + 3488\mu^4 - 5556\mu^2 + 2400) + 2c_6 (-27\mu^6 + 223\mu^4 \\
& - 517\mu^2 + 216) + c_7 (-72\mu^6 + 599\mu^4 - 1408\mu^2 + 608)] \\
& + \frac{e^2 g_A^2 \Xi_1}{384\pi^3 F^2 m^2} [c_6 (54\mu^4 - 95\mu^2 + 12) + c_7 (72\mu^4 - 131\mu^2 + 18)], \\
\gamma_{M1M1}^{(p)} = & \frac{e^2 g_A^2}{384\pi^3 F^2 (\mu^2 - 4)^2 m^2 \mu^2} [c_6 \Xi_2 (-144\mu^{10} + 1651\mu^8 - 6468\mu^6 + 9584\mu^4 \\
& - 3968\mu^2 + 128) + c_7 \Xi_2 (-180\mu^{10} + 2053\mu^8 - 7972\mu^6 + 11604\mu^4 - 4592\mu^2 + 128) \\
& + c_6 (-144\mu^8 + 1147\mu^6 - 2456\mu^4 + 976\mu^2) + c_7 (-180\mu^8 + 1423\mu^6 - 2996\mu^4 + 1120\mu^2)] \\
& + \frac{e^2 g_A^2 \Xi_1}{384\pi^3 F^2 m^2} [c_6 (144\mu^4 - 211\mu^2 + 38) + c_7 (180\mu^4 - 253\mu^2 + 42)], \\
\gamma_{E1M2}^{(p)} = & \frac{e^2 g_A^2}{384\pi^3 F^2 (\mu^2 - 4)^2 m^2} [-3c_6 \Xi_2 (12\mu^8 - 139\mu^6 + 552\mu^4 - 832\mu^2 + 312) \\
& - c_7 \Xi_2 (36\mu^8 - 411\mu^6 + 1592\mu^4 - 2276\mu^2 + 672) + c_6 (-36\mu^6 + 291\mu^4 - 650\mu^2 + 224)
\end{aligned}$$

$$\begin{aligned}
& + c_7(-36\mu^6 + 285\mu^4 - 608\mu^2 + 128)] + \frac{e^2 g_A^2 \Xi_1}{128\pi^3 F^2 m^2} [c_6(12\mu^4 - 19\mu^2 + 2) + c_7(36\mu^4 - 51\mu^2 + 2)], \\
\gamma_{\text{MIE2}}^{(p)} = & \frac{e^2 g_A^2}{384\pi^3 F^2 (\mu^2 - 4)m^2 \mu^2} [c_6 \Xi_2(-6\mu^8 + 49\mu^6 - 114\mu^4 + 48\mu^2) + c_7 \Xi_2(5\mu^6 \\
& - 24\mu^4 - 12\mu^2 + 16) - 2c_6(3\mu^6 - 14\mu^4 + 4\mu^2) + c_7(5\mu^4 + 4\mu^2)] \\
& + \frac{e^2 g_A^2 \Xi_1}{384\pi^3 F^2 m^2} [c_6 \mu^2(6\mu^2 - 13) - c_7(5\mu^2 + 6)].
\end{aligned}$$

d. Spin-dependent second-order polarizabilities

$$\begin{aligned}
\gamma_{\text{E2E2}}^{(p)} = & \frac{e^2 g_A^2}{276480\pi^3 F^2 \mu^2 (\mu^2 - 4)^3 m^4} [-6c_6 \Xi_2(2815\mu^{12} - 44860\mu^{10} + 274613\mu^8 - 793312\mu^6 \\
& + 1048500\mu^4 - 478000\mu^2 + 17920) - 6c_7 \Xi_2(4530\mu^{12} - 72615\mu^{10} + 448178\mu^8 \\
& - 1310752\mu^6 + 1768680\mu^4 - 843040\mu^2 + 38400) - c_6 \mu^2(16890\mu^8 - 210045\mu^6 \\
& + 914298\mu^4 - 1564712\mu^2 + 742400) - 4c_7 \mu^2(6795\mu^8 - 85140\mu^6 + 374947\mu^4 - 655268\mu^2 + 328480)] \\
& + \frac{e^2 g_A^2 \Xi_1}{46080\pi^3 F^2 m^4} [c_6(2815\mu^4 - 5450\mu^2 + 1263) + c_7(4530\mu^4 - 9195\mu^2 + 2348)], \\
\gamma_{\text{M2M2}}^{(p)} = & \frac{e^2 g_A^2}{276480\pi^3 F^2 \mu^2 (\mu^2 - 4)^3 m^4} [6c_7 \Xi_2(-12270\mu^{12} + 189729\mu^{10} - 1114038\mu^8 \\
& + 3028128\mu^6 - 3641480\mu^4 + 1458080\mu^2 - 78720) - 6c_6 \Xi_2(9265\mu^{12} - 143484\mu^{10} \\
& + 844403\mu^8 - 2303488\mu^6 + 2788060\mu^4 - 1132080\mu^2 + 61440) + c_6(-55590\mu^{10} \\
& + 666339\mu^8 - 2738494\mu^6 + 4234376\mu^4 - 1680256\mu^2 + 23040) + 4c_7(-18405\mu^{10} \\
& + 220176\mu^8 - 901871\mu^6 + 1385404\mu^4 - 538544\mu^2 + 7680)] \\
& + \frac{e^2 g_A^2 \Xi_1}{46080\pi^3 F^2 m^4} [c_6(9265\mu^4 - 13774\mu^2 + 3017) + 3c_7(4090\mu^4 - 5983\mu^2 + 1284)], \\
\gamma_{\text{E2M3}}^{(p)} = & \frac{e^2 g_A^2}{138240\pi^3 F^2 \mu^2 (\mu^2 - 4)^3 m^4} [6c_7 \Xi_2 \mu^2(-930\mu^{10} + 14319\mu^8 - 83402\mu^6 + 222784\mu^4 \\
& - 255000\mu^2 + 77920) - 6c_6 \Xi_2(895\mu^{12} - 13924\mu^{10} + 82397\mu^8 - 226144\mu^6 + 274020\mu^4 \\
& - 102640\mu^2 + 2560) - c_6 \mu^2(5370\mu^8 - 64749\mu^6 + 268578\mu^4 - 420872\mu^2 + 148736) \\
& - 4c_7 \mu^2(1395\mu^8 - 16596\mu^6 + 67237\mu^4 - 99788\mu^2 + 25504)] \\
& + \frac{e^2 g_A^2 \Xi_1}{23040\pi^3 F^2 m^4} [c_6(895\mu^4 - 1394\mu^2 + 231) + c_7(930\mu^4 - 1299\mu^2 + 116)], \\
\gamma_{\text{M2E3}}^{(p)} = & \frac{e^2 g_A^2}{138240\pi^3 F^2 \mu^2 (\mu^2 - 4)^2 m^4} [-6c_6 \Xi_2 \mu^2(145\mu^8 - 1808\mu^6 + 7971\mu^4 - 14020\mu^2 + 7020) \\
& - 6c_7 \Xi_2(30\mu^{10} - 513\mu^8 + 2946\mu^6 - 6120\mu^4 + 1640\mu^2 + 1920) + c_6 \mu^2(-870\mu^6 + 7803\mu^4 \\
& - 20218\mu^2 + 11008) + 4c_7(-45\mu^8 + 612\mu^6 - 2177\mu^4 + 1112\mu^2 + 480)]
\end{aligned}$$

$$\begin{aligned}
& + \frac{e^2 g_A^2 \Xi_1}{23040 \pi^3 F^2 m^4} [c_6(145\mu^4 - 358\mu^2 + 41) + 3c_7(10\mu^4 - 71\mu^2 - 28)], \\
\gamma_{\text{E1E1}\nu}^{(p)} = & \frac{e^2 g_A^2}{92160 \pi^3 F^2 \mu^2 (\mu^2 - 4)^4 m^4} [6c_6 \Xi_2 (-12795\mu^{14} + 252768\mu^{12} - 2022553\mu^{10} \\
& + 8314020\mu^8 - 18266004\mu^6 + 19956640\mu^4 - 8462400\mu^2 + 586240) \\
& + 6c_7 \Xi_2 (-17370\mu^{14} + 343603\mu^{12} - 2754238\mu^{10} + 11349720\mu^8 - 25027944\mu^6 \\
& + 27512320\mu^4 - 11801600\mu^2 + 837120) - c_6(76770\mu^{12} - 1247913\mu^{10} + 7772910\mu^8 \\
& - 22691488\mu^6 + 29783392\mu^4 - 12724992\mu^2 + 276480) - 4c_7(26055\mu^{12} - 424212\mu^{10} \\
& + 2648475\mu^8 - 7760752\mu^6 + 10258144\mu^4 - 4459456\mu^2 + 111616)] \\
& + \frac{e^2 g_A^2 \Xi_1}{15360 \pi^3 F^2 m^4} [c_6(12795\mu^4 - 22458\mu^2 + 6139) + c_7(17370\mu^4 - 30943\mu^2 + 8644)], \\
\gamma_{\text{M1M1}\nu}^{(p)} = & \frac{e^2 g_A^2}{30720 \pi^3 F^2 \mu^4 (\mu^2 - 4)^4 m^4} [2c_6 \Xi_2 (-18645\mu^{16} + 365512\mu^{14} - 2895039\mu^{12} \\
& + 11734236\mu^{10} - 25255068\mu^8 + 26691840\mu^6 - 10715712\mu^4 + 690176\mu^2 + 12288) \\
& + 2c_7 \Xi_2 (-24390\mu^{16} + 477637\mu^{14} - 3777690\mu^{12} + 15279624\mu^{10} - 32775144\mu^8 + 34427520\mu^6 \\
& - 13633152\mu^4 + 843776\mu^2 + 12288) - c_6\mu^2(37290\mu^{12} - 600509\mu^{10} + 3691774\mu^8 \\
& - 10567696\mu^6 + 13374368\mu^4 - 5340160\mu^2 + 145408) - 4c_7\mu^2(12195\mu^{12} - 196136\mu^{10} \\
& + 1203489\mu^8 - 3433800\mu^6 + 4317072\mu^4 - 1691520\mu^2 + 40448)] \\
& + \frac{e^2 g_A^2 \Xi_1}{15360 \pi^3 F^2 m^4} [c_6(18645\mu^4 - 29902\mu^2 + 7533) + c_7(24390\mu^4 - 38617\mu^2 + 9444)], \\
\gamma_{\text{EIM2}\nu}^{(p)} = & \frac{e^2 g_A^2}{230400 \pi^3 F^2 \mu^2 (\mu^2 - 4)^4 m^4} [6c_6 \Xi_2 (-28605\mu^{14} + 558752\mu^{12} - 4403315\mu^{10} \\
& + 17712684\mu^8 - 37646844\mu^6 + 38881120\mu^4 - 14719680\mu^2 + 787200) \\
& + 6c_7 \Xi_2 (-34470\mu^{14} + 670917\mu^{12} - 5260850\mu^{10} + 21003984\mu^8 - 44091984\mu^6 \\
& + 44459680\mu^4 - 15800320\mu^2 + 593920) - c_6(171630\mu^{12} - 2751807\mu^{10} + 16799538\mu^8 \\
& - 47489120\mu^6 + 58760928\mu^4 - 21684352\mu^2 + 307200) - 4c_7(51705\mu^{12} - 825408\mu^{10} \\
& + 5005722\mu^8 - 13991740\mu^6 + 16921472\mu^4 - 5799168\mu^2 + 28160)] \\
& + \frac{e^2 g_A^2 \Xi_1}{38400 \pi^3 F^2 m^4} [c_6(28605\mu^4 - 43862\mu^2 + 9569) + c_7(34470\mu^4 - 50457\mu^2 + 9404)], \\
\gamma_{\text{M1E2}\nu}^{(p)} = & \frac{e^2 g_A^2}{230400 \pi^3 F^2 \mu^4 (\mu^2 - 4)^3 m^4} [6c_7 \Xi_2 (-17370\mu^{14} + 275051\mu^{12} - 1668778\mu^{10} \\
& + 4756616\mu^8 - 6145600\mu^6 + 2653280\mu^4 - 74880\mu^2 + 5120) - 6c_6 \Xi_2 \mu^2 (14355\mu^{12} \\
& - 226956\mu^{10} + 1374373\mu^8 - 3909056\mu^6 + 5044180\mu^4 - 2201360\mu^2 + 77440) \\
& - c_6\mu^4(86130\mu^8 - 1060281\mu^6 + 4545762\mu^4 - 7588888\mu^2 + 3381184)
\end{aligned}$$

$$\begin{aligned}
& -4c_7\mu^2(26055\mu^{10} - 321384\mu^8 + 1381428\mu^6 - 2311252\mu^4 + 1010576\mu^2 + 16640)] \\
& + \frac{e^2 g_A^2 \Xi_1}{38400\pi^3 F^2 m^4} [c_6(14355\mu^4 - 25986\mu^2 + 5719) + c_7(17370\mu^4 - 31871\mu^2 + 6684)].
\end{aligned}$$

2. Neutron values

a. Spin-independent first-order polarizabilities

$$\begin{aligned}
\alpha_{E1}^{(n)} &= -\frac{e^2 g_A^2}{32\pi^3 F^2 m} (2c_6 \Xi_2(\mu^2 - 2) + 3c_7 \Xi_2(\mu^2 - 2)) - \frac{e^2 (\tilde{e}_{117} + 2\tilde{e}_{118} - e_{92} - 2e_{91})}{\pi} \\
& + \frac{e^2 \Xi_1}{96\pi^3 F^2 m} (6c_6 g_A^2 \mu^2 + 9c_7 g_A^2 \mu^2 - c_2 m) - \frac{e^2 (4c_1 + c_2 - 2c_3)}{192\pi^3 F^2}, \\
\beta_{M1}^{(n)} &= -\frac{e^2 g_A^2}{64\pi^3 F^2 (\mu^2 - 4)m} (2c_6 \Xi_2(\mu^4 - 7\mu^2 + 8) + 2c_7 \Xi_2(3\mu^4 - 20\mu^2 + 24) \\
& - c_6(4 - 3\mu^2) - 2c_7(4 - 3\mu^2)) + \frac{2e^2 (\tilde{e}_{118} - e_{91})}{\pi} + \frac{e^2}{192\pi^3 F^2} (4c_1 - c_2 - 2c_3) \\
& + \frac{e^2 \Xi_1}{96\pi^3 F^2 m} (3g_A^2 c_6(\mu^2 - 1) + 3g_A^2 c_7(3\mu^2 - 2) - c_2 m).
\end{aligned}$$

b. Spin-independent second-order polarizabilities

$$\begin{aligned}
\alpha_{E2}^{(n)} &= -\frac{e^2 g_A^2}{128\pi^3 F^2 (\mu^2 - 4)m^3} [8c_6 \Xi_2(7\mu^4 - 45\mu^2 + 60) + 4c_7 \Xi_2(20\mu^4 - 129\mu^2 + 174) \\
& - c_6(196 - 65\mu^2) - 2c_7(152 - 49\mu^2)] + \frac{e^2 (-32c_1 + 15\mu^2 c_2 - 44c_3)}{960\pi^3 F^2 \mu^2 m^2} \\
& + \frac{e^2 \Xi_1}{32\pi^3 F^2 m^3} [2g_A^2 c_6(7\mu^2 - 3) + g_A^2 c_7(20\mu^2 - 9) + c_2 m] + \frac{3e^2 (\tilde{e}_{117} - e_{92})}{2\pi m^2}, \\
\beta_{M2}^{(n)} &= -\frac{e^2 g_A^2}{128\pi^3 F^2 \mu^2 (\mu^2 - 4)^2 m^3} [24c_6 \Xi_2(2\mu^8 - 21\mu^6 + 70\mu^4 - 66\mu^2 + 8) \\
& + 4c_7 \Xi_2(22\mu^8 - 231\mu^6 + 770\mu^4 - 740\mu^2 + 80) + c_6(57\mu^6 - 412\mu^4 + 544\mu^2) \\
& + 2c_7(53\mu^6 - 382\mu^4 + 536\mu^2)] + \frac{e^2 (32c_1 + (15\mu^2 + 8)c_2 + 44c_3)}{960\pi^3 F^2 \mu^2 m^2} + \frac{3e^2 (\tilde{e}_{117} - e_{92})}{2\pi m^2} \\
& + \frac{e^2 \Xi_1}{32\pi^3 F^2 m^3} [6g_A^2 c_6(2\mu^2 - 1) + 11g_A^2 c_7(2\mu^2 - 1) + c_2 m], \\
\alpha_{E1\nu}^{(n)} &= -\frac{e^2 g_A^2}{1536\pi^3 F^2 \mu^2 (\mu^2 - 4)^2 m^3} [8c_6 \Xi_2(18\mu^8 - 197\mu^6 + 710\mu^4 - 826\mu^2 + 184) \\
& + 4c_7 \Xi_2(90\mu^8 - 969\mu^6 + 3390\mu^4 - 3740\mu^2 + 656) + c_6(135\mu^4 - 1012\mu^2 + 1408) \\
& + 6c_7(57\mu^4 - 414\mu^2 + 584)] + \frac{e^2 \Xi_1}{384\pi^3 F^2 m^3} [2g_A^2 c_6(18\mu^2 - 17) + 3g_A^2 c_7(30\mu^2 \\
& - 23) - c_2 m] + \frac{e^2 (96c_1 + (16 - 15\mu^2)c_2 + 132c_3)}{11520\pi^3 F^2 \mu^2 m^2} - \frac{e^2 (\tilde{e}_{117} - e_{92})}{8\pi m^2}, \\
\beta_{M1\nu}^{(n)} &= \frac{e^2 g_A^2}{1536\pi^3 F^2 \mu^2 (\mu^2 - 4)^3 m^3} [8c_6 \Xi_2(-29\mu^{10} + 419\mu^8 - 2212\mu^6 + 5016\mu^4 \\
& - 3976\mu^2 + 128) + 4c_7 \Xi_2(-108\mu^{10} + 1567\mu^8 - 8330\mu^6 + 19104\mu^4 - 15520\mu^2
\end{aligned}$$

$$\begin{aligned}
& + 896) - c_6(223\mu^8 - 2420\mu^6 + 8768\mu^4 - 9792\mu^2 + 512) - 2c_7(207\mu^8 - 2264\mu^6 \\
& + 8240\mu^4 - 9152\mu^2 + 512)] + \frac{e^2 \Xi_1}{384\pi^3 F^2 m^3} [2g_A^2 c_6(29\mu^2 - 13) + g_A^2 c_7(108\mu^2 \\
& - 55) - c_2 m] - \frac{e^2(32c_1 + (5\mu^2 + 8)c_2 + 44c_3)}{3840\pi^3 F^2 \mu^2 m^2} - \frac{e^2(\tilde{e}_{117} - e_{92})}{8\pi m^2}.
\end{aligned}$$

c. Spin-dependent first-order polarizabilities

$$\begin{aligned}
\gamma_{\text{E1E1}}^{(n)} &= \frac{e^2 g_A^2}{192\pi^3 F^2 (\mu^2 - 4)^2 m^2} [c_6 \Xi_2(-4\mu^6 + 43\mu^4 - 150\mu^2 + 180) + c_7 \Xi_2(-13\mu^6 \\
& + 139\mu^4 - 474\mu^2 + 516) - c_6(4\mu^4 - 29\mu^2 + 64) - c_7(13\mu^4 - 89\mu^2 + 160)] \\
& + \frac{e^2 g_A^2 \Xi_1}{192\pi^3 F^2 m^2} [c_6(4\mu^2 - 3) + c_7(13\mu^2 - 9)], \\
\gamma_{\text{M1M1}}^{(n)} &= \frac{e^2 g_A^2}{192\pi^3 F^2 (\mu^2 - 4)^2 m^2 \mu^2} [c_6 \Xi_2(-9\mu^8 + 92\mu^6 - 290\mu^4 + 216\mu^2) \\
& - c_7 \Xi_2(23\mu^8 - 239\mu^6 + 786\mu^4 - 712\mu^2 + 64) - c_6(9\mu^6 - 62\mu^4 + 56\mu^2) \\
& - c_7(23\mu^6 - 166\mu^4 + 200\mu^2)] + \frac{e^2 g_A^2 \Xi_1}{192\pi^3 F^2 m^2} [c_6(9\mu^2 - 2) + c_7(23\mu^2 - 9)], \\
\gamma_{\text{E1M2}}^{(n)} &= \frac{e^2 g_A^2}{192\pi^3 F^2 (\mu^2 - 4)^2 m^2} [c_6 \Xi_2(3\mu^6 - 32\mu^4 + 110\mu^2 - 108) + c_7 \Xi_2(-3\mu^6 \\
& + 31\mu^4 - 94\mu^2 + 84) + c_6(3\mu^4 - 23\mu^2 + 32) - c_7(3\mu^4 - 13\mu^2 + 16)] \\
& + \frac{e^2 g_A^2 \Xi_1}{192\pi^3 F^2 m^2} [c_6(2 - 3\mu^2) + c_7(3\mu^2 - 1)], \\
\gamma_{\text{M1E2}}^{(n)} &= \frac{e^2 g_A^2}{192\pi^3 F^2 m^2 \mu^2} [c_6 \Xi_2(2\mu^4 - 7\mu^2 + 2) - c_7 \Xi_2(\mu^4 + \mu^2 - 2) + (2c_6 - c_7)\mu^2] \\
& + \frac{e^2 g_A^2 \Xi_1}{192\pi^3 F^2 m^2} [c_6(3 - 2\mu^2) + c_7(\mu^2 + 3)].
\end{aligned}$$

d. Spin-dependent second-order polarizabilities

$$\begin{aligned}
\gamma_{\text{E2E2}}^{(n)} &= \frac{e^2 g_A^2}{138240\pi^3 F^2 \mu^2 (\mu^2 - 4)^3 m^4} [3c_6 \Xi_2(-895\mu^{10} + 13239\mu^8 - 72576\mu^6 \\
& + 175180\mu^4 - 164240\mu^2 + 20480) + 6c_7 \Xi_2(-795\mu^{10} + 11782\mu^8 - 64748\mu^6 \\
& + 156750\mu^4 - 147080\mu^2 + 19200) + c_6 \mu^2(-2685\mu^6 + 30197\mu^4 - 111268\mu^2 \\
& + 138080) + c_7 \mu^2(-4770\mu^6 + 53717\mu^4 - 197908\mu^2 + 241760)] \\
& + \frac{e^2 g_A^2 \Xi_1}{46080\pi^3 F^2 m^4} [c_6(895\mu^2 - 709) + 2c_7(795\mu^2 - 652)], \\
\gamma_{\text{M2M2}}^{(n)} &= \frac{e^2 g_A^2}{138240\pi^3 F^2 \mu^2 (\mu^2 - 4)^3 m^4} [3c_6 \Xi_2(-1377\mu^{10} + 19929\mu^8 - 105504\mu^6 \\
& + 238100\mu^4 - 181520\mu^2 + 17280) + 6c_7 \Xi_2(-1341\mu^{10} + 19482\mu^8 - 103812\mu^6
\end{aligned}$$

$$\begin{aligned}
& + 237490\mu^4 - 189400\mu^2 + 22080) - c_6(4131\mu^8 - 45451\mu^6 + 159284\mu^4 \\
& - 145024\mu^2 + 3840) - c_7(8046\mu^8 - 89011\mu^6 + 315884\mu^4 - 306304\mu^2 + 15360)] \\
& + \frac{e^2 g_A^2 \Xi_1}{15360\pi^3 F^2 m^4} [c_6(459\mu^2 - 217) + 2c_7(447\mu^2 - 236)], \\
\gamma_{E2M3}^{(n)} = & \frac{e^2 g_A^2}{69120\pi^3 F^2 \mu^2 (\mu^2 - 4)^3 m^4} [3c_6 \Xi_2(113\mu^{10} - 1689\mu^8 + 9408\mu^6 - 23060\mu^4 \\
& + 20080\mu^2 - 2560) - 6c_7 \Xi_2 \mu^2(51\mu^8 - 718\mu^6 + 3596\mu^4 - 7230\mu^2 + 5000) \\
& + c_6 \mu^2(339\mu^6 - 4003\mu^4 + 15452\mu^2 - 15136) + c_7 \mu^2(-306\mu^6 + 2957\mu^4 - 7828\mu^2 \\
& + 7904)] + \frac{e^2 g_A^2 \Xi_1}{23040\pi^3 F^2 m^4} [c_6(107 - 113\mu^2) + 2c_7(51\mu^2 - 4)], \\
\gamma_{M2E3}^{(n)} = & \frac{e^2 g_A^2}{69120\pi^3 F^2 \mu^2 (\mu^2 - 4)^2 m^4} [3c_6 \Xi_2(111\mu^8 - 1227\mu^6 + 4500\mu^4 - 5980\mu^2 + 1920) \\
& + 6c_7 \Xi_2(3\mu^8 - 66\mu^6 + 420\mu^4 - 1070\mu^2 + 960) + c_6(333\mu^6 - 2393\mu^4 + 4568\mu^2 - 960) \\
& + c_7(18\mu^6 - 53\mu^4 + 248\mu^2 - 960)] + \frac{e^2 g_A^2 \Xi_1}{7680\pi^3 F^2 m^4} [c_6(39 - 37\mu^2) - 2c_7(\mu^2 - 12)], \\
\gamma_{E1E1v}^{(n)} = & \frac{e^2 g_A^2}{46080\pi^3 F^2 \mu^2 (\mu^2 - 4)^4 m^4} [-3c_6 \Xi_2(1339\mu^{12} - 24999\mu^{10} + 184860\mu^8 \\
& - 674892\mu^6 + 1211040\mu^4 - 883520\mu^2 + 122880) - 6c_7 \Xi_2(1787\mu^{12} - 33422\mu^{10} \\
& + 247860\mu^8 - 909966\mu^6 + 1654880\mu^4 - 1245280\mu^2 + 184320) + c_6(-4017\mu^{10} \\
& + 61305\mu^8 - 346112\mu^6 + 833840\mu^4 - 727424\mu^2 + 84992) + c_7(-10722\mu^{10} \\
& + 163845\mu^8 - 929672\mu^6 + 2283920\mu^4 - 2071424\mu^2 + 223232)] \\
& + \frac{e^2 g_A^2 \Xi_1}{15360\pi^3 F^2 m^4} [13c_6(103\mu^2 - 69) + 2c_7(1787\mu^2 - 1256)], \\
\gamma_{M1M1v}^{(n)} = & \frac{e^2 g_A^2}{15360\pi^3 F^2 \mu^4 (\mu^2 - 4)^4 m^4} [-c_6 \Xi_2 \mu^2(1413\mu^{12} - 26345\mu^{10} + 194436\mu^8 \\
& - 708756\mu^6 + 1285760\mu^4 - 953280\mu^2 + 122880) - 2c_7 \Xi_2(1997\mu^{14} - 37266\mu^{12} \\
& + 275292\mu^{10} - 1003890\mu^8 + 1814400\mu^6 - 1334496\mu^4 + 168448\mu^2 + 6144) \\
& + c_6 \mu^2(-1413\mu^{10} + 21277\mu^8 - 117992\mu^6 + 292400\mu^4 - 256896\mu^2 + 8192) \\
& + c_7 \mu^2(-3994\mu^{10} + 60273\mu^8 - 334632\mu^6 + 818160\mu^4 - 707712\mu^2 + 31744)] \\
& + \frac{e^2 g_A^2 \Xi_1}{15360\pi^3 F^2 m^4} [c_6(1413\mu^2 - 911) + 2c_7(1997\mu^2 - 1320)], \\
\gamma_{E1M2v}^{(n)} = & \frac{e^2 g_A^2}{115200\pi^3 F^2 \mu^2 (\mu^2 - 4)^4 m^4} [3c_6 \Xi_2(-1621\mu^{12} + 29085\mu^{10} - 202572\mu^8 \\
& + 667452\mu^6 - 949760\mu^4 + 264640\mu^2 + 180480) - 6c_7 \Xi_2(3183\mu^{12} - 58600\mu^{10} \\
& + 424836\mu^8 - 1504806\mu^6 + 2553440\mu^4 - 1608800\mu^2 + 76160) - c_6(4863\mu^{10}
\end{aligned}$$

$$\begin{aligned}
& -71337\mu^8 + 376280\mu^6 - 744112\mu^4 + 285888\mu^2 + 97280) + c_7(-19098\mu^{10} \\
& + 287277\mu^8 - 1591400\mu^6 + 3681712\mu^4 - 2808768\mu^2 + 56320)] \\
& + \frac{e^2 g_A^2 \Xi_1}{38400\pi^3 F^2 m^4} [c_6(1621\mu^2 + 93) + 2c_7(3183\mu^2 - 1306)], \\
\gamma_{\text{M1E2v}}^{(n)} = & \frac{e^2 g_A^2}{115200\pi^3 F^2 \mu^4 (\mu^2 - 4)^3 m^4} [-3c_6 \Xi_2(443\mu^{12} - 6359\mu^{10} + 33208\mu^8 \\
& - 74660\mu^6 + 69680\mu^4 - 3840\mu^2 + 5120) - 6c_7 \Xi_2(2089\mu^{12} - 30692\mu^{10} + 166204\mu^8 \\
& - 391370\mu^6 + 350200\mu^4 - 42240\mu^2 + 2560) + c_6\mu^2(-1329\mu^8 + 13323\mu^6 - 40892\mu^4 \\
& + 51616\mu^2 + 33280) + c_7\mu^2(-12534\mu^8 + 137763\mu^6 - 482012\mu^4 + 542176\mu^2 \\
& + 33280)] + \frac{e^2 g_A^2 \Xi_1}{38400\pi^3 F^2 m^4} [c_6(443\mu^2 - 157) + 2c_7(2089\mu^2 - 1446)].
\end{aligned}$$

APPENDIX E: RENORMALIZATION OF THE NUCLEON MAGNETIC MOMENTS

Below, we provide the expressions for the LECs c_6 , c_7 in terms of the renormalized quantities \bar{c}_6 and \bar{c}_7 , see Sec. II C.

$$c_6 = \bar{c}_6 + \delta c_6^{(3)} + \delta c_6^{(4)}, \quad c_7 = \bar{c}_7 + \delta c_7^{(3)} + \delta c_7^{(4)}, \quad (\text{E1})$$

with

$$\begin{aligned}
\delta c_6^{(3)} = & -\frac{g_A^2}{F^2(4m^2 - M^2)} ((4(\epsilon - 4)m^2 - 3(\epsilon - 2)M^2)A_0(m) + (4(5 - 2\epsilon)m^2 + 3(\epsilon - 2)M^2)A_0(M) \\
& + (16m^4 + 2(4\epsilon - 13)M^2m^2 - 3(\epsilon - 2)M^4)B_0(m, M, m^2)) \\
& - \frac{h_A^2}{3(\epsilon - 2)(2\epsilon - 3)^3 F^2 m^2 m_\Delta^4} (-10(\epsilon - 2)(\epsilon - 1)^2(2\epsilon - 3)m^6 - 20(\epsilon - 2)^2(\epsilon - 1)(2\epsilon - 1)m_\Delta m^5 \\
& + (20(\epsilon - 1)^2(2\epsilon - 5)(2\epsilon - 3)M^2 + (\epsilon - 2)^2(\epsilon(4\epsilon(7\epsilon - 18) - 13) + 47)m_\Delta^2)m^4 \\
& + 2(\epsilon - 2)(2\epsilon - 3)m_\Delta(10(\epsilon - 1)(3\epsilon - 4)M^2 + (\epsilon(\epsilon(14\epsilon - 43) + 10) + 2)m_\Delta^2)m^3 \\
& + 2(\epsilon - 2)(5(\epsilon - 1)^2(2\epsilon - 3)M^4 + (7 - \epsilon(8\epsilon((\epsilon - 5)\epsilon + 3) + 25))m_\Delta^2 M^2 \\
& + (\epsilon(\epsilon(8\epsilon^2 - 50\epsilon + 71) - 51) + 35)m_\Delta^4)m^2 + 2(\epsilon - 2)(M^2 - m_\Delta^2)m_\Delta(((\epsilon - 2)\epsilon(12(\epsilon - 3)\epsilon + 47) \\
& + 20)m_\Delta^2 - 20(\epsilon - 1)^2 M^2)m - 3(\epsilon - 1)(2\epsilon^2 - 7\epsilon + 6)^2 m_\Delta^2 (m_\Delta^2 - M^2)^2)A_0(M) \\
& + \frac{h_A^2}{3(\epsilon - 2)(2\epsilon - 3)^3 F^2 m^2 m_\Delta^4} (10(\epsilon - 2)(\epsilon - 1)^2(2\epsilon - 3)m^6 + 20(\epsilon - 2)^2(\epsilon - 1)(2\epsilon - 1)m_\Delta m^5 \\
& + (-20(\epsilon - 2)(\epsilon - 1)^2(2\epsilon - 3)M^2 - (\epsilon(\epsilon(\epsilon(4\epsilon(7\epsilon - 36) + 207) + 111) \\
& - 460) + 248)m_\Delta^2)m^4 + 2m_\Delta((\epsilon(\epsilon(\epsilon(4\epsilon(13\epsilon - 94) + 1035) - 1306) + 754) \\
& - 172)m_\Delta^2 - 10(\epsilon - 2)(\epsilon - 1)(\epsilon(2\epsilon - 7) + 4)M^2)m^3 + 2(\epsilon - 2)(5(\epsilon - 1)^2(2\epsilon - 3)M^4 \\
& - 5(\epsilon(\epsilon(4(\epsilon - 5)\epsilon + 27) - 13) + 4)m_\Delta^2 M^2 + (\epsilon(2\epsilon(5\epsilon(2\epsilon - 11) + 91) - 141) \\
& + 62)m_\Delta^4)m^2 + 2(\epsilon - 2)(M - m_\Delta)m_\Delta(M + m_\Delta)((\epsilon - 2)\epsilon(12(\epsilon - 3)\epsilon + 47) \\
& + 20)m_\Delta^2 - 20(\epsilon - 1)^2 M^2)m - 3(\epsilon - 1)(2\epsilon^2 - 7\epsilon + 6)^2 m_\Delta^2 (m_\Delta^2 - M^2)^2)A_0(m_\Delta) \\
& + \frac{h_A^2((m + m_\Delta)^2 - M^2)}{3(2\epsilon - 3)^3 F^2 m^2 m_\Delta^4} (-10(\epsilon - 1)^2(2\epsilon - 3)m^6 + 20(\epsilon - 1)m_\Delta m^5 \\
& + (2\epsilon - 3)(20(\epsilon - 1)^2 M^2 + (\epsilon(\epsilon(14\epsilon - 23) - 39) + 38)m_\Delta^2)m^4 + 2m_\Delta((\epsilon(4(22 \\
& - 5\epsilon)\epsilon - 159) + 98)m_\Delta^2 - 10(\epsilon - 1)(2\epsilon - 1)M^2)m^3 + 2(2\epsilon - 3)(-5(\epsilon - 1)^2 M^4
\end{aligned}$$

$$\begin{aligned}
& + 5(\epsilon(\epsilon(2\epsilon - 7) + 7) - 4)m_\Delta^2 M^2 + (7 - 2(\epsilon - 1)\epsilon(5\epsilon - 12))m_\Delta^4) m^2 \\
& + 2(M^2 - m_\Delta^2)m_\Delta(20(\epsilon - 1)^2 M^2 + (\epsilon(4(10 - 3\epsilon)\epsilon - 59) + 34)m_\Delta^2)m \\
& + 3(3 - 2\epsilon)^2(\epsilon - 2)(\epsilon - 1)m_\Delta^2(M^2 - m_\Delta^2)^2 B_0(M, m_\Delta, m^2),
\end{aligned} \tag{E2}$$

$$\begin{aligned}
\delta c_7^{(3)} = & -\frac{4(1 - \epsilon)g_A^2 m^2}{F^2(4m^2 - M^2)}(2A_0(m) - A_0(M)) + \frac{2g_A^2 m^2(4m^2 - 2(1 - \epsilon)M^2)}{F^2(4m^2 - M^2)}B_0(m, M, m^2) \\
& - \frac{2h_A^2}{3F^2(\epsilon - 2)(2\epsilon - 3)^3 mm_\Delta^4}((\epsilon - 2)(\epsilon - 1)^2(2\epsilon - 3)m^5 + 2(\epsilon - 2)^2(\epsilon - 1)(2\epsilon \\
& - 1)m_\Delta m^4 + (-2(\epsilon - 1)^2(2\epsilon - 5)(2\epsilon - 3)M^2 - (\epsilon - 2)^2(\epsilon(4(\epsilon - 3)\epsilon + 5) \\
& + 2)m_\Delta^2)m^3 - (\epsilon - 2)(2\epsilon - 3)m_\Delta(2(\epsilon - 1)(3\epsilon - 4)M^2 + (\epsilon(2\epsilon(2\epsilon - 7) + 11) \\
& - 5)m_\Delta^2)m^2 + (\epsilon - 2)(M^2 - m_\Delta^2)((\epsilon(2\epsilon - 7)(2(\epsilon - 2)\epsilon + 3) + 7)m_\Delta^2 \\
& - (\epsilon - 1)^2(2\epsilon - 3)M^2)m + 4(\epsilon - 2)(\epsilon - 1)^2 m_\Delta(M^2 - m_\Delta^2)^2)A_0(M) \\
& - \frac{2h_A^2}{3F^2(\epsilon - 2)(2\epsilon - 3)^3 mm_\Delta^4}(-4(\epsilon - 2)(\epsilon - 1)^2 m_\Delta^5 + (\epsilon - 2)(\epsilon(2\epsilon - 7)(2(\epsilon - 2)\epsilon \\
& + 3) + 7)mm_\Delta^4 + (((\epsilon - 1)\epsilon(8\epsilon((\epsilon - 6)\epsilon + 12) - 59) - 2)m^2 + 8(\epsilon - 2)(\epsilon \\
& - 1)^2 M^2)m_\Delta^3 + m((- \epsilon(2\epsilon - 5)(\epsilon(\epsilon(2\epsilon - 7) + 8) + 2) - 14)m^2 \\
& - (\epsilon - 2)(\epsilon(\epsilon(4(\epsilon - 5)\epsilon + 27) - 13) + 4)M^2)m_\Delta^2 \\
& + 2(\epsilon - 2)(\epsilon - 1)(m^2 - M^2)((\epsilon - 2)(2\epsilon - 1)m^2 + 2(\epsilon - 1)M^2)m_\Delta \\
& + (\epsilon - 2)(\epsilon - 1)^2(2\epsilon - 3)m(m - M)^2(m + M)^2)A_0(m_\Delta) \\
& - \frac{2h_A^2((m + m_\Delta)^2 - M^2)}{3F^2(2\epsilon - 3)^3 mm_\Delta^4}(-(\epsilon - 1)^2(2\epsilon - 3)m^5 + 2(\epsilon - 1)m_\Delta m^4 + (2\epsilon - 3)(2(\epsilon \\
& - 1)^2 M^2 + ((2\epsilon - 5)\epsilon^2 + 2)m_\Delta^2)m^3 + m_\Delta((-4\epsilon^2 + 6\epsilon - 2)M^2 + (\epsilon(-4(\epsilon - 5)\epsilon \\
& - 39) + 25)m_\Delta^2)m^2 - (2\epsilon - 3)(M^2 - m_\Delta^2)((\epsilon - 1)^2 M^2 + (\epsilon(-2(\epsilon - 4)\epsilon - 9) \\
& + 5)m_\Delta^2)m + 4(\epsilon - 1)^2 m_\Delta(M^2 - m_\Delta^2)^2)B_0(m_\Delta, M, m^2),
\end{aligned} \tag{E3}$$

$$\begin{aligned}
\delta c_6^{(4)} = & -\frac{g_A^2 c_6 M^2 B_0(m, M, m^2)}{2F^2(4m^2 - M^2)}(8m^2(2\epsilon - 2) + M^2(5 - 6\epsilon)) \\
& + \frac{A_0(M)}{2F^2 m(2\epsilon - 4)(4m^2 - M^2)}(c_6 m(2\epsilon - 4)(8m^2(g_A^2(2\epsilon - 2) - 1) \\
& + M^2(2 - 3g_A^2(2\epsilon - 2))) + 4(4m^2 - M^2)(2c_4 m^2(2\epsilon - 4) + 3c_2 M^2)) \\
& - \frac{g_A^2 c_6 A_0(m)}{2F^2(4m^2 - M^2)}(4m^2(2\epsilon - 1) + M^2(5 - 6\epsilon)) + \frac{4M^2}{m}(c_1 c_6 + 4e_{106} m^2),
\end{aligned} \tag{E4}$$

$$\begin{aligned}
\delta c_7^{(4)} = & -\frac{g_A^2 M^2 B_0(m, M, m^2)}{2F^2(4m^2 - M^2)}(c_6(2M^2 - 4m^2(2\epsilon + 1)) - 3c_7(M^2(2\epsilon - 3) + 8m^2)) \\
& - \frac{A_0(M)}{2F^2(4m^2 - M^2)}(c_6(4m^2(g_A^2(2\epsilon + 1) - 1) + (1 - 3g_A^2)M^2) + 3g_A^2 c_7(M^2(2\epsilon - 4) + 8m^2) \\
& + 4c_4 m(4m^2 - M^2)) + \frac{g_A^2 A_0(m)}{2F^2(4m^2 - M^2)}(c_6(8m^2(2\epsilon - 1) - 2M^2) \\
& + 3c_7(4m^2(2\epsilon - 1) + M^2(2\epsilon - 3))) + \frac{4M^2}{m}(c_1 c_7 + 2m^2(2e_{105} - e_{106})),
\end{aligned} \tag{E5}$$

with the space-time dimension $d = 4 - 2\epsilon$. The expressions for the loop integrals are provided in Appendix F.

APPENDIX F: LOOP INTEGRALS

The loop integral functions are defined as

$$\begin{aligned} A_0(m) &= \frac{1}{i} \int \frac{d^d l}{(2\pi)^d} \frac{\mu^{4-d}}{l^2 - m_0^2 + i\varepsilon}, \\ B_0(m_1, m_2, p^2) &= \frac{1}{i} \int \frac{d^d l}{(2\pi)^d} \frac{\mu^{4-d}}{(l^2 - m_1^2 + i\varepsilon)[(l - p)^2 - m_2^2 + i\varepsilon]}. \end{aligned} \quad (\text{F1})$$

The renormalization scale μ in all integrals is set to $\mu = m$.

- [1] M. Tanabashi *et al.* (Particle Data Group), *Phys. Rev. D* **98**, 030001 (2018).
- [2] J. Ahrens *et al.* (GDH and A2 Collaborations), *Phys. Rev. Lett.* **87**, 022003 (2001).
- [3] H. Dutz *et al.* (GDH Collaboration), *Phys. Rev. Lett.* **91**, 192001 (2003).
- [4] M. Camen, K. Kossert, F. Wissmann, J. Ahrens, H. J. Arends, R. Beck, G. Caselotti, P. Grabmayr, P. D. Harty, O. Jahn, P. Jennewein, R. Kondratiev, M. I. Levchuk, V. Lisin, A. I. Lvov, J. C. McGeorge, A. Natter, V. OlmosdeLeon, M. Schumacher, B. Seitz, F. Smend, A. Thomas, W. Weihofen, and F. Zapadka, *Phys. Rev. C* **65**, 032202(R) (2002).
- [5] P. P. Martel *et al.* (A2 Collaboration at MAMI), *Phys. Rev. Lett.* **114**, 112501 (2015).
- [6] D. Paudyal *et al.* (A2 Collaboration), *Phys. Rev. C* **102**, 035205 (2020).
- [7] Y. Prok *et al.* (CLAS Collaboration), *Phys. Lett. B* **672**, 12 (2009).
- [8] M. Amarian *et al.* (Jefferson Lab E94010 Collaboration), *Phys. Rev. Lett.* **93**, 152301 (2004).
- [9] N. Guler *et al.* (CLAS Collaboration), *Phys. Rev. C* **92**, 055201 (2015).
- [10] O. Gryniuk, F. Hagelstein, and V. Pascalutsa, *Phys. Rev. D* **94**, 034043 (2016).
- [11] A. Deur, in *Proceedings of the 9th International Workshop on Chiral Dynamics (CD18) Durham, NC, USA, September 17–21, 2018* (2019), https://misportal.jlab.org/ul/publications/view_pub.cfm?pub_id=15828.
- [12] W. Detmold, B. C. Tiburzi, and A. Walker-Loud, *Phys. Rev. D* **81**, 054502 (2010).
- [13] J. M. M. Hall, D. B. Leinweber, and R. D. Young, *Phys. Rev. D* **89**, 054511 (2014).
- [14] M. Lujan, A. Alexandru, W. Freeman, and F. X. Lee, *Phys. Rev. D* **89**, 074506 (2014).
- [15] W. Freeman, A. Alexandru, M. Lujan, and F. X. Lee, *Phys. Rev. D* **90**, 054507 (2014).
- [16] E. Chang, W. Detmold, K. Orginos, A. Parreno, M. J. Savage, B. C. Tiburzi, and S. R. Beane (NPLQCD Collaboration), *Phys. Rev. D* **92**, 114502 (2015).
- [17] R. Bignell, D. Leinweber, W. Kamleh, and M. Burkardt, PoS **INPC2016**, 287 (2017).
- [18] R. Bignell, J. Hall, W. Kamleh, D. Leinweber, and M. Burkardt, *Phys. Rev. D* **98**, 034504 (2018).
- [19] V. Bernard, N. Kaiser, and Ulf-G. Meißner, *Phys. Rev. Lett.* **67**, 1515 (1991).
- [20] V. Bernard, N. Kaiser, and Ulf-G. Meißner, *Nucl. Phys. B* **373**, 346 (1992).
- [21] V. Bernard, N. Kaiser, and Ulf-G. Meißner, *Int. J. Mod. Phys. E* **4**, 193 (1995).
- [22] K. B. Vijaya Kumar, J. A. McGovern, and M. C. Birse, *Phys. Lett. B* **479**, 167 (2000).
- [23] G. C. Gellas, T. R. Hemmert, and Ulf-G. Meißner, *Phys. Rev. Lett.* **85**, 14 (2000).
- [24] T. R. Hemmert, B. R. Holstein, and J. Kambor, *Phys. Rev. D* **55**, 5598 (1997).
- [25] V. Bernard, *Prog. Part. Nucl. Phys.* **60**, 82 (2008).
- [26] T. Becher and H. Leutwyler, *Eur. Phys. J. C* **9**, 643 (1999).
- [27] T. Fuchs, J. Gegelia, G. Japaridze, and S. Scherer, *Phys. Rev. D* **68**, 056005 (2003).
- [28] J. Gegelia and G. Japaridze, *Phys. Rev. D* **60**, 114038 (1999).
- [29] D. Siemens, V. Bernard, E. Epelbaum, A. Gasparyan, H. Krebs, and Ulf-G. Meißner, *Phys. Rev. C* **94**, 014620 (2016).
- [30] T. R. Hemmert, B. R. Holstein, and J. Kambor, *J. Phys. G* **24**, 1831 (1998).
- [31] V. Bernard, E. Epelbaum, H. Krebs, and Ulf-G. Meißner, *Phys. Rev. D* **87**, 054032 (2013).
- [32] D.-L. Yao, D. Siemens, V. Bernard, E. Epelbaum, A. M. Gasparyan, J. Gegelia, H. Krebs, and Ulf-G. Meißner, *J. High Energy Phys.* **05** (2016) 038.
- [33] D. Siemens, J. Ruiz de Elvira, E. Epelbaum, M. Hoferichter, H. Krebs, B. Kubis, and Ulf-G. Meißner, *Phys. Lett. B* **770**, 27 (2017).
- [34] J. Rijneveen, N. Rijneveen, H. Krebs, A. Gasparyan, and E. Epelbaum, [arXiv:2006.03917](https://arxiv.org/abs/2006.03917).
- [35] V. Pascalutsa and D. R. Phillips, *Phys. Rev. C* **67**, 055202 (2003).
- [36] L. S. Geng, J. Martin Camalich, L. Alvarez-Ruso, and M. J. Vicente Vacas, *Phys. Rev. D* **78**, 014011 (2008).
- [37] J. M. Alarcon, J. M. Martin Camalich, and J. A. Oller, *Phys. Rev. D* **85**, 051503(R) (2012).
- [38] J. M. Alarcón, F. Hagelstein, V. Lensky, and V. Pascalutsa, *Phys. Rev. D* **102**, 014006 (2020).
- [39] J. M. Alarcón, F. Hagelstein, V. Lensky, and V. Pascalutsa, *Phys. Rev. D* **102**, 114026 (2020).
- [40] V. Lensky, J. McGovern, and V. Pascalutsa, *Eur. Phys. J. C* **75**, 604 (2015).
- [41] D. Babusci, G. Giordano, A. I. L'vov, G. Matone, and A. M. Nathan, *Phys. Rev. C* **58**, 1013 (1998).
- [42] B. R. Holstein, D. Drechsel, B. Pasquini, and M. Vanderhaeghen, *Phys. Rev. C* **61**, 034316 (2000).
- [43] V. Olmos de Leon *et al.*, *Eur. Phys. J. A* **10**, 207 (2001).
- [44] D. Drechsel, B. Pasquini, and M. Vanderhaeghen, *Phys. Rept.* **378**, 99 (2003).

- [45] R. P. Hildebrandt, H. W. Griesshammer, T. R. Hemmert, and B. Pasquini, *Eur. Phys. J. A* **20**, 293 (2004).
- [46] B. Pasquini, D. Drechsel, and M. Vanderhaeghen, *Phys. Rev. C* **76**, 015203 (2007).
- [47] A. Gasparyan and M. F. M. Lutz, *Nucl. Phys. A* **848**, 126 (2010).
- [48] A. Gasparyan, M. Lutz, and B. Pasquini, *Nucl. Phys. A* **866**, 79 (2011).
- [49] J. Wess and B. Zumino, *Phys. Lett. B* **37**, 95 (1971).
- [50] E. Witten, *Nucl. Phys. B* **223**, 422 (1983).
- [51] N. Fettes, Ulf-G. Meißner, M. Mojzis, and S. Steininger, *Annals Phys.* **283**, 273 (2000).
- [52] H.-B. Tang and P. J. Ellis, *Phys. Lett. B* **387**, 9 (1996).
- [53] H. Krebs, E. Epelbaum, and Ulf-G. Meißner, *Phys. Lett. B* **683**, 222 (2010).
- [54] J. Gasser and H. Leutwyler, *Annals Phys.* **158**, 142 (1984).
- [55] T. R. Hemmert, Ph.D. thesis, Massachusetts U., Amherst (1997), <http://wwwlib.umi.com/dissertations/fullcit?p9809346>.
- [56] S. Weinberg, *Nucl. Phys. B* **363**, 3 (1991).
- [57] J. Gasser, M. E. Sainio, and A. Svarc, *Nucl. Phys. B* **307**, 779 (1988).
- [58] A. Denner, S. Dittmaier, M. Roth, and D. Wackerlo, *Nucl. Phys. B* **560**, 33 (1999).
- [59] A. Denner and S. Dittmaier, *Nucl. Phys. B Proc. Suppl.* **160**, 22 (2006).
- [60] T. Fuchs, J. Gegelia, and S. Scherer, *J. Phys. G* **30**, 1407 (2004).
- [61] V. Lensky, F. Hagelstein, V. Pascalutsa, and M. Vanderhaeghen, *Phys. Rev. D* **97**, 074012 (2018).
- [62] H. W. Griesshammer and T. R. Hemmert, *Phys. Rev. C* **65**, 045207 (2002).
- [63] I. Guiasu and E. Radescu, *Annals Phys.* **120**, 145 (1979).
- [64] C. Ditsche, M. Hoferichter, B. Kubis, and Ulf-G. Meißner, *J. High Energy Phys.* **06** (2012) 043.
- [65] Wolfram Research, Inc., Mathematica, Version 12.0 (Champaign, IL, 2019), <https://www.wolfram.com/mathematica>.
- [66] J. Kuipers, T. Ueda, J. A. M. Vermaseren, and J. Vollinga, *Comput. Phys. Commun.* **184**, 1453 (2013).
- [67] H. H. Patel, *Comput. Phys. Commun.* **218**, 66 (2017).
- [68] E. Epelbaum *et al.*, *Eur. Phys. J. A* **56**, 92 (2020).
- [69] E. Epelbaum, H. Krebs, and P. Reinert, *Front. in Phys.* **8**, 98 (2020).
- [70] R. J. Furnstahl, N. Klco, D. R. Phillips, and S. Wesolowski, *Phys. Rev. C* **92**, 024005 (2015).
- [71] J. A. Melendez, S. Wesolowski, and R. J. Furnstahl, *Phys. Rev. C* **96**, 024003 (2017).
- [72] J. A. Melendez, R. J. Furnstahl, D. R. Phillips, M. T. Pratola, and S. Wesolowski, *Phys. Rev. C* **100**, 044001 (2019).
- [73] E. Epelbaum, PoS **CD2018**, 006 (2019).
- [74] J. A. McGovern, D. R. Phillips, and H. W. Griesshammer, *Eur. Phys. J. A* **49**, 12 (2013).
- [75] V. Lensky and J. A. McGovern, *Phys. Rev. C* **89**, 032202(R) (2014).
- [76] V. Pascalutsa, *Phys. Lett. B* **503**, 85 (2001).
- [77] H. Krebs, E. Epelbaum, and Ulf-G. Meißner, *Phys. Rev. C* **80**, 028201 (2009).
- [78] H. W. Griesshammer, J. A. McGovern, and D. R. Phillips, *Eur. Phys. J. A* **52**, 139 (2016).
- [79] V. Bernard, N. Kaiser, and Ulf-G. Meißner, *Nucl. Phys. A* **615**, 483 (1997).
- [80] H. Krebs, A. M. Gasparyan, and E. Epelbaum, *Phys. Rev. C* **98**, 014003 (2018).
- [81] F. Hagelstein, R. Miskimen, and V. Pascalutsa, *Prog. Part. Nucl. Phys.* **88**, 29 (2016).
- [82] V. Lensky, J. M. Alarcón, and V. Pascalutsa, *Phys. Rev. C* **90**, 055202 (2014).
- [83] C. W. Kao, T. Spitzenberg, and M. Vanderhaeghen, *Phys. Rev. D* **67**, 016001 (2003).
- [84] A. Aleksejevs and S. Barkanova, *Nucl. Phys. Proc. Suppl.* **245**, 17 (2013).
- [85] H. W. Griesshammer, J. A. McGovern, and D. R. Phillips, *Eur. Phys. J. A* **54**, 37 (2018).
- [86] M. C. Birse, X.-D. Ji, and J. A. McGovern, *Phys. Rev. Lett.* **86**, 3204 (2001).
- [87] G. C. Gellas, T. R. Hemmert, and Ulf-G. Meißner, *Phys. Rev. Lett.* **86**, 3205 (2001).